

ท่อคาร์บอนนาโนดัดแปรเพื่่อการประกยุกต์ใช้ในการนำสงยา



นางสาวจุฬารัตน์ เอี่ยมสมัย

ศูนย์วิทยพัทยากร  
จุฬาลงกรณ์มหาวิทยาลัย

วิทยานิพนธ์นี้เป็นส่วนหนึ่งของการศึกษาตามหลักสูตรปริญญาวิทยาศาสตรดุษฎีบัณฑิต

สาขาวิชาวิทยาศาสตร์นาโนและเทคโนโลยี (สหสาขาวิชา)

บัณฑิตวิทยาลัย จุฬาลงกรณ์มหาวิทยาลัย

ปีการศึกษา 2553

ลิขสิทธิ์ของจุฬาลงกรณ์มหาวิทยาลัย

# MODIFIED CARBON NANOTUBES FOR DRUG DELIVERY APPLICATIONS



Miss Chularat Iamsamai

ศูนย์วิทยทรัพยากร

A Dissertation Submitted in Partial Fulfillment of the Requirements  
for the Degree of Doctor of Philosophy Program in Nanoscience and Technology

(Interdisciplinary Program)

Graduate School

Chulalongkorn University

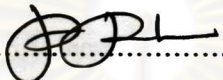
Academic Year 2010

Copyright of Chulalongkorn University


Thesis title	<b>MODIFIED CARBON NANOTUBES FOR DRUG DELIVERY APPLICATIONS</b>
By	Miss Chularat Iamsamai
Field of study	Nanoscience and Technology
Thesis Advisor	Professor Supot Hannongbua, Ph.D.
Thesis Co-advisor	Stephan Thierry Dubas, Ph.D. Uracha Ruktanonchai, Ph.D. Apinan Soottitantawat, Ph.D.

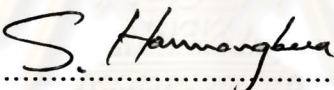
---

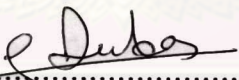
Accepted by the Graduate School, Chulalongkorn University in Partial Fulfillment of the Requirements for the Doctoral Degree.

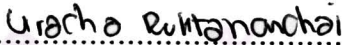
  
.....Dean of the Graduate School  
(Associate Professor Pornpote Piumsomboon, Ph.D.)

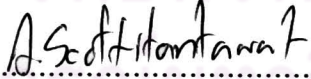
**THESIS COMMITTEE**

  
.....Chairman  
(Associate Professor Vudhichai Parasuk, Ph.D.)

  
.....Thesis Advisor  
(Professor Supot Hannongbua, Ph.D.)

  
.....Thesis Co-advisor  
(Stephan Thierry Dubas, Ph.D.)

  
.....Thesis Co-advisor  
(Uracha Ruktanonchai, Ph.D.)

  
.....Thesis Co-advisor  
(Apinan Soottitantawat, Ph.D.)

  
.....Examiner  
(Assistant Professor Sukkaneste Tungasamita, Ph.D.)

  
.....Examiner  
(Associate Professor Suwabun Chirachanchai, Ph.D.)

  
.....External Examiner  
(Associate Professor Satit Puttipipatkachorn, Ph.D.)

## 4989718720 : MAJOR NANOSCIENCE AND TECHNOLOGY

KEYWORDS: CARBON NANOTUBES / SURFACE MODIFICATION / DRUG DELIVERY

CHULARAT IAMSAMAI: MODIFIED CARBON NANOTUBES FOR DRUG DELIVERY APPLICATIONS. THESIS ADVISOR: PROFESSOR. SUPOT HANNONGBUA, Ph.D., THESIS COADVISORS: STEPHAN THIERRY DUBAS, Ph.D., URACHA RUKTANONCHAI, Ph.D., APINAN SOOTTITANTAWAT, Ph.D. 140 pp.

Noncovalent surface modification of multiwall carbon nanotubes (MWCNTs) using chitosan coating as a monolayer is presented. The different degree of deacetylation (%DD) (61%, 71%, 78%, 84%, 90% and 93%) of chitosan and chitosan concentration affected to carbon nanotubes's dispersion efficiency and their stability. Results showed that the dispersion of MWCNTs could be improved when using chitosan with the lowest degree of deacetylation (61%DD). Zeta potential measurements confirmed that the chitosan surface coverage on the MWCNTs was twice as high when modifying the nanotubes surface with the 61%DD than when using the 93%DD chitosan. To study how a chitosan-polysaccharide increases the dispersion efficiency and stability of CNTs, molecular dynamics simulation done on the three models: *i*) two pristine CNTs (*p*CNT-*p*CNT), *ii*) a pristine CNT-a chitosan wrapped CNT (*p*CNT-*c*WCNT) and *iii*) two chitosan wrapped CNTs (*c*WCNT-*c*WCNT). As a result, the CNT aggregation was found in *p*CNT-*p*CNT and *p*CNT-*c*WCNT due to van der Waals interaction between the tube-tube aromatic rings, and intertube bridging by chitosan, respectively. In case of *c*WCNT-*c*WCNT, charge-charge repulsion was found to separate the two tubes and well disperse in aqueous solution. Although the monolayer coating MWCNTs with low %DD chitosan was improved the dispersion of MWCNTs, their stability was insufficient to be used as drug carrier. Therefore, the layer-by-layer deposition technique was selected as a potential method for preparing multilayers between poly(diallyldimethylammonium chloride) (PDADMAC) and poly(sodium 4-styrenesulfonate) (PSS) coating on treated MWCNTs surface. Interestingly, we found the simple method to prepare primary, secondary and tertiary layers on treated MWCNT with "just enough polyelectrolyte" without centrifugation process. Multilayer coating on MWCNT was provided high stability in aqueous solution. Gentian violet and diclofenac were used as hydrophilic model drugs for loading on modified MWCNTs. Gentian violet selectively loaded on negatively charged surface of MWCNT while diclofenac cannot be achieved to load in any kind of MWCNTs. The cytotoxicity of modified MWCNTs with different functional groups was evaluated by MTT assay. Treated MWCNTs were toxic to L929 cells when the concentration reached 25 $\mu$ g/ml while primary coating MWCNTs with PDADMAC was toxic at concentration 12.5 $\mu$ g/ml.

Field of study: ..Nanoscience and Technology... Student's signature... *C. Iamsamai*.....

Academic year: .....2010.....

Advisor's signature... *S. Hannongbua*.....

Co-advisor's signature... *S. Dubas*.....

*U. Ruktanonchai*.....

*A. Soottitantawat*.....

จุฬารัตน์ เขียมสมัย : ท่อคาร์บอนนาโนดัดแปรเพื่อการประยุกต์ใช้ในการนำส่งยา.

(MODIFIED CARBON NANOTUBES FOR DRUG DELIVERY APPLICATIONS)

อ.ที่ปรึกษาวิทยานิพนธ์หลัก : ศาสตราจารย์ ดร. สุพจน์ หารหนองบัว, อ.ที่ปรึกษาวิทยานิพนธ์ร่วม :  
ดร. สเตฟาน เทียร์ ดูบาส, ดร. อรุชา รัชชตานนท์ชัย, ดร. อภินันท์ สุทธิธรรวัช, 140 หน้า.

การดัดแปรพื้นผิวของท่อคาร์บอนนาโนผนังหลายชั้น (MWCNTs) แบบนอนโควาเลนต์ โดยการเคลือบพื้นผิวแบบชั้นเดียวด้วยโคโคซานได้ถูกนำเสนอในงานวิจัยนี้ ระดับการกำจัดหมู่อะซิทีล (%DD) ของโคโคซาน (61%, 71%, 78%, 84%, 90% และ 93%) และความเข้มข้นของโคโคซานที่แตกต่างกัน มีผลต่อความสามารถในการกระจายตัวและความเสถียรของท่อคาร์บอนนาโนผนังหลายชั้น ผลการทดลองแสดงว่า โคโคซานที่มีระดับการกำจัดหมู่อะซิทีลต่ำที่สุด (61%) สามารถปรับปรุงการกระจายตัวของท่อคาร์บอนนาโนผนังหลายชั้น จากการวัดค่า zeta potential ยืนยันได้ว่า โคโคซานที่มีระดับการกำจัดหมู่อะซิทีล 61% สามารถปกคลุมพื้นผิวท่อคาร์บอนนาโนผนังหลายชั้นได้สูงกว่าสองเท่าเมื่อเทียบกับโคโคซานที่มีระดับการกำจัดหมู่อะซิทีล 93% เพื่อศึกษาโคโคซานซึ่งเป็นพอลิแคโรได์ช่วยเพิ่มความสามารถในการกระจายตัวและความเสถียรให้กับท่อคาร์บอนนาโนได้อย่างไร ดังนั้น Molecular Dynamics Simulation ถูกนำมาใช้เพื่อทำการศึกษาระบบ ได้แก่ i) ท่อคาร์บอนนาโนที่ไม่ผ่านการดัดแปรทั้งคู่ (pCNT-pCNT), ii) ท่อคาร์บอนนาโนที่ไม่ผ่านการดัดแปรกับโคโคซานที่มีระดับการกำจัดหมู่อะซิทีล 60% (pCNT-cwCNT) และ iii) ท่อคาร์บอนนาโนที่ไม่ผ่านการดัดแปรด้วยโคโคซานที่มีระดับการกำจัดหมู่อะซิทีล 60% ทั้งคู่ (cwCNT-cwCNT) การรวมตัวกันของท่อคาร์บอนนาโนเกิดขึ้นในกรณีที่เป็น pCNT-pCNT และ pCNT-cwCNT เนื่องจากแรง van der Waals ที่เกิดขึ้นระหว่างวงแหวนอะโรมาติกของท่อคาร์บอนนาโนและการเกาะกันระหว่างท่อคาร์บอนนาโนด้วยโคโคซาน ตามลำดับ ส่วนในกรณี cwCNT-cwCNT พบว่า เกิดการผลักกันระหว่างประจุส่งผลให้ทั้งสองแยกออกจากกันและกระจายตัวได้ในสารละลาย แม้ว่าท่อคาร์บอนนาโนผนังหลายชั้นที่ไม่ผ่านการดัดแปรโดยการเคลือบพื้นผิวแบบชั้นเดียวด้วยโคโคซานที่มีระดับการกำจัดหมู่อะซิทีลต่ำ จะสามารถปรับปรุงความสามารถในการกระจายตัวของท่อคาร์บอนนาโนผนังหลายชั้นได้ แต่ความเสถียรของท่อคาร์บอนนาโนดัดแปรด้วยโคโคซานดังกล่าวยังไม่เพียงพอต่อการนำมาใช้เพื่อเป็นตัวนำส่งยา ด้วยเหตุนี้เทคนิค layer-by-layer deposition เป็นวิธีที่มีศักยภาพที่ถูกเลือกใช้เพื่อเตรียมฟิล์มบางหลายชั้นระหว่างพอลิ(ไดอัลลิลไดเมทิลแอมโมเนียม คลอไรด์) (PDADMAC) และพอลิ(ไฮเดียม 4-สไตรีน ซัลโฟเนต) (PSS) เพื่อเคลือบบนท่อคาร์บอนนาโนที่ไม่ผ่านการดัดแปรทางเคมี เป็นที่น่าสนใจว่า การเตรียมฟิล์มบางชั้นที่ 1, 2 และ 3 บนท่อคาร์บอนนาโนที่ไม่ผ่านการดัดแปรทางเคมี สามารถเตรียมได้ด้วยวิธีที่ง่ายโดยใช้ “just enough polyelectrolyte” ซึ่งปราศจากการผ่านขั้นตอนการปั่นเหวี่ยง ทำให้ท่อคาร์บอนนาโนดัดแปรด้วยวิธีดังกล่าวมีความเสถียรอยู่ในสารละลายสูง ท่อคาร์บอนนาโนดัดแปรดังกล่าวถูกนำมาใช้เพื่อ load ยาโมเดลที่ละลายน้ำ ได้แก่ ยาเจนเชียนไวโอเลตและยาโคโคพิแนค พบว่า ยาเจนเชียนไวโอเลตสามารถ load ลงบนท่อคาร์บอนนาโนดัดแปรที่มีพื้นผิวเป็นประจุลบได้ดี ในขณะที่ยาโคโคพิแนคไม่สามารถ load ลงบนท่อคาร์บอนนาโนดัดแปรชนิดใดได้เลย ทั้งนี้ท่อคาร์บอนนาโนที่ไม่ผ่านการดัดแปรด้วยหมู่ดัดแปรที่แตกต่างกันถูกนำมาทดสอบเพื่อประเมินค่าความเป็นพิษต่อเซลล์ L929 ด้วย MTT assay พบว่า ท่อคาร์บอนนาโนที่ไม่ผ่านการดัดแปรทางเคมี ปริมาณ 25 ไมโครกรัม/มิลลิลิตร มีความเป็นพิษต่อเซลล์ L929 ในขณะที่ท่อคาร์บอนนาโนดัดแปรที่เคลือบหนึ่งชั้นด้วย PDADMAC มีความเป็นพิษต่อเซลล์ L929 ที่ปริมาณ 12.5 ไมโครกรัม/มิลลิลิตร

สาขาวิชา...วิทยาศาสตร์นาโนและเทคโนโลยี... ลายมือชื่อนิสิต.....

ปีการศึกษา.....2553.....

ลายมือชื่อ อ.ที่ปรึกษาวิทยานิพนธ์หลัก.....

ลายมือชื่อ อ.ที่ปรึกษาวิทยานิพนธ์ร่วม.....

อ.ดร. อภินันท์ สุทธิธรรวัช

## ACKNOWLEDGEMENTS

I wish to express my deepest gratitude to Professor Dr. Supot Hannongbua, Dr. Stephan Thierry Dubas, Dr. Uracha Ruktanonchai and Dr. Apinan Soottitantawat, my advisors team, for their valuable guidance, advice and encouragement throughout this research work.

I wish to extend my sincere thanks to committee; Associate Professor Dr. Vudhichai Parasuk, Associate Professor Dr. Satit Puttipipatkhajorn, Associate Professor Dr. Suwabun Chirachanchai, and Assistant Professor Dr. Sukkaneste Tungasamita for their advice, motivating comments, participation as dissertation committees and assistance for my study and the Doctor of Philosophy Program in Nanoscience and Technology, Graduate School, Chulalongkorn University for graduate courses and financial supporting throughout my Ph. D study.

I gratefully acknowledge the generous access to research facilities and chemical support from Metallurgy and Materials Science Research Institute, Chulalongkorn University and Dr. Kritsana Siralermukul. I would like to thank Thailand Graduate Institute of Science and Technology, (TGIST) and Graduate School, Chulalongkorn University for providing special research scholarships: TGIST (TG-55-09-50-059D) and The 90<sup>th</sup> Anniversary of Chulalongkorn University Fund (Ratchadaphiseksomphot Endowment Fund), respectively.

I would like to thank Dr. Thanyada Rungrotmongkol, Miss Uthumporn Arsawang and Mr. Arthit Vongachariya for supporting computational simulation data to fulfill my research work. I would like to sincere thank to all colleagues, nano-friends and Miss Chindarat Pinkeaw for their encouragement and help along my Ph.D. study in this program.

Finally, I would like to express my deepest appreciation to my *FAMILY* for their love, great encouragement and worthy moral support throughout my whole life's study.

# CONTENTS

	Page
ABSTRACT (THAI).....	iv
ABSTRACT (ENGLISH).....	v
ACKNOWLEDGEMENTS.....	vi
CONTENTS.....	vii
LIST OF TABLES.....	xiv
LIST OF FIGURES.....	xv
LIST OF ABBREVIATIONS.....	xxii
CHAPTER	
I INTRODUCTION.....	1
II THEORY AND LITERATURE REVIEW.....	4
2.1 Introduction to Carbon Nanotubes.....	6
2.2 Carbon nanotubes synthesis.....	9
2.2.1 Electric Arc Discharge technique.....	9
2.2.2 Laser Ablation Technique.....	10
2.2.3 Chemical Vapor Deposition Technique.....	11
2.3 Surface modification of carbon nanotubes.....	12
2.3.1 Noncovalent surface modification.....	13
2.3.2 Covalent surface modification.....	15
2.4 Theory of Layer-by-Layer self assembly.....	16
2.4.1 Definition and general description of polyelectrolyte.....	16
2.4.2 Formation of polyelectrolyte multilayer thin films.....	19
2.4.3 Parameters controlling the growth of PEM.....	21
2.4.3.1 Type of polyelectrolyte.....	21
2.4.3.2 Effect of polymer charge density.....	22
2.4.3.3 Influence of ionic strength.....	22
2.5 Layer-by-layer surface modification of carbon nanotubes.....	24
2.6 Wrapping carbon nanotubes with polymer by noncovalent surface modification: Molecular Dynamics Simulation.....	28
2.7 Carbon nanotubes in drug delivery application.....	29

CHAPTER	Page
2.8 Carbon nanotubes cytotoxicity: <i>In Vitro</i> .....	31
III EXPERIMENTAL.....	35
3.1. Chitosan synthesis.....	35
3.1.1 Chemicals and Materials.....	35
3.1.2 Methodology of chitosan synthesis with various degree of deacetylation.....	35
3.1.3 Determination of degree of deacetylation of chitosan using first derivative UV-Vis Spectroscopy technique.....	36
3.1.4 Determination of average molecular weight of chitosan using gel permeation chromatography (GPC Waters 600E).....	39
3.1.4.1 Sample preparation.....	39
3.2 Effect of the degree of deacetylation of chitosan on its dispersion of carbon nanotubes.....	39
3.2.1 Chemicals and Materials.....	39
3.2.2 Effect of chitosan concentration on the dispersion of MWCNTs.....	40
3.2.3 Effect of sonication times on MWCNTs dispersion with chitosan.....	40
3.2.4 Effect of %DD of chitosan on the dispersion of MWCNTs.....	41
3.2.5 Surface charge of the modified MWCNTs.....	41
3.3 Molecular Dynamics Simulation: Dispersion and separation of chitosan wrapping on SWCNTs by noncovalently modification.....	42
3.3.1 Materials and methods.....	43
3.4 Covalent surface modification of multiwall carbon nanotubes with acid oxidation (H <sub>2</sub> SO <sub>4</sub> and HNO <sub>3</sub> ).....	44
3.4.1 Chemicals and materials.....	44
3.4.2 Acid treatment of carbon nanotubes.....	45



CHAPTER	Page
3.5 Layer-by-layer deposition on treated carbon nanotubes with polyelectrolyte; PDADMAC and PSS without centrifugation process.....	45
3.5.1 Chemicals and materials.....	45
3.5.2 Deposition of polyelectrolyte multilayers on multiwall carbon nanotubes via layer-by-layer technique.....	46
3.5.3 Stability of modified MWCNT (treated MWCNT and primary coating MWCNT with PDADMAC).....	48
3.5.3.1 Effect of salt concentration on stability of modified MWCNT.....	48
3.5.3.2 Effect of pH on stability of modified MWCNT.....	48
3.5.4 Characterization Technique.....	48
3.6 Hydrophilic model drugs: gentian violet and diclofenac loading and recovery on modified multiwalled carbon nanotubes.....	49
3.6.1 Chemicals and materials.....	49
3.6.1.1 Gentian violet.....	49
3.6.1.2 Diclofenac.....	50
3.6.2 Preparation of phosphate buffer saline.....	50
3.6.3 Layer-by-layer deposition on treated multiwall carbon nanotubes with polyelectrolyte in 0.1xPBS buffer.....	50
3.6.4 Preparation of primary and secondary layers coating on MWCNTs with polyelectrolyte.....	51
3.6.4.1 Deposition of primary layer on carbon nanotubes.....	51
3.6.4.2 Deposition of secondary layer on carbon nanotubes.....	51
3.6.5 Loading and recovery gentian violet from modified multiwall carbon nanotubes; Treated MWCNT, Primary coating MWCNT with PDADMAC and Secondary coating MWCNT with PDADMAC/PSS.....	52

CHAPTER	Page
3.6.6 Loading and recovery diclofenac sodium from modified multiwall carbon nanotubes; Treated MWCNT, Primary coating MWCNT with PDADMAC and Secondary coating MWCNT with PDADMAC/PSS.....	52
3.7 Cytotoxicity of modified carbon nanotubes using MTT assay.....	53
3.7.1 Chemicals and Materials.....	53
3.7.2 L929 fibroblast cells preparation.....	54
3.7.3 Interference of formazan adsorption on untreated and treated multiwall carbon nanotubes.....	54
3.7.4 Cytotoxicity test: MTT Assay.....	55
3.7.5 Effect of functional groups of modified multiwall carbon nanotubes on their cytotoxicity.....	55
3.7.5.1 Preparation of modified carbon nanotubes with poly(diallyldimethyl ammonium chloride) and poly(sodium 4-styrene sulfonate).....	55
3.7.5.2 Preparation of modified multiwall carbon nanotubes for testing MTT assay.....	56
3.7.5.3 Cytotoxicity: MTT Assay.....	56
3.8 Characterization Technique.....	57
3.8.1 UV-Vis spectroscopy.....	57
3.8.2 Zeta potential measurement.....	58
3.8.3 Transmission electron microscopy (TEM).....	58
3.8.4 Scanning electron microscopy (SEM).....	58
3.8.5 Gel permeation chromatography (GPC).....	59
3.8.6 Fourier Transform Infrared spectroscopy (FTIR).....	59
3.8.7 Raman spectroscopy.....	59
IV RESULTS AND DISCUSSION.....	60
4.1 Surface modification of carbon nanotubes.....	60
4.1.1 Noncovalent surface modification of multiwall carbon nanotubes with various degree of deacetylation of chitosan.....	60

CHAPTER	Page
4.1.1.1 Chitosan synthesis.....	61
4.1.1.2 Effect of sonication times on carbon nanotubes dispersion with chitosan.....	65
4.1.1.3 Effect of chitosan concentration on carbon nanotubes dispersion.....	66
4.1.1.4 Effect of degree of deacetylation of chitosan on carbon nanotubes dispersion.....	68
4.1.1.5 Surface charge of modified carbon nanotubes with different degree of deacetylation of chitosan.....	70
4.1.2 Molecular Dynamics Simulation: Dispersion and separation of chitosan wrapping on SWCNTs by noncovalently modification.....	73
4.1.2.1 Dispersion and solubility of CNTs.....	75
4.1.2.2 Role of chitosan fragments.....	77
4.1.3 Covalent surface modification of multiwall carbon nanotubes with acid oxidation (H <sub>2</sub> SO <sub>4</sub> and HNO <sub>3</sub> ).....	79
4.1.4 Layer-by-layer deposition on treated carbon nanotubes with polyelectrolyte; PDADMAC and PSS without centrifugation process.....	82
4.1.4.1 Primary layer coating on treated MWCNTs with PDADMAC.....	84
4.1.4.1.1 Effect of PDADMAC concentration on the stability of treated MWCNTs.....	84
4.1.4.1.2 Stability of treated and primary coating on MWCNT in different salt concentrations and pH condition.....	90
4.1.4.2 Secondary layer coating on MWCNTs.....	92
4.1.4.3 Tertiary layer coating on MWCNTs.....	94
4.2 Loading and recovery of hydrophilic model drugs of modified multiwall carbon nanotubes.....	98

CHAPTER	Page
4.2.1 Loading and recovery of gentian violet of treated multiwall carbon nanotubes, primary and secondary coating multiwall carbon nanotubes .....	98
4.2.2 Loading and recovery of diclofenac of treated multiwall carbon nanotubes, primary and secondary coating multiwall carbon nanotubes .....	104
4.3 Cytotoxicity of modified carbon nanotubes.....	105
4.3.1 Interference of adsorption formazan by carbon nanotubes.....	106
4.3.2 Cytotoxicity of untreated, treated, coating primary (PDADMAC), secondary (PDADMAC/PSS), tertiary MWCNT(PDADMAC/PSS/PDADMAC) on L929 cells.....	107
4.3.2.1 Cytotoxicity of untreated and treated MWCNT.....	107
4.3.2.2 Cytotoxicity of primary coating MWCNT with PDADMAC, secondary coating MWCNT with PDADMAC/PSS and tertiary coating MWCNT with PDADMAC/PSS/PDADMAC.....	109
4.3.2.2.1 Cytotoxicity of primary coating MWCNT with PDADMAC, secondary coating MWCNT with PDADMAC/PSS and tertiary coating MWCNT with PDADMAC/PSS/PDADMAC : In case of solution.....	112
4.3.2.2.2 Cytotoxicity of primary coating MWCNT with PDADMAC, secondary coating MWCNT with PDADMAC/PSS and tertiary coating MWCNT with PDADMAC/PSS/PDADMAC : In case of powder.....	115

CHAPTER	Page
V CONCLUSIONS.....	119
REFERENCES.....	121
APPENDIX.....	130
VITAE.....	134



ศูนย์วิทยทรัพยากร  
จุฬาลงกรณ์มหาวิทยาลัย

**LIST OF TABLES**

TABLE	Page
2.1 Structures of ionic sites of polyelectrolyte.....	18
3.1 Gel Permeation Chromatography test condition.....	39



ศูนย์วิทยทรัพยากร  
จุฬาลงกรณ์มหาวิทยาลัย

## LIST OF FIGURES

FIGURE	Page
2.1 Carbon Allotropes; (a) Diamond, (b) Graphite, (c) Fullerene (C <sub>60</sub> ), (d) Single Walled Carbon Nanotube, and (e) Amorphous Carbon.....	5
2.2 (a) Crystallographic configurations of CNTs, (b) Direction of rolled hexagonal sheet of graphite to form a CNT.....	7
2.3 Arc discharge apparatus produced the first carbon nanotubes.....	10
2.4 Laser ablation apparatus for producing carbon nanotubes.....	11
2.5 Carbon nanotubes synthesis using chemical vapor deposition technique.....	12
2.6 Chemical structure of (a) sodium poly(styrene sulfonate) and (b) poly(diallyldimethylammonium chloride).....	16
2.7 Chemical structure of the weak synthetic polyelectrolytes (a) poly(acrylic acid) and (b) poly(ethylene imine) and weak natural polyelectrolytes (c) chitosan and (d) alginate.....	17
2.8 Schematic of the electrostatic self-assembly (ESA).....	20
2.9 Variety of substrates for deposition polyelectrolyte multilayers via layer-by-layer technique.....	21
2.10 TEM image of coating multiwall carbon nanotubes with polyelectrolyte.....	24
2.11 Representative the deposition of PDMAEMA, PSS, and HSA.....	25
2.12 The process of solubilizing PAH-MWCNTs and assembly bionanomultilayers.....	26
2.13 The schematic illustration of the detection for AFP based on sandwich-type CLIA. The upper part I–V is the schematics of layer-by-layer electrostatic self-assembly of HRP on carbon nanotube template: (I) treatment of MWCNTs generating negatively charged carboxylic functionalized groups; (II) assembling of positively charged PDDA; (III) assembling of negatively charged HRP; (IV) repetition of II and III until the desired layers are obtained; (V) additional assembling of positively charged PDDA layer and negatively charged PSS layer; (VI) adsorption of AFP secondary antibody (Ab <sub>2</sub> ).....	27

FIGURE	Page
2.14 TEM images of modified SWCNTs. (a) Cut SWCNTs, (b) ALG-SWCNTs, (c) CHI-SWCNTs, (d) CHI/ALG-SWCNTs, (e) DOX-SWCNTs, (f) DOX-ALG-SWCNTs, (g) DOX-CHI-SWCNTs and (h) DOX-CHI/ALG-SWCNTs.....	28
2.15 (a) The effect of CNT structure on phagocytosis by macrophages and clearing from tissues. (b) In addition to their dimensions, other considerations relevant to the safety of CNTs include increasing their solubility and preventing their aggregation.....	32
2.16 Effect of functional groups of SWCNT on cell viability.....	33
3.1 Chemical structure of Chitosan: $x$ = N-acetyl-D-glucosamine unit, $y$ = D-glucosamine unit: $x > 50\%$ = Chitin, $y > 50\%$ = Chitosan.....	35
3.2 First derivative absorbance of N-acetyl-D-glucosamine with different concentrations(g/l).....	37
3.3 Calibration curve of N-acetyl-D-glucosamine in acetic acid 0.1 M with (a) Height (H) of derivative absorbance and (b) Height (H) in mm from zero crossing point as a function of the concentration of N-acetyl-D-glucosamine.....	38
3.4 Morphology image of pristine CNT characterized by scanning electron microscope (Phillips XL30CP), a diameter in a range of 110-170 nm and length in a range of 5-9 $\mu\text{m}$ .....	40
3.5 Schematic views of (a) two pristine CNTs ( $p\text{CNT}-p\text{CNT}$ ), (b) a pristine CNT -a wrapped CNT with chitosan ( $p\text{CNT}-c\text{wCNT}$ ), and (c) two chitosan-wrapped CNTs ( $c\text{wCNT}-c\text{wCNT}$ ) where the SWCNT and the polymer used are the (8,8) armchair and 60% <i>DD</i> chitosan, respectively. The distances ( $d(Cgi-Cgj)$ ) and ( $d(Sgi-Sgj)$ ) and torsion angle ( $\tau$ ) between the two SWCNTs were defined through the center of gravity ( $Cg$ ) and the surface of each tube in which $\tau = 0^\circ$ and the two tubes are parallel.....	42
3.6 Chemical structure of chitosan 60% <i>DD</i> were alternate the repeating unit between N-Acetyl-D-Glucosamine and D-Glucosamine.....	43



FIGURE	Page
3.7 Transmission electron microscopic image of pristine multiwall carbon nanotubes (baytubes® C 150 P).....	44
3.8 Chemical structure of poly(diallyldimethylammonium chloride): PDADMAC.....	46
3.9 Chemical structure of poly(sodium 4-styrene sulfonate): PSS.....	46
3.10 Diagram of modified carbon nanotubes with PDADMAC and PSS as polyelectrolyte multilayers.....	47
3.11 Chemical structure of Gentian violet (crystal violet, Methyl Violet 10B, hexamethyl pararosaniline chloride).....	49
3.12 Chemical structure of Diclofenac (2-(2,6-dichloranilino)phenylacetic acid)....	50
3.13 Chemical structure of MTT; (3-(4,5-Dimethylthiazol-2-yl)-2,5 diphenyltetrazolium bromide, a yellow tetrazole).....	53
4.1 Chemical structure of Chitosan: $x$ = N-acetyl-D-glucosamine unit, $y$ = D-glucosamine unit: $x > 50\%$ = Chitin, $y > 50\%$ = Chitosan.....	61
4.2 Plot of degree of deacetylation of chitosan which investigated by first derivative UV-Visible spectroscopy technique as a function of deacetylation time.....	62
4.3 Schematic of deacetylated reaction of chitin under concentrated alkaline.....	62
4.4 Molecular weight of chitosan as a function of deacetylation time.....	64
4.5 Hypothesis model of noncovalent surface modification of MWCNTs with chitosan.....	64
4.6 The dispersion of MWCNTs with 5 mM of different degree of deacetylation chitosan (61, 78 and 93% <i>DD</i> ) as a function of sonication time.....	66
4.7 Plot of the changes in absorbance of a CNT solution as function of the 61% <i>DD</i> chitosan concentration (0-10mM).....	67
4.8 Plots of the changes in absorbance of a dispersion of MWCNTs in a 5 mM chitosan solution of various degree of deacetylation before (squares) and after (triangles) centrifugation at 2000 rpm for 10 minutes.....	70

FIGURE	Page
4.9 Zeta potential of modified MWCNT (circles) and normalized chitosan adsorption ratio onto the MWCNT (triangles) as a function of the %DD of chitosan.....	72
4.10 Schematic views of (a) two pristine CNTs ( <i>p</i> CNT- <i>p</i> CNT), (b) a pristine CNT – a wrapped CNT with chitosan ( <i>p</i> CNT- <i>cw</i> CNT), and (c) two chitosan- wrapped CNTs ( <i>cw</i> CNT- <i>cw</i> CNT) where the SWCNT and the polymer used are the (8,8) armchair and 60%DD chitosan, respectively. The distances ( $d(Cg_i-Cg_j)$ ) and ( $d(S_i-S_j)$ ) and torsion angle ( $\tau$ ) between the two SWCNTs were defined through the center of gravity ( <i>Cg</i> ) and the surface of each tube in which $\tau = 0^\circ$ and the two tubes are parallel. The molecular structure of the chitosan's repeating units was shown (d).....	74
4.11 Distance (blue line), $d(Cg_i-Cg_j)$ , between the two centers of gravity of SWCNT and torsion angle (red line), $\tau$ (see Figure 4.10 for definition), as a function of the simulation time for the three systems, (a) <i>p</i> CNT- <i>p</i> CNT, (b) <i>p</i> CNT- <i>cw</i> CNT and (c) <i>cw</i> CNT- <i>cw</i> CNT, where their corresponding structures taken from the MD simulation were also shown in (d), (e) and (f).....	75
4.12 RDFs from the nitrogen atoms on the N-acetyl-D-glucosamine (N(NAG), blue line) and D-glucosamine (N(GLS), red line) of chitosan (see Figure 4.10(d) for definition) to the carbon atoms of the wrapped CNTs (a) CNT#1 for the <i>p</i> CNT- <i>cw</i> CNT, (b) both CNT#1 and CNT#2 for the <i>cw</i> CNT- <i>cw</i> CNT and (c) oxygen atoms of water.....	77
4.13 Raman spectra of pristine MWCNT and treated MWCNTs.....	80
4.14 FTIR spectra of pristine MWCNT and treated MWCNTs.....	81
4.15 Transmission electron micrograph of (a) pristine MWCNTs and (b) treated MWCNTs.....	82

FIGURE	Page
4.16 Stability of modified MWCNT 6.25 $\mu\text{g/ml}$ with different poly(diallyldimethylammonium chloride) concentration (0-0.05 mM) (a) Solutions of treated MWCNT and the modified MWCNT with various PDADMAC concentrations, (b) Plots of the changes in absorbance of modified MWCNT with various PDADMAC concentration after preparing for 1 week, (c) Plots of reversal zeta potential of modified MWCNT with various PDADMAC concentrations.....	85
4.17 Plots of the changes in absorbance of modified MWCNT (6.25, 12.5 and 25 $\mu\text{g/ml}$ ) with various PDADMAC concentrations (0-0.25mM) after preparing for 1 week.....	88
4.18 Plots of zeta potential of modified CNT 12.5, 25, 50 $\mu\text{g/ml}$ with various PDADMAC concentrations.....	89
4.19 Mass ratio between PDADMAC and treated carbon nanotubes as a primary layer.....	89
4.20 Stability of modified MWCNT, treated MWCNT and PDADMAC coated on MWCNTs, as a function of salt concentration for 1 week.....	91
4.21 Stability of modified MWCNT, treated MWCNT and PDADMAC coated on MWCNTs, as a function of <i>pH</i> for 1 day.....	92
4.22 Plots of changes in absorbance of primary coating MWCNT with PDADMAC as a function of PSS concentrations, final amount of MWCNT: 12.5 $\mu\text{g/ml}$ ....	93
4.23 Plots of the reversal zeta potential of primary coating MWCNT with PDADMAC as a function of PSS concentrations, final amount of MWCNT: 12.5 $\mu\text{g/ml}$ .....	94
4.24 Plots of changes in absorbance of secondary coating MWCNT with PDADMAC/PSS as a function of PDADMAC concentrations, final amount of MWCNT: 6.25 $\mu\text{g/ml}$ .....	95
4.25 Plots of the changed in zeta potential of secondary coating MWCNT with PDADMAC/PSS as a function of PDADMAC concentrations, final amount of MWCNT: 6.25 $\mu\text{g/ml}$ .....	95

FIGURE	Page
4.26 Zeta potential of pristine MWCNT, treated MWCNT, primary coating MWCNT with PDADMAC, secondary coating MWCNT with PDADMAC/PSS, and tertiary coating MWCNT with PDADMAC/PSS /PDADMAC.....	96
4.27 Transmission electron micrograph of (a) pristine MWCNT scale bar 50 nm, (b) tertiary coating MWCNT with PDADMAC/PSS /PDADMAC scale bar 50 nm, (c),(d) and tertiary coating MWCNT with PDADMAC/PSS /PDADMAC scale bar 100 nm.....	97
4.28 The reversal charge when the CNTs were modified with primary, secondary, and tertiary layer in 0.1xPBS buffer.....	99
4.29 Calibration curve of gentian violet in 0.1 PBS buffer with different concentrations.....	100
4.30 Comparison concentrations of gentian violet adsorption in 0.1 PBS and recover in ethanol from treated MWCNT.....	101
4.31 Comparison concentrations of gentian violet adsorption in 0.1 PBS and recover in ethanol from primary coating CNT with PDADMAC.....	102
4.32 Comparison concentrations of gentian violet adsorption in 0.1 PBS and recover in ethanol from secondary coating MWCNT with PDADMAC/PSS.....	103
4.33 The remaining of diclofenac concentrations in 0.1 PBS after loading to modified carbon nanotubes.....	105
4.34 The absorbance of formazan solution at 570 nm after exposed with pristine and treated MWCNT with various concentrations.....	106
4.35 The absorbance of formazan after convert from MTT by exposing L929 cells with different concentrations of pristine and treated CNT for 24 hr.....	108
4.36 % Cell viability of L929 cell after exposed with untreated and treated MWCNT with different concentrations for 24 hr.....	109
4.37 The absorbance of formazan after convert from MTT by exposing L929 cells with different concentrations of PDADMAC solution for 24 hr.....	110

FIGURE	Page
4.38 % Cell viability of L929 after exposed with PDADMAC solution with different concentrations for 24 hr.....	111
4.39 L929 cells morphology after exposed with PDADMAC concentration (a) 0.1 mM and (b) 0.5 mM for 24 hr.....	111
4.40 L929 cells morphology after exposed with PSS concentration (a) 0.1 mM and (b) 0.5 mM for 24 hr.....	112
4.41 The absorbance of formazan after L929 cells were exposed with different concentrations of primary coating MWCNT with PDADMAC, secondary coating MWCNT with PDADMAC/PSS, tertiary coating MWCNT with PDADMAC/PSS/PDADMAC for 24 hr.....	113
4.42 % Cell viability of L929 cells after exposed with primary coating CNT with PDADMAC, secondary coating CNT with PDADMAC/PSS, tertiary coating CNT with PDADMAC/PSS/PDADMAC with different concentrations for 24 hr.....	114
4.43 L929 cells morphology, (a) Cell control (b) Cell after exposed with primary coating MWCNT with PDADMAC 12.5 µg/ml, (c) secondary coating MWCNT with PDADMAC/PSS 6.25 µg/ml, and (d) tertiary coating MWCNT with PDADMAC/PSS/PDADMAC 3.125 µg/ml.....	115
4.44 The absorbance of formazan after L929 cells were exposed with different concentrations of primary coating MWCNT with PDADMAC, secondary coating MWCNT with PDADMAC/PSS, tertiary coating MWCNT with PDADMAC/PSS/PDADMAC for 24 hr.....	116
4.45 % Cell viability of L929 cells after exposed with primary coating MWCNT with PDADMAC, secondary coating MWCNT with PDADMAC/PSS, tertiary coating MWCNT with PDADMAC/PSS/PDADMAC with different concentrations for 24 hr.....	117
4.46 L929 cells morphology, (a) Cell control (b) Cell after exposed with primary coating MWCNT with PDADMAC 50 µg/ml, (c) secondary coating MWCNT with PDADMAC/PSS 50 µg/ml, and (d) tertiary coating MWCNT with PDADMAC/PSS/PDADMAC 50 µg/ml.....	118

## LIST OF ABBREVIATIONS

CNT(s)	:	Carbon nanotube(s)
MWCNT(s)	:	Multiwall carbon nanotube(s)
SWCNT(s)	:	Singlewall carbon nanotube(s)
DD	:	Degree of deacetylation
PEL	:	Polyelectrolyte
PEM	:	Polyelectrolyte Multilayer Thin Films
LbL	:	Layer-by-Layer technique
ESA	:	Electrostatic self - assembly
PDADMAC	:	Poly(diallyldimethylammonium chloride)
PSS	:	Poly(sodium 4-styrene sulfonate)
RDF	:	Radial Distribution Function
$\tau$	:	Torsion angle
$S_g$	:	Distance between CNTs surface
$C_g$	:	Distance between center of mass of CNTs
$C_w$	:	Chitosan wrapped
$p$	:	Pristine
mM	:	milli Molar
M	:	Molar
nm	:	nanometer
$\text{\AA}$	:	Angstrom
min	:	minute
ps	:	picosecond
fs	:	femtosecond
<i>et al.</i>	:	<i>et alii</i>

# CHAPTER I

## INTRODUCTION

Problems associated with the administration of free drugs such as limited solubility, poor biodistribution, lack of selectivity between drug and targeted cells, unfavourable pharmacokinetics and healthy tissue damage can be overcome and improved by the use of a targeted drug delivery system. Nanocarriers such as nanoparticles, nanotubes and nanowires, nanospheres, nanocapsules, dendrimers, polymeric micelles, etc. are widely promising vehicles which are used in drug delivery systems because they present targeted delivery to targeted cells while providing drug efficiency. Nanocarriers can deliver drugs to specific areas within the body. Furthermore, they can overcome resistance from the physicochemical barriers in the body. Therefore, efficient delivery of drugs to various parts of the body is successful because it is directly affected by nanoparticles. Drug delivery systems can be improved by nanocarriers such as increasing the solubility of poorly soluble drugs in order to enhance bioavailability for timed release of drug molecules and precise drug targeting. The surface properties of nanocarriers can be modified in order to reduce drug toxicity and provide more efficient drug distribution.

Among attractive nanomaterials, carbon nanotubes (CNTs), have been studied in a wide variety of scientific research and applications. Because CNTs possess unique properties, CNTs exhibit excellent thermal and chemical stabilities. In addition, they also possess semi- and metallic-conductive properties. For these reasons, CNTs have been widely used in many applications and impacted to the scientific breakthroughs in the present. Integrating CNTs in biomedical applications as a drug carrier is one of the major challenges of CNTs research to date for therapeutic molecules in drug delivery systems. Due to the unique physicochemical properties of CNTs which maintain their structure in any conditions, CNTs are suitable materials to be used as drug carriers. Moreover, CNTs offer some interesting advantages over the spherical nanoparticles for biomedical applications. The large inner volume of CNTs allows the loading of small biomolecules while their outer surface can be modified by covalent and noncovalent surface modification. Since CNTs can hardly be dispersed in any kind of solvent and tend to aggregate due to

van der Waals interaction of intertube, the development of efficient methodologies for surface modification of CNTs is needed to overcome this obstacle. Two main approaches of surface modification of CNTs have been proposed including covalent and non-covalent surface modification to overcome this barrier. Surface modification of CNTs, especially, using modified CNTs as a drug carrier in drug delivery application, dispersion and stability efficiency of CNTs are necessary improved. In term of dispersion, the modified CNTs provide high specific surface area for high adsorption with other molecules while in term of stability, individual CNT after dispersing should be stable in the solution without any precipitation. To apply CNTs in biomedical applications, cytotoxicity of CNT is another concern which was still argued in scientific research until now. However, many different toxicity results of CNTs have been published and proposed where there are five S factors concerned with CNT toxicity including size, source, shape, surface chemistry and surface area.

In this work, CNTs were modified both by noncovalent and covalent modification to improve CNTs dispersion and stability which are having hydrophilic species either positive or negative charge at their surface. Molecular dynamics simulation was carried out for the pristine CNT and non-covalent modified CNT, with 60%DD chitosan, in aqueous solution. This aims to understand and explain their solubility at molecular level and to confirm the result of noncovalent surface modification of CNT with various degree of deacetylation of chitosan in experimental method. For drug loading, modified CNT with multilayers thin film between PDADMAC and PSS were used as a drug reservoir. The coating multilayers on CNT were loaded with model hydrophilic drugs; gentian violet and diclofenac sodium salt. Furthermore, drug loading were quantified by releasing in ethanol. Cytotoxicity of modified CNT and pristine CNT was evaluated with L929 mouse fibroblast cell using MTT assay. In addition, the interference of formazan adsorption on CNT surface was investigated in order to confirm the potential of this assay. The characterization techniques used in this work are UV-Vis spectroscopy, zeta potential measurement, transmission electron microscopy, gel permeation chromatography, fourier transform infrared spectroscopy and raman spectroscopy.

UV-Vis spectroscopy was used to investigate the dispersion efficiency and stability of modified CNTs. In addition, the drug loading and drug release from modified



CNTs in individual tubes and film were detected using UV-Vis spectroscopy. Modified CNTs with polyelectrolyte via layer-by-layer technique was monitored using transmission electron microscopy. To confirm the surface charge of modified CNTs, electrical charge in term zeta potential was investigated using zeta sizer instrument.

The results obtained from this study can be used as a guidance for preparing CNTs by modifying their surface properly to apply as drug carriers in drug delivery application in future.



ศูนย์วิจัยทรัพยากร  
จุฬาลงกรณ์มหาวิทยาลัย

## CHAPTER II

### THEORY AND LITERATURE REVIEW

*'There's plenty of room at the bottom'*, was the title of Richard Feynman's talk, when he gave a lecture at American Physical Society Meeting at Caltech in 1959 [1]. This valuable phrase has been the mainspring of scientific inspiration for scientists around the world to initiate the scientific movement of tiny level which is nowadays called "Nanoscience and Nanotechnology". Nanoscience is the study of phenomena and manipulation of materials at atomic, molecular and macromolecular scales, where properties differ significantly from those at larger scale while nanotechnology is the design, characterization, production and application of structures, devices and systems by controlling shape and size at nanometer scale [2].

Nanotechnology deals with materials and systems having the following key properties [3];

- They have at least one dimension smaller than 100 nm.
- They are designed through processes that exhibit fundamental control over the physical and chemical characteristics of molecular scale structure.
- They can be combined into larger structures.

A wide group of nanomaterials enables access to the new ranges of electronic, magnetic, mechanical and optical properties. One of interesting nanomaterials which has attracted the attention of many researchers since the last decade is "Carbon Nanotubes" (CNTs) [4]. There are many allotropes of carbon structures which have been well known in nowadays such as diamond, graphite, fullerene ( $C_{60}$ ) and carbon nanotube. The major allotropes of carbon; diamond and graphite, should be considered and compared with carbon nanotube in term of their structure as shown in Figure 2.1. The chemical bonding of carbon nanotubes is composed entirely of  $sp^2$  bonds, similar to graphite. This bonding structure, which is stronger than the  $sp^3$  bonds found in diamonds, provides the molecules with their unique strength. Nanotubes naturally align themselves into "ropes" held together by van der Waals forces [5]. In diamond, each carbon atom is bonded to four others in a three dimensional lattice while in graphite, each carbon atoms is attached to three others in a same plane and form a hexagonal lattice. The remaining bond in graphite

structure is used to hold the other planes above and below. However, the bonds in the plane of graphite are stronger than in diamond but the interplanar bonds are relatively weak and enable the planes to slide [6].

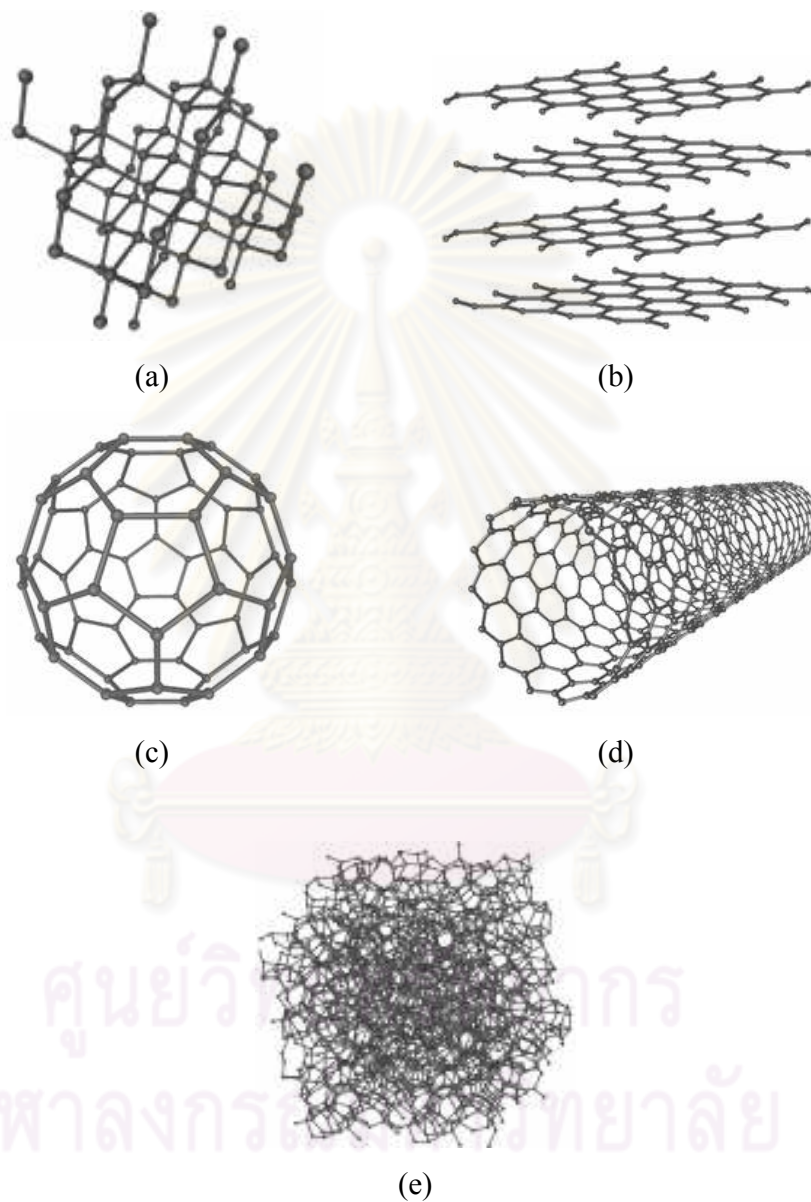


**Figure 2.1** Carbon Allotropes; (a) Diamond, (b) Graphite, (c) Fullerene ( $C_{60}$ ), (d) Single Walled Carbon Nanotube and (e) Amorphous Carbon.

## 2.1 Introduction to Carbon Nanotubes

Since the discovery of multiwalled carbon nanotubes in 1991 by Iijima [7] and singlewalled carbon nanotubes in 1993 by Iijima's team from NEC, Japan [8] and Bethune's team from IBM, California, U.S.A. [9], the breakthrough of carbon nanotubes in last decade has been illustrated by a great number of scientific publications in multidisciplinary field. Among their remarkable properties; high tensile strength, high stability in thermal and chemical, high electrical conductivity and biocompatibility, all of these properties become important reason that carbon nanotubes to be integrated in wide variety of applications. Carbon nanotubes are nanoscale graphene cylinder covered their edge by a half of fullerene. There are two main types of carbon nanotubes which are singlewall carbon nanotubes and multiwall carbon nanotubes. Singlewall carbon nanotubes (SWCNTs) are a roll of monolayered graphene sheet while multiwall carbon nanotubes (MWCNTs) are several graphitic concentric layers. The diameter varies from 0.4 to 2 nm for SWCNT and from 1.4 to 100 nm for MWCNT, while their length can be reached in several micrometers [10].

Three crystallographic configurations of carbon nanotubes; zigzag, armchair, and chiral of CNTs (Figure 2.2(a)) depend on how the graphene sheet is rolled up. These groups are determined by the chiral vector which received by the equation (1)

$$Ch = n\hat{a}_1 + m\hat{a}_2 \dots\dots\dots (1)$$

Where  $\hat{a}_1$  and  $\hat{a}_2$  are unit vectors in the two dimensional hexagonal lattice, and  $n$  and  $m$  are integers. Another important factor is the chiral angle (Figure 2.2(b)), which is the angle between  $Ch$  and  $\hat{a}_1$ . When  $n = m$  and the chiral angle is 30 degrees, it is known as an armchair type. When  $n$  or  $m$  is zero and the chiral angle is equal to zero, the nanotube is known as zigzag. Chiral nanotubes are formed when the chiral angles are ranged between  $0^\circ$  and  $30^\circ$ .

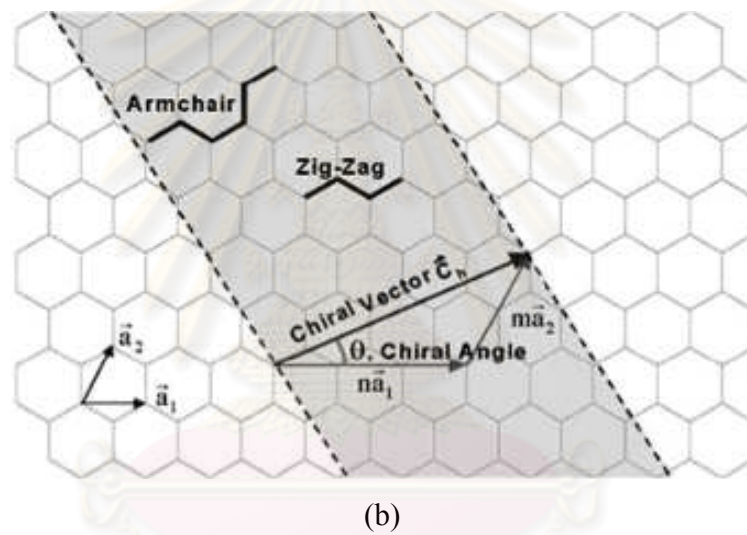
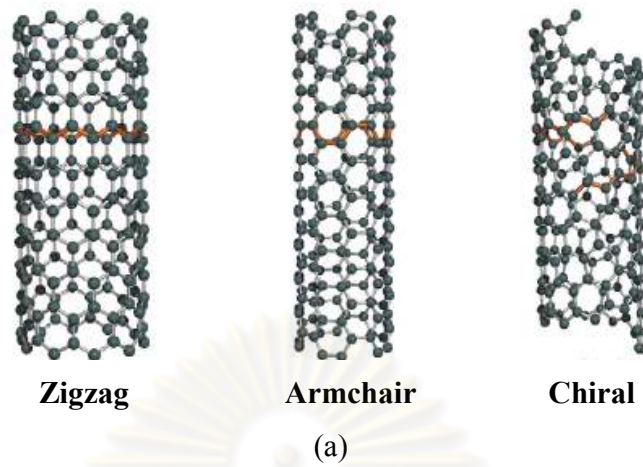


**Figure 2.2** (a) Crystallographic configurations of CNTs [11], (b) Direction of rolled hexagonal sheet of graphite to form a CNT [12].

In addition, radius of carbon nanotube can be calculated follow equation (2)

$$R = \frac{Ch}{2\pi} \dots\dots\dots(2)$$

$R$  = radius of carbon nanotube,  $Ch$  = Chiral vector

Diameter of carbon nanotube can be calculated follow equation (3)

$$D = \frac{c}{\pi} \dots\dots\dots(3)$$

$D$  = diameter of carbon nanotube,  $c$  = circumference

Length of chiral vector can be calculated follow equation (4)

$$C = |Ch| = a\sqrt{(n^2 + nm + m^2)} \dots\dots\dots(4)$$

$C$  = Length of chiral vector,  $a$  = length of unit vector,  $n, m$  = integer

Length of unit vector can be calculated follow equation (5)

$$a = |\hat{a}_1| = |\hat{a}_2| = a_{cc}\sqrt{3} \dots\dots\dots(5)$$

$a_{cc}$  = 0.1421 nm (bond length of C-C)

$a$  = 0.1421x1.732 = 0.2411nm

Chiral angle which is the angle between Ch harvest zigzag C-C bond can be calculated follow equation (6)

$$\theta = \tan^{-1}\left(\frac{m\sqrt{3}}{m+2n}\right) \dots\dots\dots(6)$$

$n, m$  = integer

The unique electrical property of carbon nanotubes which is an important parameter should also be considered that which the crystallographic configuration of carbon nanotubes was provided metallic carbon nanotube and semiconductor carbon nanotube. It's depend on the difference of integer of unit vector as follow,

$$|n-m| = 3q \quad \text{metallic - armchair}$$

$$|n-m| = 3q \pm 1 \quad \text{semiconductor - zigzag}$$

$q$  = integer 0,1,2,3...

Intershell spacing of multiwall carbon nanotubes can be calculated (7).

$$D = 0.344 + 0.1 \exp\left(\frac{-c}{4\pi}\right) \dots\dots\dots(7)$$

$D$  = intershell spacing of MWCNTs,  $c$  = circumference

## 2.2 Carbon nanotubes synthesis

### 2.2.1 Electric Arc Discharge technique

The most widely used technique to produce nanotubes is the electric arc discharge (Figure 2.3). The synthesis is performed in a water-cooled reaction chamber first evacuated and then filled with an inert gas atmosphere (helium or argon, 660 mbar). Two graphite rods are used as electrodes: one is fixed while another one can be moved by a translation mechanism. The mobile electrode (the anode) is moved towards the cathode until the distance between them is less than 1 mm that a current (100 A) passes through the electrodes and plasma is created between them. The average temperature in the inter-electrode plasma region is extremely high (of the order of 4000 K) and therefore the carbon is sublimated and the positive electrode is consumed. In order to maintain the arc between the electrodes, the anode has to be continuously translated to keep a constant distance between the rods.

The deposit consists of a hard grey outer shell and a soft fibrous black core. The outer hard shell is formed of nanoparticles and MWCNTs fused together whereas the core contains about one-thirds polyhedral graphitic nanoparticles and two-thirds MWCNTs. To synthesize SWCNTs, the electrodes are doped with a small amount of metallic catalyst particles. Among the two methods, the arc discharge has the advantage of being much cheaper than the laser ablation method [13, 14].

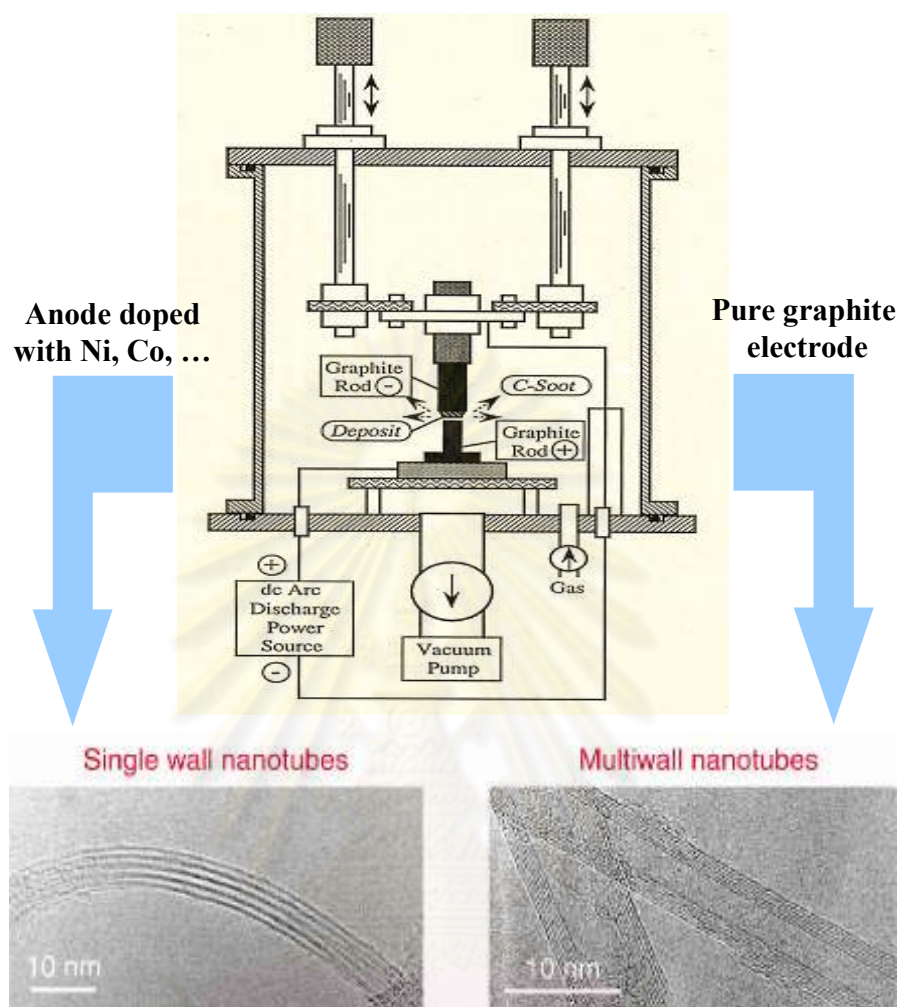


**Figure 2.3** Arc discharge apparatus produced the first carbon nanotubes[15,16]

### 2.2.2 Laser Ablation Technique

The laser ablation technique (Figure 2.4) operates at similar conditions to arc discharge. Both methods use the condensation of carbon atoms generated from the vaporization of graphite targets. Also, SWCNTs are formed when graphite targets containing catalyst. Such as Ni, Co, Pt, are vaporized by a laser. The graphite target is placed in a quartz tube surrounded by a furnace (at 1,200 °C).

A constant gas flow (Ar or He) is passed through the tube in order to transfer the soot generated to a water-cooled Cu collector. The SWCNTs usually condense as ropes



or bundles consisting of several individual SWCNTs. By products such as amorphous carbon or encapsulated metal catalyst particles are also present. When just a pure graphite target is used, MWCNTs are found only. These nanotubes are formed with 4 to 24 graphitic layers and their length can reach 300 nm. The laser ablation technique favors the growth of SWCNTs, while MWCNTs are usually not generated with this method. A disadvantage of this method is that it requires expensive lasers [13, 14].

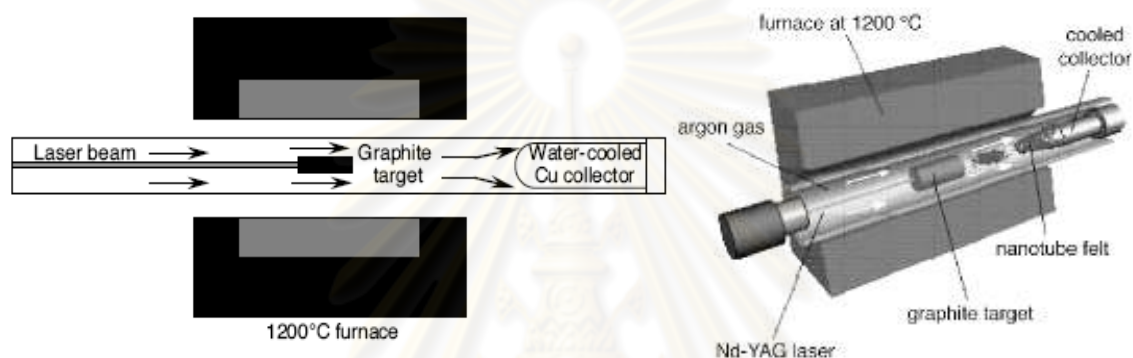


**Figure 2.4** Laser ablation apparatus for producing carbon nanotubes[13,17].

### 2.2.3 Chemical Vapor Deposition Technique

Most of chemical vapor deposition (CVD) method uses methane, carbon monoxide, ethylene, or acetylene as the carbon feedstock, and the growth temperature is typically in the range of 823-1023 K. Iron, Nickel, or Cobalt nanoparticles are often used as the catalysts. In the CVD process growth as shown in Figure 2.5 involves heating a catalyst material to high temperature in a tube furnace using a hydrocarbon gas pass through the tube reactor over a period of time. The basic mechanism in this process is the dissociation of hydrocarbon molecules catalyzed by the transition metal and saturation of carbon atoms in the metal nanoparticle. Precipitation of carbon from the metal particle leads to the formation of tubular carbon solid.

This process has two main advantages: the nanotubes are obtained at much lower temperature, although this is at the cost of lower quality, and the catalyst can be deposited on a substrate, which allows for the formation of novel structures [12-14].

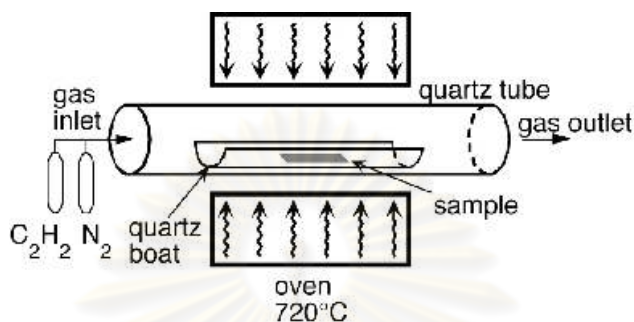


**Figure 2.5** Carbon nanotubes synthesis using chemical vapor deposition technique[16].

### 2.3 Surface modification of carbon nanotubes

According to the van der Waals force between nanotubes surface, carbon nanotubes tend to aggregate to each other as a bundle. Therefore, this major problem lead carbon nanotubes hardly dispersed in any kind of solvent and induced the next problem which was how to disperse carbon nanotubes before applying in any application. The necessary properties of carbon nanotubes and even the other nanomaterials were provided the high specific surface area and their individual unique property. The surface modification of carbon nanotubes were the important solution to overcome this problem by reducing the van der Waals force of intertubes for improving their dispersion and provide the ionic functional groups on nanotube surface for improving their stability in aqueous solution. From the relevant literatures, there have been proposed two main approaches for modifying carbon nanotubes surface; *i*) noncovalent and *ii*) covalent surface modification. To provide a wide variety of functional groups on carbon nanotubes surface, covalent surface modification were the impact method for dispersion and stability improvement. However, the disadvantages of this technique are that the abundant of conjugated bond which were the important for the electronic property of carbon nanotubes, were loose during the favor chemical reaction on nanotubes surface.

While the noncovalent surface modification still provided the carbon nanotubes integrity using polymer, surfactant, biomolecules base on the interaction as electrostatic, hydrogen bonding, hydrophobic, and even van der Waals. However, the noncovalent surface modification still provide the weak interaction between the dispersing species and carbon nanotubes surface when compare with covalent surface modification, it's possible to loose their stability when the condition were not suitable.

### 2.3.1 Noncovalent surface modification

Several ways of dispersion have been explored and can be basically divided in two main approaches. One procedure consists on the noncovalent modification of CNTs with surfactant, nucleic acid, peptides, and polymers. The noncovalent interactions are based on van der Waals, hydrophobic and  $\pi$ - $\pi$  stacking interactions. The advantage of this method is the preservation of the electronic structure of CNTs surface.

*Chengguo Hu et al.* [18] demonstrated a new noncovalent approach for the dissolution and exfoliation of SWNTs in water by a rigid, planar and conjugated diazo dye, Congo red (CR). The mixture of SWNTs and CR can be dissolved in water with a solubility as high as 3.5 mg/ml for SWNTs. High-resolution transmission electron microscope images showed that the SWNTs bundles were efficiently exfoliated into individual SWNTs or small ropes. The pi-stacking interaction between adsorbed CR and SWNTs was considered responsible for the high solubility.

Individual single-walled carbon nanotubes (SWNTs) have been suspended in aqueous media using various anionic, cationic, nonionic surfactants and polymers were reported by *Valerie C. Moore et al.* [19]. The surfactants are compared with respect to their ability to suspend individual SWNTs and the quality of the absorption and fluorescence spectra. For the ionic surfactants, sodium dodecylbenzene sulfonate (SDBS) gives the most well resolved spectral features. For the nonionic systems, surfactants with higher molecular weight suspend more SWNT material and have more pronounced spectral features.

*Junping Zhang et al.* presented their work that focuses on manipulating the dispersion of pristine CNTs with a series of versatile derivatives of chitosan (CTS) by

using  $pH$  as a stimulus [20]. Derivatives of CTS could be used to disperse CNTs homogeneously while endowing them with biocompatibility and maintaining their intact electronic structure. The substitution degree of CTS derivatives could also be used to manipulate the dispersion of CNTs more specifically.  $pH$  sensitivity of the CTS/CNTs, CMCTS/CNTs and NSC/CNTs systems as well as completely homogeneous dispersion of CNTs by using HACC may open new possibilities for using CNTs for various biomedical applications.

Moreover, polyelectrolyte multilayers can be immobilized onto carbon nanotubes via electrostatic interaction by Layer-by-Layer technique to disperse carbon nanotubes. *Decher et al.* have developed a new technique for the preparation of polymer thin film from polyelectrolyte solution by Layer-by-Layer technique or electrostatic self-assembly technique (ESA) [21]. The principle of this technique can be summarized as follow. A substrate is successively dipped in dilutes solution of oppositely charged polyelectrolyte leading to a Layer-by-Layer deposition mode. Each adsorption step leads to a reversal of the charges allowing the deposition of the next layer until it becomes polyelectrolyte multilayer thin films (PEMs) [22]. PEMs have been fabricated using mainly electrostatic attraction as the driving force for multilayers. There are many other interactions that have been used successfully for multilayers deposition such as donor-accepter interaction, hydrogen bonding, covalent bond, etc. *Agata Zykwinska et al.* demonstrated that a new general procedure for carbon nanotube modification based on polyelectrolyte layer-by-layer assembly [23]. They demonstrated noncovalently modified surface of carbon nanotubes by layer-by-layer deposition with synthetic polyelectrolytes. The thickness of the adsorbed polyelectrolyte layers increases linearly with the bilayers number up to reach 6 nm. The adsorbed polyelectrolyte layers were used as anchoring ones to subsequently graft a natural biopolymer. This opens the promising way to design new biodevices based on carbon nanotubes. *Alvaro Carrillo et al.* described a strategy for functionalizing graphite and carbon nanotube surfaces with multilayered polymeric films [24]. Poly(amphiphiles) adsorb noncovalently onto these surfaces from aqueous solutions, due to hydrophobic interactions. The covalent attachment of a second polymer layer to this initial adsorbed layer results in the formation of a cross-linked polymer bilayer; additional layers can be deposited by the covalent or electrostatic attachment of

polyelectrolytes. They used these multilayered polymer films to mediate the attachment of gold nanoparticles to graphite, single-walled nanotube (SWNT), and multiwalled nanotube (MWNT) surfaces. This approach provides a convenient method for attaching other nanostructures, biological molecules, or ligands to carbon nanotubes.

### 2.3.2 Covalent surface modification

Another approach is based on CNTs covalent functionalization. First, CNTs are cut and oxidized to generate a certain number of carboxylic groups subsequently dramatized with different types of molecules. Alternatively, CNT side walls can be directly functionalized by addition reactions.

*Maxim N. Tchoul et al.* demonstrated that oxidation of single-walled carbon nanotubes (SWNTs) with nitric acid increases their dispersability in water, methanol, and N,N-dimethylformamide [25]. The dispersability of all types of nanotubes increased substantially after 1 hr of sonication and after 2-4 hr of reflux. Longer treatments resulted in little further improvement in dispersability and at reflux degraded the SWNTs. Concurrent with improved dispersability, oxidation resulted in smaller diameters and shorter lengths show mostly bundles rather than individual tubes. Functionalization of carbon nanotubes via 1,3-dipolar cycloadditions was demonstrated by *Nikos Tagmatarchis and Maurizio Prato* [26]. The organic functionalization of carbon nanotubes has opened new avenues with opportunities to fabricate novel nanostructures by improving both their solubility and processibility. The 1,3-dipolar cycloaddition of azomethine ylides onto carbon nanotube (CNT) networks may play a relevant role towards this direction. CNT-based materials have been synthesized possessing differently functionalized solubilizing chains and hold strong promise as useful building blocks for the construction of novel hybrids for nano- and bio-technological applications.

## 2.4 Theory of Layer-by-Layer self assembly

### 2.4.1 Definition and general description of polyelectrolyte [27]

The term “polyelectrolyte” (PEL) is employed for polymer systems consisting of a macroion i.e., a macromolecule carrying covalently bound anionic or cationic groups, and low molecular “counterions” securing for electroneutrality. Example of an anionic and a cationic polyelectrolyte (PEL) are presented in Figure 2.6.

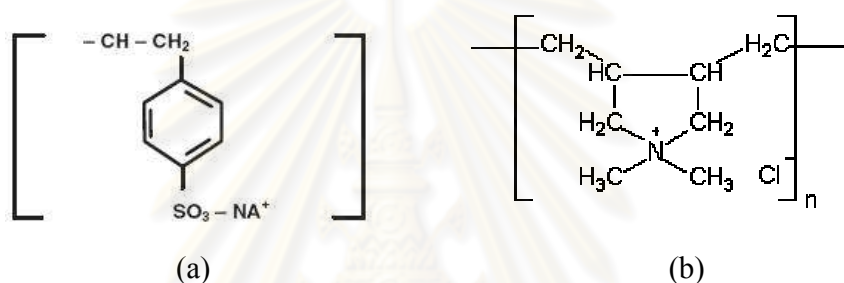


**Figure 2.6** Chemical structure of (a) sodium poly(styrene sulfonate) and (b) poly(diallyldimethylammonium chloride).

Both Na-polystyrene sulfonate and poly(diallyldimethylammonium chloride) are dissociated into macroion and counterion in aqueous solution in the total  $pH$  range between 0 and 14. Also polymers like poly(acrylic acid) and poly(ethylene imine) are usually classified as polyelectrolytes, in spite of the fact that they form a polyion-counterion system only in a limited  $pH$  range, and remain as an undissociated polyacid in the acid range or undissociated polybase in the alkaline range, respectively (Figure 2.7 (a), (b)), a behavior typical for weak polyelectrolytes (Figure 2.7 (c), (d)) and quite analogous to weak low molecular electrolytes.

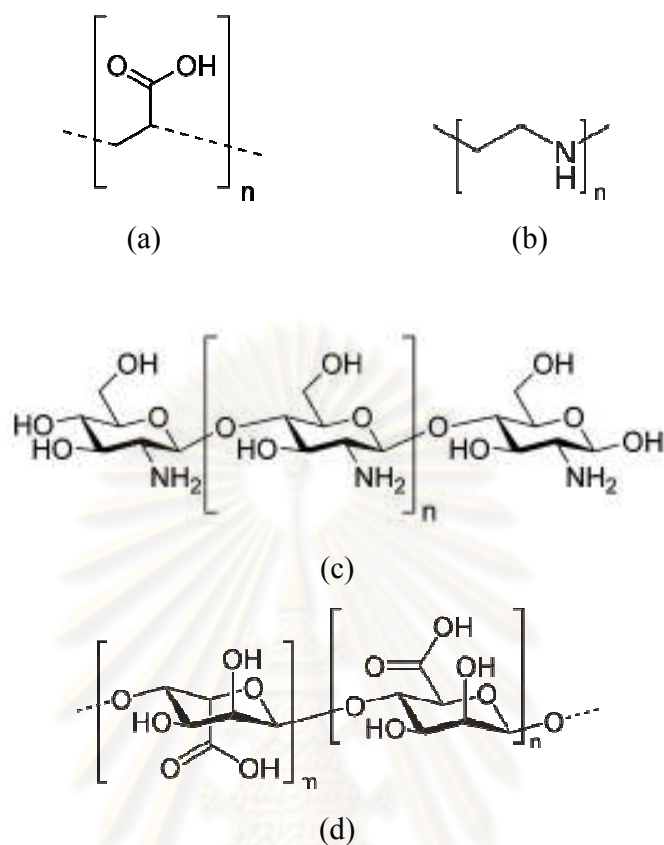


**Figure 2.7** Chemical structure of the weak synthetic polyelectrolytes (a) poly(acrylic acid) and (b) poly(ethyleneimine) and weak natural polyelectrolytes (c) chitosan and (d) alginate.

A special case of polyelectrolytes, the “polyampholytes,” carrying both anionic and cationic groups covalently bound to the macromolecule, are presented in nature by an abundant number of proteins but can also be obtained by various synthetic routes.

In principle, any macromolecular chemical structure can be transformed into a polyelectrolyte structure by covalently attaching a reasonable number of ionic groups to the polymer backbone, with linear or branched macromolecules at a compound soluble in an aqueous medium of appropriate  $pH$  after introducing a sufficient number of ionic groups.

Today’s commercial polyelectrolytes are predominantly obtained by a polymerization, polycondensation, or polyaddition process. Also numerous important

PEL also originate from nature, such as gelatin, as a representative of the widespread class of proteins or pectins belonging to the group of anionic polysaccharides. Furthermore, some PEL of practical importance result from a chemical modification of nonionic natural polymers such as cellulose or starch.

In contrast to the huge variability of the polymer backbone structure, the number of different chemical structures of anionic or cationic sites responsible for the peculiar behavior of PEL in solution is rather small (Table 2.1)

**Table 2.1** Structures of ionic sites of polyelectrolyte.

Cationic groups	Anionic groups
$-\text{COO}^-$	$-\text{NH}_3^+$
$-\text{CSS}^-$	$=\text{NH}_2^+$
$-\text{OSO}_3^-$	$\equiv\text{NH}^+$
$-\text{SO}_3^-$	$-\text{NR}_3^+$
$-\text{OPO}_3^{2-}$	

These ionic groups are usually classified as anionic and cationic; a further subdivision into weakly and strongly acid and basic groups is reasonable in analogy to “strong” and “weak” acids and bases of low molecular chemistry with the sulfonate, the sulfonate-half ester, and the tetraalkylammonium group being representative for the so-called “strong PEL.”

Besides the acid or base strength of the ionic site, the average distance between the adjacent anionic or cationic charges along the polymer chain is a decisive parameter determining PEL behavior, especially in the dissolved state. This charge carrier density or charge density is defined as the average distance between ionic sites, taking into account chain bond geometry, or as the average number of ionic sites per monomer unit in the case of copolymers, with the latter definition yielding comparable data only within the same class of copolymer with an ionic component. Besides this average charge density, the regularity of distribution of ionic sites along the chain can also influence PEL properties significantly, for example, with regard to solubility. As a rule, typical PEL



behavior can be expected if more than 1 ionic site per 10 monomeric units is present in a copolymer.

#### **2.4.2 Formation of polyelectrolyte multilayer thin films**

Polyelectrolyte multilayer films created via Layer-by-Layer (LbL) deposition are currently used to modify the surface properties of materials. These polyelectrolyte based films are capable of self-organization. The self-organization process of polyelectrolyte films, also referred to as electrostatic self-assembly (ESA), has been well documented over the past ten years.

Starting in the early 1990s, Decher's group began work on the realistic method for the ESA of nanolayers over charged substrate. The process developed by Decher has increased in popularity since its introduction. This is a result of the method's simplicity and the fact that polyelectrolytes as well as charged nano objects can be deposited in a controlled manner. Biological compounds, conducting and light emitting polymers, and dyes have also been deposited onto suitable substrates via ESA.

The LbL process is based on the alternating adsorption of charged cationic and anionic species. The process begins by properly charging a substrate. The charged substrate is then primed by adsorbing a layer of a polyelectrolyte with an opposite charge sign to that imparted to the substrate. Once the substrate is primed, it is then dipped into a solution of a counterion polyelectrolyte. A rinse step is included between the two adsorption processes to remove excess as well as to prevent cross-contamination of the polyelectrolyte solutions. These simple steps complete the LbL deposition of the nanolayers. Multiple layers can be created by simply dipping the substrate in alternating anionic and cationic baths [28].

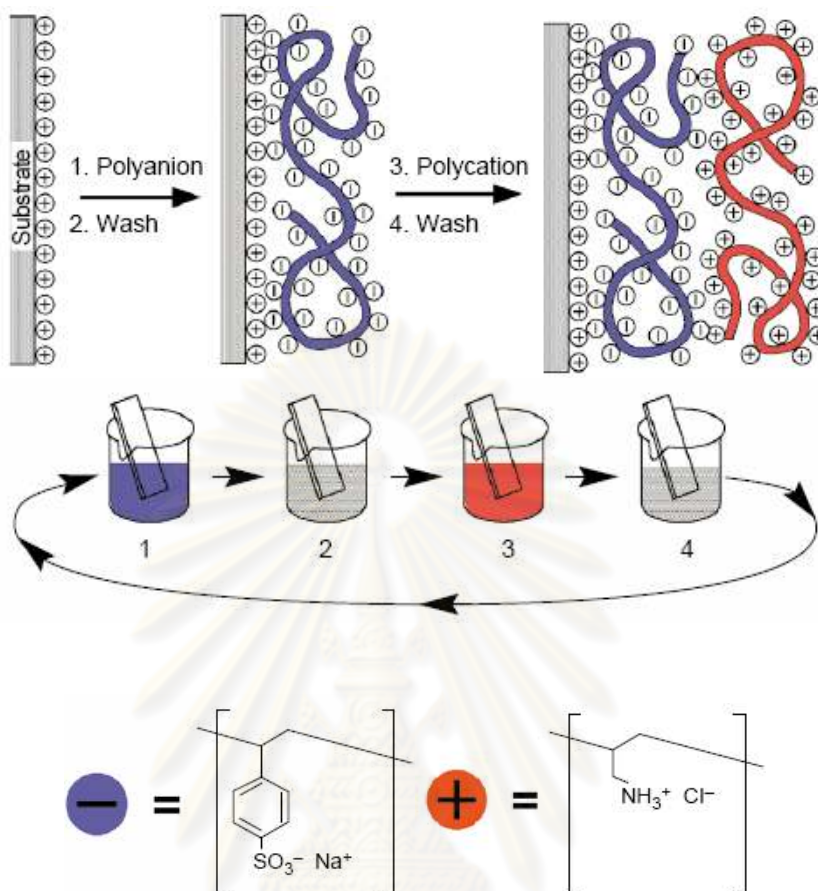


**Figure 2.8** Schematic of the electrostatic self-assembly (ESA) [21].

From Figure 2.8 top: Simplified molecular concept of the first two adsorption steps depicting film deposition starting with a positively charged substrate. The polyanion conformation and layer interpenetration are an idealization of the surface charge reversal with each adsorption step which is the basis of the electrostatically driven multilayer build up depicted here. Counterions are omitted for clarity. Figure 2.8 Bottom: Schematic of the film deposition process using glass slides and beakers. Steps 1 and 3 represent the adsorption of a polyanion and polycation respectively, and steps 2 and 4 are washing steps. The four steps are the basic buildup sequence for the simplest film architecture  $(A/B)_n$  where  $n$  is the number of deposition cycles. The construction of more complex film architectures requires additional beakers and an extended deposition sequence.

Therefore, Layer-by-layer technique is the most versatile and facile approach based on electrostatic self-assembly between oppositely charged polyelectrolytes [29]. This technique can produce the multilayers thin film on any shape, any size and any substrate as shown in Figure 2.9.

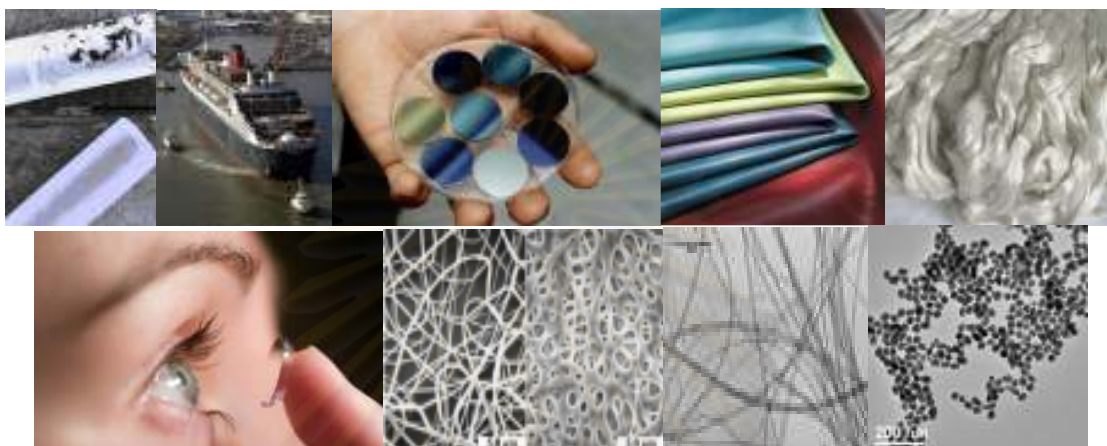


**Figure 2.9** Variety of substrates for deposition polyelectrolyte multilayers via layer-by-layer technique.

### 2.4.3 Parameters controlling the growth of PEM [30]

The parameters controlling the growth of PEM were studied because there are important for the multilayer formation.

#### 2.4.3.1 Type of polyelectrolyte

The type of polyelectrolyte affects the total thickness. For instance, the multilayer thickness increases in the order: poly (acrylamide sulfonate)/poly (diallyldimethylammonium chloride) (PAMS/PDADMAC) < poly (styrene sulfonate) /poly (allylamine hydrochloride) (PSS/PAH) < PSS/PDADMAC. All these polyelectrolytes are flexible. The intrinsic persistence length for PSS, PAMS and PAH is similar (approx. 1 nm) while the intrinsic persistence length of PDADMAC is slightly

higher. Therefore the chain stiffness cannot be the only reason for the differences in multilayer thickness. It is assumed that the balance between hydrophobicity and hydrophilicity of the polyelectrolytes plays an important role for the thickness. While PSS has a hydrophobic backbone and is not water soluble below a degree of charge of 0.33 even the neutral PAMS is water soluble.

The type of multilayer growth depends also on the type of polyelectrolytes. The thickness of PSS/PAH multilayers increases linearly with the number of deposition cycles, while the thickness of PSS/PDADMAC multilayers increases linearly or exponentially depending on the charge density of PDADMAC. The exponential growth is related to a higher surface roughness and internal roughness than in the case of linear growth [31].

#### **2.4.3.2 Effect of polymer charge density**

A minimum charge density is required for the formation of multilayers. Below this charge threshold the charge reversal is not sufficient. In the case of strong polyelectrolytes the charge density is varied by changing the chemical structure. For instance, a PSS/PDADMAC multilayer can be built up at polycation charges  $\geq 70\%$ . Above this threshold the charge density does not affect the polymer density (electron density between 0.374 and 0.393  $\text{Å}^{-3}$ ) [32].

Not only the average charge density, but also the distribution of the charges along the chains plays an important role for building up multilayers. The adsorption of block-copolymers showed that a short strongly charged block (10–20% of the total number of monomer units per chain) is sufficient for the formation of multilayers, even if the average charge density is below the charge threshold that is required for multilayer formation [33].

#### **2.4.3.3 Influence of ionic strength**

The total multilayer thickness can be controlled with angstrom precision by adding salt to the aqueous polyion solutions. Due to the screening of the charges along

the polyelectrolyte chains the polymer molecules are more entangled with increasing salt concentration. The results are in a larger thickness and a stronger internal and external roughness of the adsorbed layers. The increase in thickness  $d$  is proportional to  $IB$  ( $I$ : ionic strength). Most of the studies in the literature report an exponent  $B$  of the salt dependence between 0.5 and 1 for different polyelectrolytes. *Lošche et al.*, showed by neutron reflectivity that the thickness of a layer pair (PSS/PAH) varies linearly with the ionic strength of the dipping solutions in the concentration range 0.5–3 mol/l NaCl additive [34]. At low ionic strength, i.e. below 0.5 mol/l NaCl, a deviation from this linear behavior towards an  $I^{0.5}$  dependence is stated. The latter behavior is also reported by other groups against air or water. Above a salt concentration of 1 mol/l the thickness increase is less pronounced, but nevertheless,  $d$  increases up to a concentration of 3 mol/l.

PSS/PDADMAC multilayers increases proportional to  $I$  or  $I^{0.5}$  depending on the PDADMAC charge density.

Beside the segment–segment repulsion also the attraction between the polyelectrolyte and the oppositely charged interface is screened. Therefore, one would expect a decrease of adsorbed amount at high ionic strength. For some systems, as, e.g. PAMS/PDADMAC or PSS/PDADMAC, this decrease has been observed, but the thickness of PSS/PAH multilayers increases even above an ionic strength of 1 mol/l. There seems to be a paradox: On one hand a minimum polymer charge density is required to form multilayers, on the other hand multilayers can be built up at high ionic strength where the electrostatic interactions are screened. These results indicate that macroscopic mean field theories like the *Gouy Chapman* theory do not describe the multilayer formation at high ionic strength. Two other explanations for the adsorption of polyelectrolytes are possible: Firstly, beside enthalpy contributions also the gain in entropy plays an important role due to the release of counterions during multilayer formation. Furthermore, charge (or ion) fluctuations near the surface should be taken into account. They make the surface ‘visible’ for the oppositely charged polyelectrolyte despite of (mean field) screening.

## 2.5 Layer-by-layer surface modification of carbon nanotubes

An interesting issue for noncovalent surface modification of carbon nanotubes was layer-by-layer deposition technique. The coating CNTs with polyelectrolyte from this technique provided a wide variety of ionic functional groups on CNT surface lead to obtain high dispersion efficiency and their stability in aqueous solution. In 2004, *Bumsu Kim et al.* [35] were successfully functionalized carbon nanotubes with gold nanoparticle composites. Treated carbon nanotubes were deposited with cationic polyelectrolyte; poly(diallyldimethylammonium chloride) alternate with anionic polyelectrolyte; polystyrene sulfonate for bilayers. *Alexander B. Artyukhin et al.* [36] has been reported noncovalent surface modification of carbon nanotubes by deposit the primer layer as pyrene ionic derivative. PDADMAC and PSS were used to alternately deposit on the modified carbon nanotubes. *Hao Kongfor et al.* [37] were proposed preparation, characterization and layer-by-layer self-assembly of polyelectrolyte-functionalized multiwall carbon nanotubes. The results confirmed that multiwall carbon nanotubes have a high efficiency loading polyelectrolytes by the layer-by-layer approach as shown in Figure 2.10 and Figure 2.11.

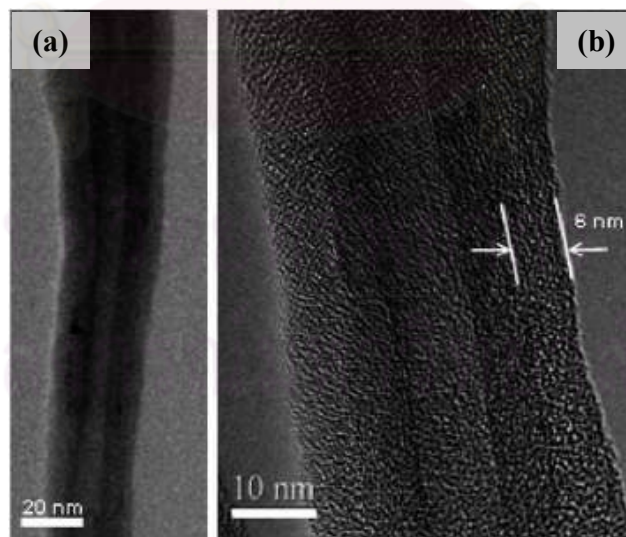


**Figure 2.10** TEM image of coating multiwall carbon nanotubes with polyelectrolyte [37].

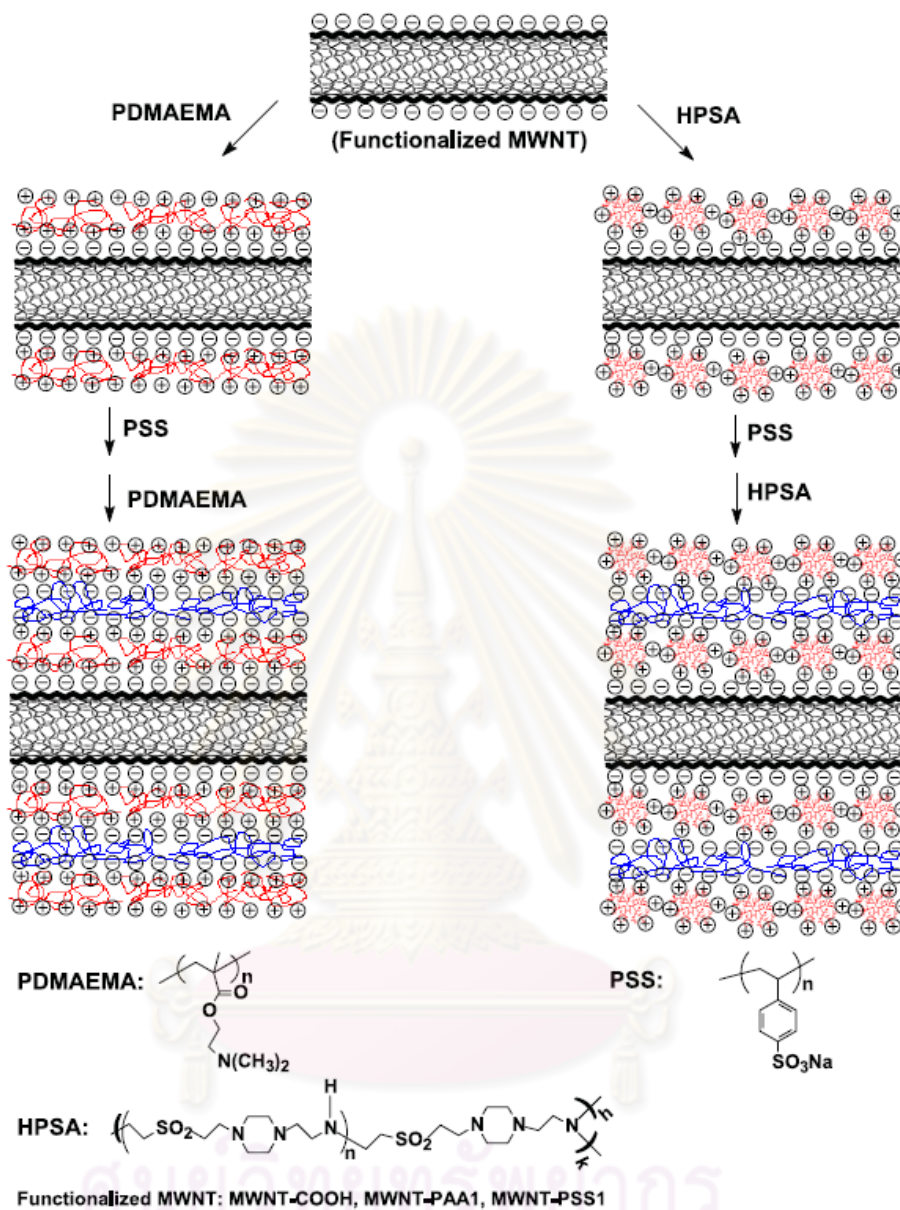


**Figure 2.11** Representative the deposition of PDMAEMA, PSS, and HPSA [37].

To apply coating carbon nanotubes with polyelectrolyte multilayers on their surface, there are many application. *Lijun Liu et al.* [38] found that water-soluble multiwall carbon nanotubes coating poly(allylamine hydrochloride) were successfully coated as bionanomultilayers with a model enzyme; horseradish peroxidase (HRP) by layer-by-layer technique as shown in Figure 2.12 The bionanomultilayers were

constructed as highly sensitive phenolic biosensor which having the detection limit of 0.6  $\mu\text{M}$ . Therefore, the developed bionanomultilayer biosensor exhibited a fast, sensitive, and stable detection.

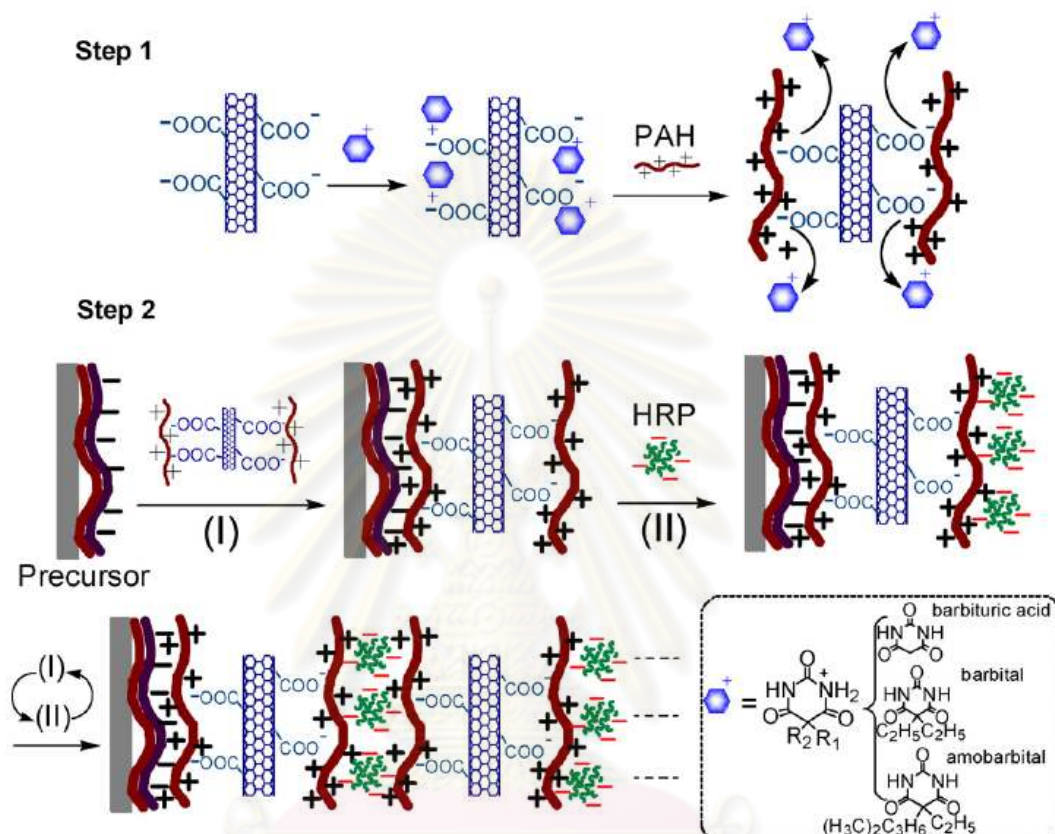


**Figure 2.12** The process of solubilizing PAH-MWCNTs and assembly bionanomultilayers on PAH-MWCNTs [38].

*Sai Bi et al.* [39] found that treated multiwall carbon nanotubes were coated with many ingredients; poly(diallyldimethyl ammonium chloride) (PDPA), horseradish peroxidase, alpha phetoprotein, and alpha phetoprotein primary and secondary antibody via layer-by-layer technique as shown in Figure 2.13. The results showed the detection limit which was two orders of magnitude lower than standard ELISA method. Therefore, this hybrid material can be used as a biolabel for ultrasensitive chemiluminescence immunoassay of cancer biomarker.



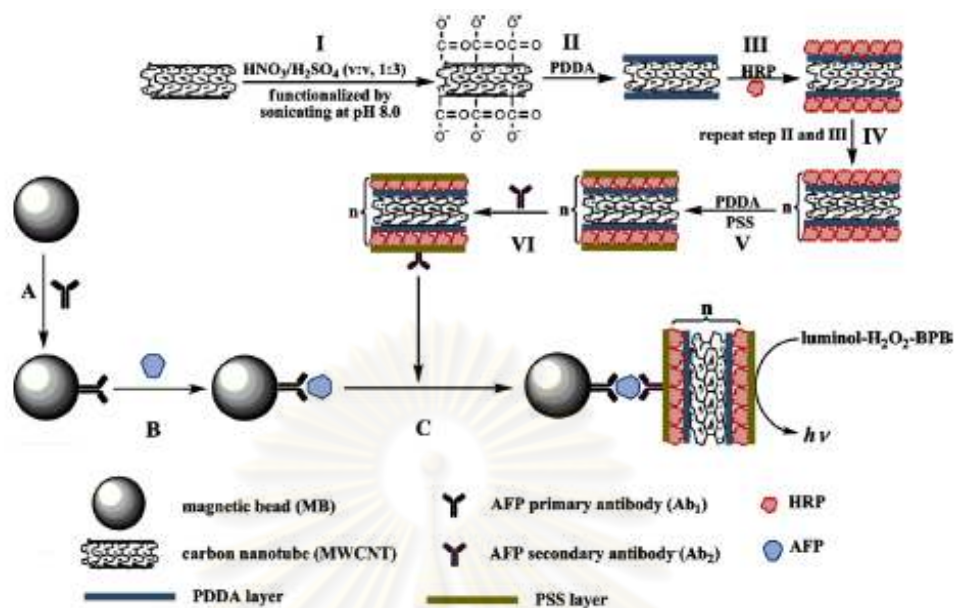


**Figure 2.13** The schematic illustration of the detection for AFP based on sandwich-type CLIA. The upper part I–V is the schematics of layer-by-layer electrostatic self-assembly of HRP on carbon nanotube template: (I) treatment of MWCNTs generating negatively charged carboxylic functionalized groups; (II) assembling of positively charged PDDA; (III) assembling of negatively charged HRP; (IV) repetition of II and III until the desired layers are obtained; (V) additional assembling of positively charged PDDA layer and negatively charged PSS layer; (VI) adsorption of AFP secondary antibody ( $\text{Ab}_2$ ) [39].

Recently, *Xiaoke Zhang et al.* [40] have been reported that treated singlewall carbon nanotubes were deposited with polysaccharides which were polycation chitosan and polyanion alginate via layer-by-layer technique. The coating carbon nanotubes were successfully controlled release anticancer drug; doxorubicin to cancer cells as shown Figure 2.14.

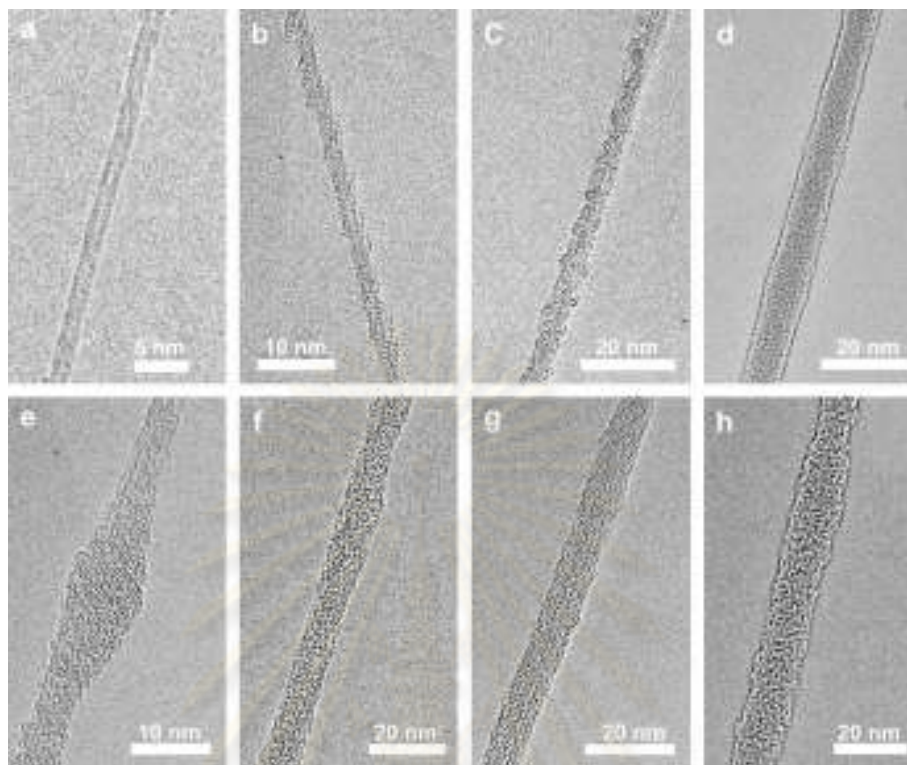


**Figure 2.14** TEM images of modified SWCNTs. (a) Cut SWCNTs, (b) Alginate-SWCNTs, (c) Chitosan-SWCNTs, (d) Chitosan/Alginate- SWCNTs, (e) Doxorubicin-SWCNTs, (f) Doxorubicin-Alginate-SWCNTs, (g) Doxorubicin-Chitosan-SWCNTs and (h) Doxorubicin-Chitosan/Alginate-SWCNTs [40].

## 2.6 Wrapping carbon nanotubes with polymer by noncovalent surface modification: Molecular Dynamics Simulation

Molecular dynamics (MD) simulation is a specific tool used to demonstrate and understand the dynamics and thermodynamics in many fields of science (e.g. biological and material systems). They can afford molecular information that is complicated or unfeasible to achieve from experimental techniques alone. The wrapping phenomenon of modified CNTs with polymer has been proposed as a general phenomenon in both of previous theoretical and experimental publications [41, 42]. Not only synthetic polymer

but natural polymer has also been proposed wrapping phenomenon on CNT surface by the molecular dynamics simulation study.

Molecular dynamics (MD) simulations are performed on the complex amylose-nanotube system to study the mode of interaction between the initially separated amylose and SWNT fragments, which can be either wrapping or encapsulation. *Y.H. Xie et al.* [43] found that the van der Waals force is dominant and it always plays an important role in promoting non-covalent association. The influence of the size of nanotube on MD simulation is also studied. Our study illustrates that amylose molecules can be used to bind with nanotubes and, thus, favor non-covalent functionalization of carbon nanotubes.

Recently, *Yingzhe Liu et al.* [44] have been reported that carbon nanotubes coated with alginic acid through noncovalent functionalization have been shown to be soluble and dispersed in water. Alginic acid can wrap around SWCNT by virtue of van der Waals attractions and organize into a compact helical structure, a process induced in the gas phase by hydrogen-bonding interactions. In contrast, in an alginate aqueous solution, a loose helical wrapping mode is found to be favored by virtue of electrostatic repulsions in conjunction with the weakening of hydrogen-bonding interactions. This work shed meaningful light on the potential of noncovalent functionalization for solubilizing carbon nanotubes, and open exciting perspectives for the design of new wrapping agents that are envisioned to form the basis of innovative nanomaterials targeted at chemical and biomedical applications.

## **2.7 Carbon nanotubes in drug delivery application**

The one of familiar application of modified carbon nanotubes which was put attempt to deep study was biomedical application especially drug delivery application.

The application of modified CNTs as new nanocarriers for drug delivery was apparent immediately after the first demonstration of the capacity of this material to penetrate into the cell. An important characteristic of modified CNTs is their high propensity to cross cell membranes. Two routes of internalization have been proposed. It has been found that modified CNTs penetrate following a passive diffusion across lipid bilayer similar to a “nanoneedle” able to perforate the cell membrane without causing cell

death [45]. Alternatively, when CNTs were used to deliver proteins by adsorbing them onto their external surface, they seem to be uptaken by endocytosis [46, 47].

*Alberto Bianco et al.* were successful in preparing CNTs containing both fluorescein and amphotericin B (AmB) [48]. Their studies revealed that AmB covalently linked to CNTs is taken up by mammalian cells without presenting any specific toxic effect. Modified CNTs with AmB, one of the most effective antibiotic molecules for the treatment of chronic fungal infection, are rapidly internalized by mammalian cells with a reduced toxicity in comparison to the drug administered alone. In addition, *Hongjie Dai et al.* [49] showed that the property of CNTs to adsorb near infrared irradiation was used to kill cancer cells. Pristine SWNT were wrapped with poly(ethylene glycol)(PEG) modified with a phospholipid (PL) moiety and folic acid (FA). Because tumor cell are known to overexpress folate receptors, the PL-PEG-FA/SWNTs construct was only internalized inside cancer cells, which were then destroyed by using a laser wavelength of 808 nm.

Recently, supramolecular chemistry on water-soluble carbon nanotubes for drug loading and delivery was proposed by *Hongjie Dai et al.*[50]. Water-soluble SWNTs with poly(ethylene glycol) (PEG) functionalization via these routes allow for surprisingly high degrees of  $\pi$ -stacking of aromatic molecules, including a cancer drug (doxorubicin). Binding of molecules to nanotubes and their release can be controlled by varying the pH. The strength of  $\pi$  -stacking of aromatic molecules is dependent on nanotube diameter, leading to a method for controlling the release rate of molecules from SWNTs by using nanotube materials with suitable diameter. Soluble Single-Walled Carbon Nanotubes as Longboat Delivery Systems for Platinum(IV) Anticancer Drug Design were demonstrated by *Stephen J. Lippard et al.* [51]. SWNTs tethered to substrates by disulfide linkages use the reducing environment of endosomes into which they are taken to selectively release their cargo only following cellular internalization. By combining the ability of platinum(IV) complexes that resist ligand substitution with the proven capacity of SWNTs to act as a longboat, shuttling smaller molecules across cell membranes, they have constructed a SWNT tethered platinum(IV) conjugate that effectively delivers a lethal dose of cis-[Pt(NH<sub>3</sub>)<sub>2</sub>Cl<sub>2</sub>] upon reduction inside the cell. *Balaji Panchapakesan et al.* [52] hypothesized that monoclonal antibodies that are specific to the IGF1 receptor

and HER2 cell surface antigens could be bound to single wall carbon nanotubes (SWCNT) in order to concentrate SWCNT on breast cancer cells for specific near-infrared phototherapy. SWCNT modified with HER2 and IGF1R specific antibodies showed selective attachment to breast cancer cells compared to SWCNT functionalized with non-specific antibodies. After the complexes were attached to specific cancer cells, SWCNT were excited by  $\sim 808$  nm infrared photons at  $\sim 800$  mW cm<sup>-2</sup> for 3 min. Cells incubated with SWCNT/non-specific antibody hybrids were still alive after photo-thermal treatment due to the lack of SWNT binding to the cell membrane. All cancerous cells treated with IGF1R and HER2 specific antibody/SWCNT hybrids and receiving infrared photons showed cell death after the laser excitation. Following multi-component targeting of IGF1R and HER2 surface receptors, integrated photo-thermal therapy in breast cancer cells led to the complete destruction of cancer cells.

## **2.8 Carbon nanotubes cytotoxicity: *In Vitro***

Toxicity of carbon nanotubes has been an important issue that attracted the researcher in laboratory and even in public to realize and consider advantages and disadvantages in the same time before integrating carbon nanotubes in any applications. Nowadays, carbon nanotubes's toxicity still be argued and discussed in academic research by world wide researcher because of their different results. Especially, the attempt to integrate carbon nanotubes in biomedical application such as drug carrier, toxicity and biocompatibility of carbon nanotubes was an important that should be considered as well. However, the beginning conclusion was that the toxicity of carbon nanotubes depends on factors which were size, shape, surface area, surface chemistry, solubility and impurity as a transition metal catalyst. *Kostas Kostarelos* [53] has been reported as news and views that experimental evidence to date clearly indicates that long and rigid carbon nanotubes should be avoided for in vivo applications and that chemical functionalization should be optimized to ensure adequate dispersibility, individualization, and excretion rates sufficient to prevent tissue accumulation as shown in Figure 4.15.

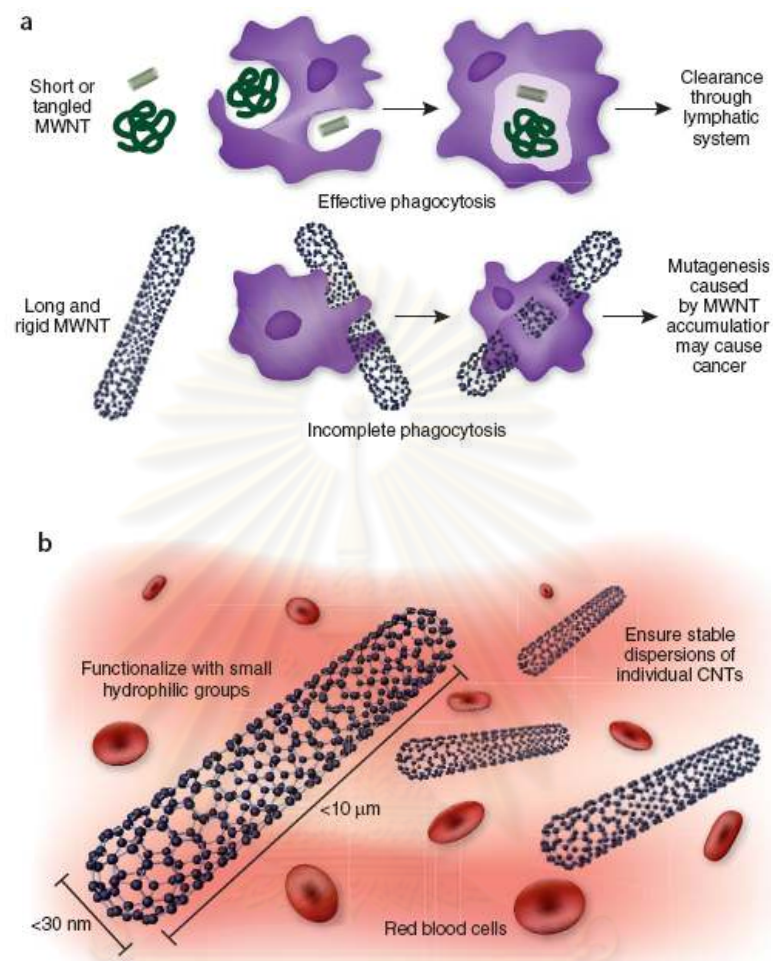


**Figure 2.15** (a) The effect of CNT structure on phagocytosis by macrophages and clearing from tissues. Whereas macrophages can engulf MWNTs with a low aspect ratio (ratio of length to width) before their clearance by draining lymph vessels, MWNTs with a high aspect ratio cannot be cleared and accumulate in tissues, where they promote carcinogenesis. (b) In addition to their dimensions, other considerations relevant to the safety of CNTs include increasing their solubility and preventing their aggregation, to facilitate urinary excretion and thereby prevent tissue accumulation [53].

*Guang Jia et al.* [54] found that the cytotoxicity of carbon nanomaterials with different geometric structures exhibited quite different cytotoxicity and bioactivity in alveolar macrophage. The cytotoxicity in vitro follows a sequence order on a mass basis: SWCNT > MWCNT > Quartz > C<sub>60</sub>.

*Christie M. Sayes et al.* [55] reported that cytotoxicity of singlewall carbon nanotubes; *In Vitro* depend on the functionalization density of carbon nanotubes surface. The modified CNT surface consist of SWNT-phenyl-SO<sub>3</sub>X (ratio of CNT/ phenyl-SO<sub>3</sub>X equal 18, 41, and 80), SWNT-phenyl-(COOH)<sub>2</sub> (ratio of CNT/ phenyl-(COOH)<sub>2</sub> equal 23) and underivatived SWNT stabilized in 1% Pluronic F108. The results showed that the degree of sidewall functionalization increases, SWCNT become less cytotoxic as shown in Figure 2.16

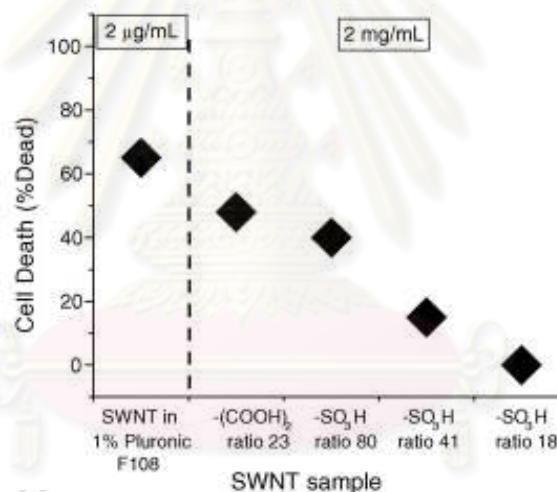


**Figure 2.16** Effect of functional groups of SWCNT on cell viability [55].

While *Alexandra Porter et al.* [56] have found that acid treated CNT were less aggregated within the cell when compared with pristine CNT. After 4 days of exposure, bundles and individual acid-treated CNT was found inside the lysosomes and cytoplasm where the caused no significant changes in cell viability or structure. *Peter Wick et al.* [57] reported that the well-dispersed carbon nanotubes effect to their cytotoxicity. Suspended carbon nanotubes-bundles were less toxic than asbestos, ropes like

agglomerated CNTs induced more cytotoxic effect than asbestos fiber at the same concentrations.

In addition, the cytotoxicity testing technique was a crucial problem as well because for cell viability test, indicator dyes such as MTT, WST-1, Neutral red, Alamar blue, and Commassie blue were needed to assess. *A. Casey et al.* [58] has been reported the indicator dyes are not appropriate for the quantitative toxicity assessment because carbon nanotubes can interact with colorimetric indicators resulted in a false positive toxic effect. *Larisa Belyanskaya et al.* [59] also reported the limit of the MTT reduction assay for carbon nanotubes-cell interaction. Improvement of carbon nanotubes suspension with polyoxyethylene sorbitan monooleate and sodium dodecyl sulfate still interfered with MTT assay as well. Therefore, the question how toxic is CNT remain unanswered and will remain uncertain until new screening techniques are developed which do not involve the use of colorimetric dye. To avoid using colorimetric dyes for cytotoxicity studies, *Eva Herzog et al.* [60] has been proposed the clonogenic assay which was the new approach for toxicity test. Employing the clonogenic assay, without any such interaction, this technique was more reliable method for in vitro cytotoxicity test which measure the colony surface area and colony number.



## CHAPTER III

### EXPERIMENTAL

#### 3.1 Chitosan synthesis

##### 3.1.1 Chemicals and Materials

Chitin extracted from shrimp and used in the synthesis of chitosan was obtained from A.N. (aquatic nutrition lab) Ltd., Thailand. Concentrated sodium hydroxide (NaOH) 50 % w/w was purchased from Vittayasom Co., Ltd., Thailand. Commercial grade ethanol was purchased from Italmar Co. Ltd., Thailand.

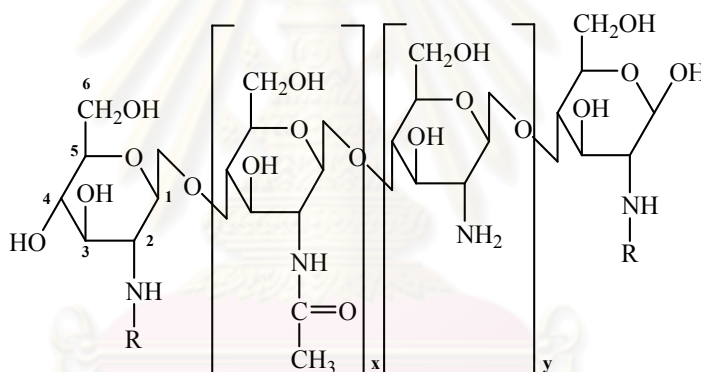


**Figure 3.1** Chemical structure of Chitosan:  $x$  = N-acetyl-D-glucosamine unit,  $y$  = D-glucosamine unit:  $x > 50\%$  = Chitin,  $y > 50\%$  = Chitosan.

##### 3.1.2 Methodology of chitosan synthesis with various degree of deacetylation

Chitosan with various degree of deacetylation (%DD) were prepared by reacting 50 g of chitin extracted from shrimp with 750 ml of concentrated sodium hydroxide (50%w/w) under constant shaking (ratio 1 g : 15 ml). Different chitosan batches of increasing %DD were obtained by varying the reaction time from 2 to 7 days at ambient temperature. The resulting chitosan powder was then filtered and rinsed with water until

obtaining neutral *pH* in the rinsed water. Thereafter, chitosan batches were rinsed with ethanol 50%, 70%, and 95% and finally air-dried. The chitosan, which was deacetylated for 7 days, was secondly deacetylated with concentrated sodium hydroxide for 3 days. The secondary deacetylated chitosan was deacetylated again with concentrated sodium hydroxide for 3 days to obtain high degree of deacetylation of chitosan. The %*DD* of each chitosan batches was measured by first derivative technique using a UV-Vis spectrophotometer (SPECORD S 100, Analytikjena). In addition, the average molecular weights of the chitosan were investigated using gel permeation chromatography.

### 3.1.3 Determination of degree of deacetylation of chitosan using first derivative UV-Vis Spectroscopy technique

First derivative UV-Vis spectroscopy technique was used to determine degree of deacetylation of resulting chitosan [61]. Chitosan powder (0.01 g) were dissolved in 0.01M diluted acetic acid 100 ml, then UV-Vis absorption spectras in term first derivative were obtained at fixed wavelength 201.4 nm by using UV-Vis spectrophotometer. %*DD* can be calculated from the equation [1] as follow,

$$\%DD = \left\{ 1 - \left\{ \frac{A}{\frac{((10 \times W) - 204A)}{161} + A} \right\} \right\} \times 100 \quad \dots\dots\dots [1]$$

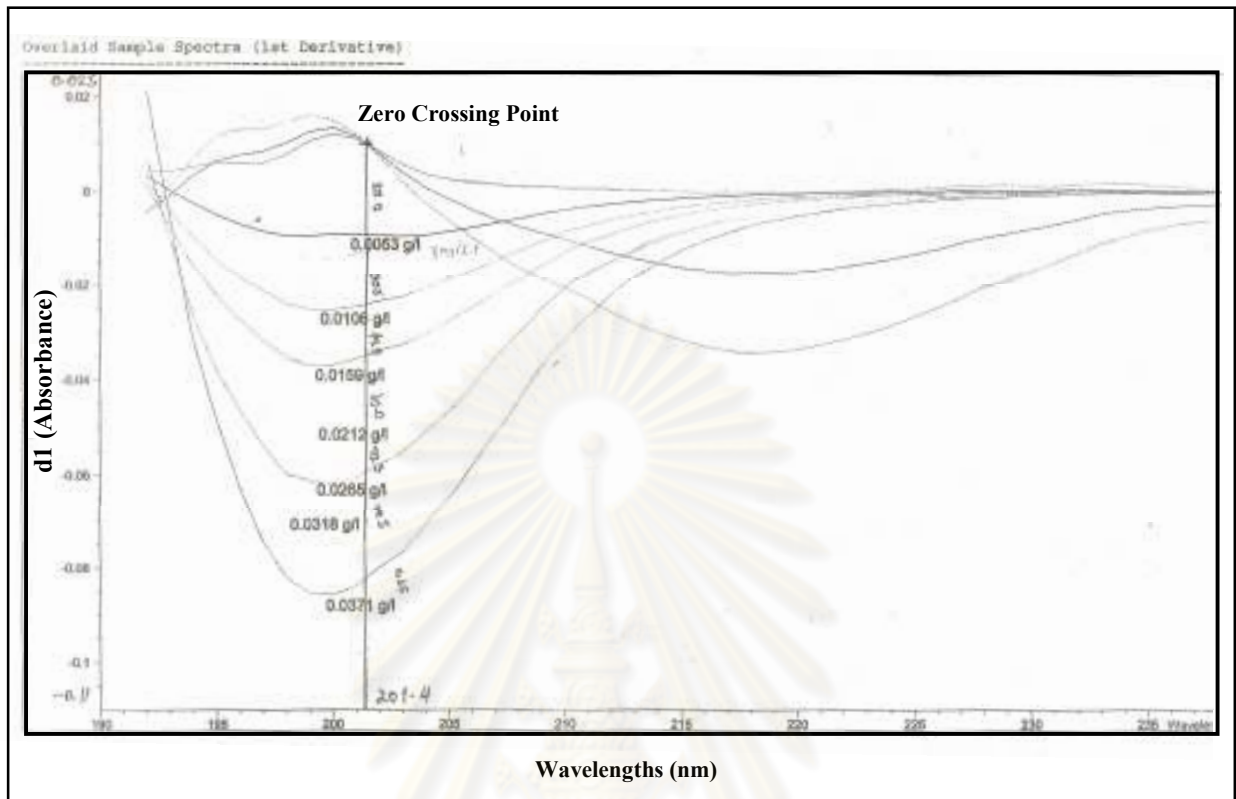
$$A = \frac{\text{Concentration of N - acetyl - D - glucosamine (g/lit)}}{204}$$

*W* = Weight of chitosan in 0.01M acetic acid

161 = Molecular weight of D-glucosamine

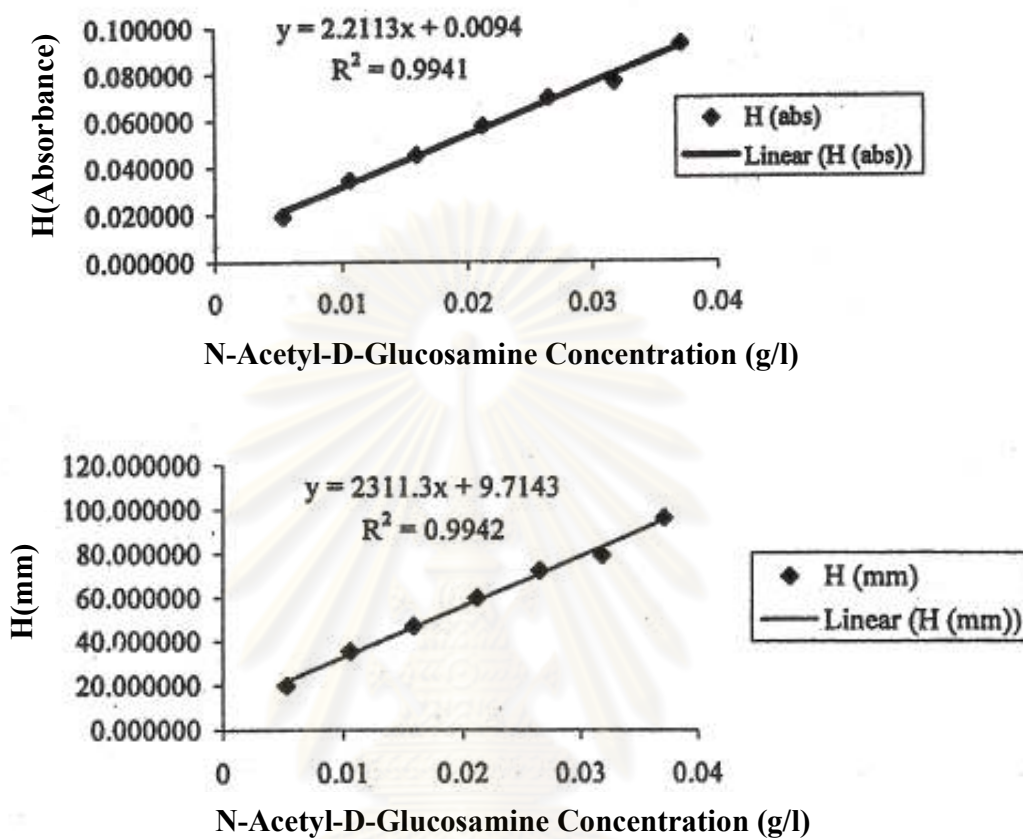
204 = Molecular weight of N-acetyl-D-glucosamine

To identify the N-acetyl-D-glucosamine in chitosan structure, the calibration curve of N-acetyl-D-glucosamine in various concentrations were prepared by plotting from first derivative absorbance spectra (Figure 3.2) at wavelength 201.4 nm as a function of N-acetyl-D-glucosamine concentration as shown in Figure 3.3.



**Figure 3.2** First derivative absorbance of N-acetyl-D-glucosamine with different N-acetyl-D-glucosamine concentrations (g/l).

ศูนย์วิทยทรัพยากร  
จุฬาลงกรณ์มหาวิทยาลัย

**Standard curve of N-Acetyl-D-Glucosamine (blank: acetic acid)**

**Figure 3.3** Calibration curve of N-acetyl-D-glucosamine in acetic acid 0.1 M with (a) Height (H) of derivative absorbance and (b) Height (H) in mm from zero crossing point as a function of the concentration of N-acetyl-D-glucosamine.

### 3.1.4 Determination of average molecular weight of chitosan using gel permeation chromatography (GPC Waters 600E)

**Table 3.1** Gel Permeation Chromatography test condition.

Types	Condition
Eluent	Acetate buffer pH~4
Flow rate	0.6 ml/min
Injection volume	20 $\mu$ l
Temperature	30 $^{\circ}$ C
Column set	Ultrahydrogel linear 1 column (MW resolving range 1,000-20,000,000) 1 column + guard column Standard pollulans (MW 5,900-788,000)
Calibration method	Polysaccharide standard calibration
Detector	Refractive Index Detector

#### 3.1.4.1 Sample preparation

Chitosan with different degree of deacetylation (61, 70, 78, 84, 90, and 93%DD) 2 mg/ml were dissolved in eluent and filtered using nylon 66 membrane (pore size 0.45  $\mu$ m) before injection.

## 3.2 Effect of the degree of deacetylation of chitosan on its dispersion of carbon nanotubes

### 3.2.1 Chemicals and Materials

Multiwall carbon nanotubes with a diameter of 110-170 nm and length of 5-9 micrometer were purchased from Aldrich, Thailand. Chitosan with various degree of deacetylation (61, 71, 78, 84, 90, and 93%DD) and their molecular weight in a range of 630-530 kDa. Analytical grade glacial acetic acid was purchased from Labscan Asia Co.,

Ltd., Thailand. All chemicals and solvents were used as received without any further purification. Double distilled water was used in all experiments.

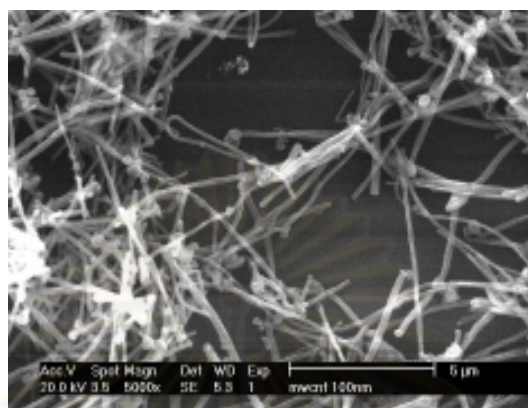


**Figure 3.4** Morphology image of pristine CNT characterized by scanning electron microscope (Phillips XL30CP), a diameter in a range of 110-170 nm and length in a range of 5-9  $\mu\text{m}$ .

### 3.2.2 Effect of chitosan concentration on the dispersion of MWCNTs

UV-Vis spectroscopy was used to determine the efficiency of the dispersion of the carbon nanotubes by turbidity measurements at 550 nm. 5 mg of MWCNT were mixed in 100 ml of a 0.01 mM chitosan solution (%DD = 61). The pH of the solution was adjusted to pH 4 with 20 mM of acetic acid. The absorbance of the solution was measured after each adjunction of chitosan until the final concentration of 10 mM chitosan was reached. In each step, the mixture was stirred and sonicated for 10 minutes using an ultrasonic bath (CREST Model 275D, USA).

### 3.2.3 Effect of sonication times on MWCNTs dispersion with chitosan

5 mg of MWCNT were mixed in 100 ml of a 5 mM chitosan solution (%DD = 61, 78 and 93). The mixture was stirred and sonicated using an ultrasonic bath with varying sonication time (15 to 150 minutes). In each period with different sonication time, the

turbidity of carbon nanotubes dispersion were determined by UV-Vis spectroscopy at wavelength 550 nm.

#### **3.2.4 Effect of %DD of chitosan on the dispersion of MWCNTs**

To evaluate the effect of the %DD on the dispersion efficiency of MWCNT by chitosan, 2.5 mg of MWCNTs were added to different solutions of chitosan having a fixed volume of 50 ml and a fixed concentration of 5 mM but increasing %DD (61, 71, 78, 84, 90, and 93%). After mixing, the MWCNT and the chitosan solutions were stirred and sonicated for 30 minutes. The absorbance at 550 nm of the pitch-black solution was then measured by using UV-Vis spectroscopy and recorded.

#### **3.2.5 Surface charge of the modified MWCNTs**

To evaluate the surface charge of each MWCNT modified with chitosan of various %DD, samples of the prepared solutions were measured with a Zetasizer (NanoZS4700 nanoseries, Malvern Instruments, UK). The samples were taken from the solutions of MWCNTs modified with 5 mM chitosan having various degree of deacetylation (61, 71, 78, 84, 93%DD) and sonicated for 10 minutes. The modified MWCNT with chitosan solution were centrifuged at 4,000 rpm for 15 minutes in order to remove the excess of chitosan. While the supernatant was removed, 25 ml acetic acid, 20 mM, was added to the remaining MWCNT and re-dispersed by vortex and sonication. The precipitation and re-dispersion step was repeated 3 times in order to remove the excess chitosan. Zeta potential of modified MWCNTs with chitosan were obtained as the average of three measurements at 25 °C.

### 3.3 Molecular Dynamics Simulation: Dispersion and separation of chitosan wrapping on SWCNTs by noncovalently modification.

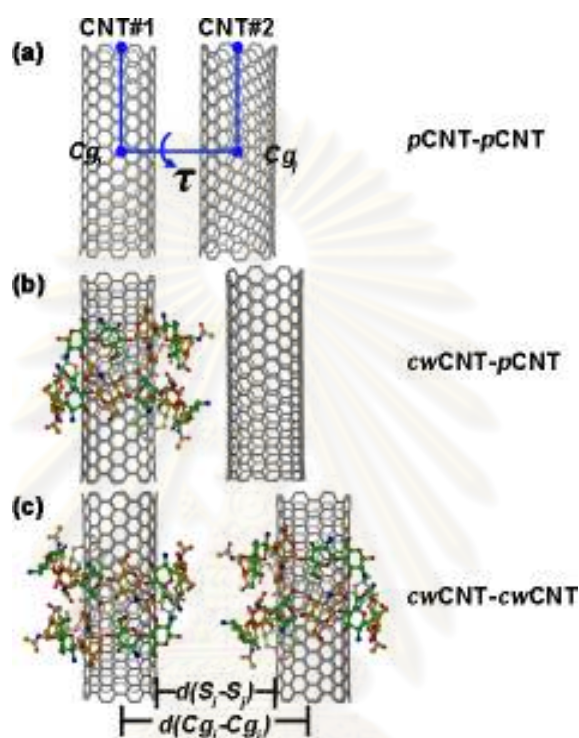


**Figure 3.5** Schematic views of (a) two pristine CNTs (pCNT-pCNT), (b) a pristine CNT - a wrapped CNT with chitosan (pCNT-cwCNT), and (c) two chitosan-wrapped CNTs (cwCNT-cwCNT) where the SWCNT and the polymer used are the (8,8) armchair and 60%DD chitosan, respectively. The distances ( $d(Cg_i-Cg_j)$ ) and ( $d(S_i-S_j)$ ) and torsion angle ( $\tau$ ) between the two SWCNTs were defined through the center of gravity ( $Cg$ ) and the surface of each tube in which  $\tau = 0^\circ$  and the two tubes are parallel.



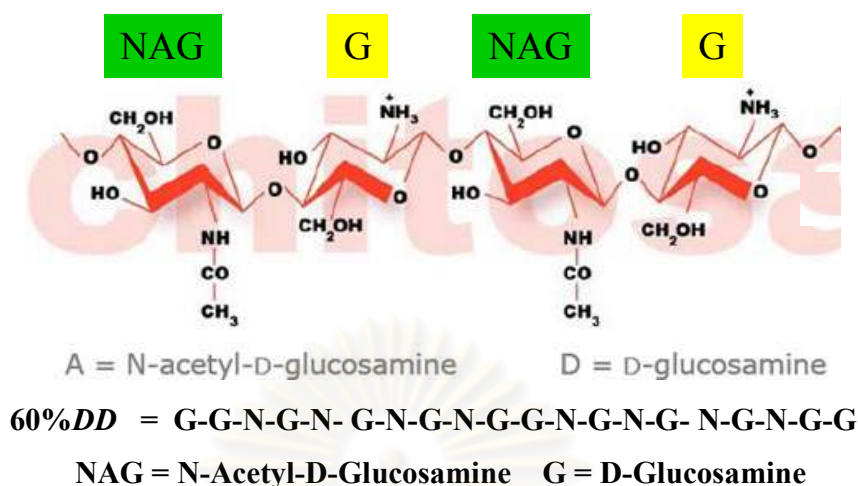


**Figure 3.6** Chemical structure of chitosan 60%DD were alternate the repeating unit between N-Acetyl-D-Glucosamine and D-Glucosamine.

### 3.3.1 Materials and methods

The 20 repeating units of 60%DD chitosan and the (8,8) armchair of SWCNTs with diameter of 11 Å, chiral vectors  $n=8$  and  $m=8$ , and 12 repeating units were constructed using Material Studio 4.3 package. The three models, as shown in Figure 3.5, are (a) two pristine CNTs (*p*CNT-*p*CNT), (b) a pristine CNT – a chitosan wrapped CNT (*p*CNT-*cw*CNT), and (c) two chitosan wrapped CNTs (*cw*CNT-*cw*CNT). Each model was solvated in aqueous solution. The MD simulations were set up and carried out according to our previous works [62, 63]. The CNT and chitosan were parameterized by AMBER03 [64] and GLYCAM06 [65] force fields, respectively. The SPC/E water model with octagonal box over 12 Å from the system surface was applied to all systems. The simulations were calculated using the AMBER10 programme package [66] with the NPT ensemble at 1 atm and a time step of 2 fs. The SHAKE algorithm was applied to all bonds involving hydrogen atoms to constraint their motions. The periodic boundary conditions were applied and the cutoff function was set at 12 Å for nonbonded interactions and particle mesh Ewald method. The whole system was heated from 10 K to 300 K for 200 ps and equilibrated at 300 K for 5 ns. Finally, the production stage was performed until 20 ns and the structural coordinates were saved every 1 ps for analysis.

### 3.4 Covalent surface modification of multiwall carbon nanotubes with acid oxidation ( $\text{H}_2\text{SO}_4$ and $\text{HNO}_3$ )

#### 3.4.1 Chemicals and materials

Multiwall carbon nanotubes: MWCNT (baytubes® C 150 P, outer diameter distribution 5-20 nm and length 1 - >10  $\mu\text{m}$ , (Figure 3.7)) were kindly donated from Bayer Co., Ltd., Thailand. Concentrated sulfuric acid 98% and nitric acid 90% A.R. grade were purchased Labscan Asia Co., Ltd., Thailand. Sodium hydroxide was purchased from Aldrich, Thailand. All chemicals and solvents were used as received without any further purification. Double distilled water was used in all experiments.

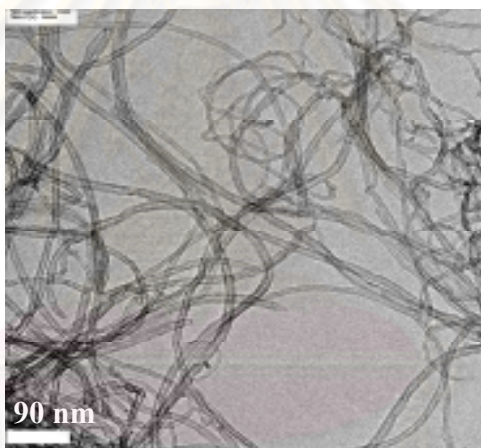


**Figure 3.7** Transmission electron microscopic image of pristine multiwall carbon nanotubes (baytubes® C 150 P).

### **3.4.2 Acid treatment of carbon nanotubes**

To prepare multiwall carbon nanotubes surface prior to coating with multilayer thin film, MWCNTs were properly treated with strong acid to provide a negative charge on their surface. 0.5 g of MWCNTs was mixed with  $\text{H}_2\text{SO}_4$ :  $\text{HNO}_3 = 3:1$  (v/v) in 80 ml, and sonicated for 2 hr at temperature 50 °C. The treated MWCNTs mixture was then neutralized with NaOH until the pH reached a value of 7. Treated MWCNT were dialyzed in distilled water for 4 days in order to remove salt ions from the acid and base used. Finally the treated carbon nanotubes were centrifuged at 4,000 rpm for 30 minutes and collected as in powder form.

The treated multiwalled carbon nanotubes were characterized on their chemical structure using Raman spectroscopy (Perkin Elmer Spectrum-GX, USA) and FTIR spectroscopy (Perkin Elmer Spectrum One, USA).

### **3.5 Layer-by-layer deposition on treated carbon nanotubes with polyelectrolyte; PDADMAC and PSS without centrifugation process**

#### **3.5.1 Chemicals and materials**

Treated multiwall carbon nanotubes were obtained from acid treatment. Poly(diallyldimethylammonium chloride): PDADMAC (medium molecular weight, 20 wt% in water, typical Mw 200,000 – 350,000) and poly(sodium 4-styrene sulfonate): PSS (typical Mw 70,000) were purchased from Aldrich, Thailand. Sodium hydroxide was purchased from Aldrich, Thailand. All chemicals and solvents were used as received without any further purification. Double distilled water was used in all experiments.

##### **3.5.1.1 Poly(diallyldimethylammonium chloride)**

PDADMAC (medium molecular weight, 20 wt% in water, typical Mw 200,000 – 350,000), was a strong cationic polyelectrolyte with positive charges along the backbone chain. The chemical structure of PDADMAC is shown in Figure 3.8.

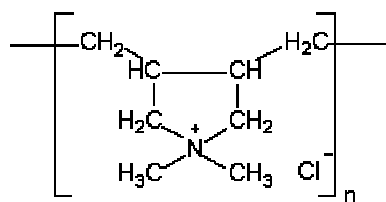


**Figure 3.8** Chemical structure of poly(diallyldimethylammonium chloride): PDADMAC.

### 3.5.1.2. Poly(sodium 4-styrene sulfonate)

PSS (typical  $M_w$  70,000), was a strong anionic polyelectrolyte with negative charges along the backbone chain. The chemical structure of PSS is shown in Figure 3.9.

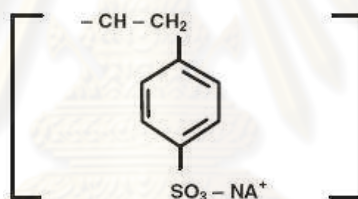


**Figure 3.9** Chemical structure of poly(sodium 4-styrene sulfonate): PSS.

## 3.5.2 Deposition of polyelectrolyte multilayers on multiwall carbon nanotubes via layer-by-layer technique

For the primary coating of the MWCNT, various amounts of carbon nanotubes (5, 10 and 20 mg) were dispersed by sonication in 400 ml of 1 mM NaOH in order to deprotonate carboxylic acid become to carboxylate group which provided negatively charged MWCNT. In different vials, 20 ml of PDADMAC with concentrations ranging from 0.0005 to 0.25 mM were mixed with 20 ml of carbon nanotubes solutions. For the deposition of the secondary layer of polyanionic PSS on the positively charged primary

coated MWCNT, aliquots of 20 ml taken from a 200 ml of the CNT mixed with 0.15 mM PDADMAC were mixed 20 ml of PSS having concentration ranging from 0.001-0.3 mM.

Finally for the deposition of the tertiary layer of PDADMAC on the negatively charged carbon nanotubes, aliquots of 20 ml were taken from a 200 ml solution containing of 0.09 mM of PSS as secondary layers were added to 20 ml of PDADMAC having concentrations ranging from 0.001 to 0.1mM. All of mixture solutions were investigated on their stability by measuring the turbidity of carbon nanotubes solution using UV-Vis spectroscopy and their surface charge density using zeta potential measurement as shown in Figure 3.10.

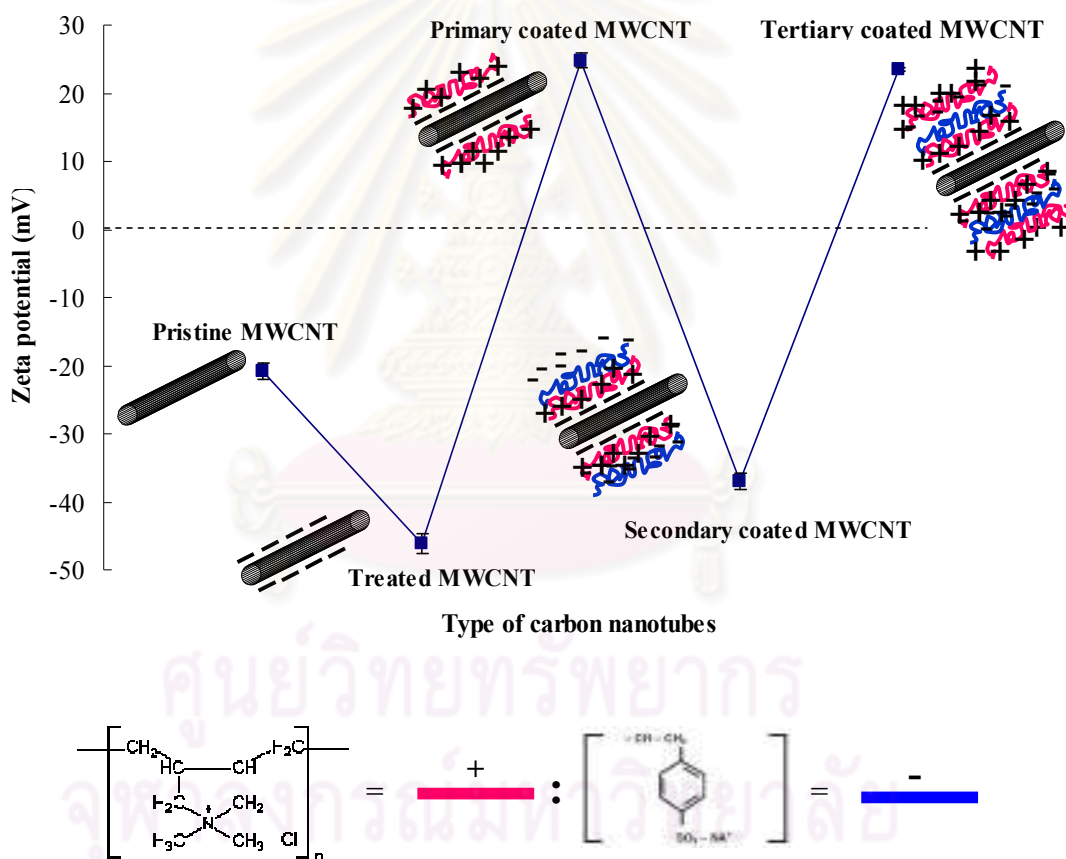


**Figure 3.10** Diagram of modified carbon nanotubes with PDADMAC and PSS as polyelectrolyte multilayers.

### **3.5.3 Stability of modified MWCNT (treated MWCNT and primary coating MWCNT with PDADMAC)**

#### **3.5.3.1 Effect of salt concentration on stability of modified MWCNT**

25  $\mu\text{g/ml}$  of treated MWCNT and primary coating MWCNT with PDADMAC 20 ml were mixed with 20 ml of different concentrations of NaCl (0-1.5 M). The mixture solution was stored at the room temperature for 1 week. The turbidity of the mixture solutions were measured by UV-Vis spectroscopy at a wavelength of 550 nm.

#### **3.5.3.2 Effect of pH on stability of modified MWCNT**

25  $\mu\text{g/ml}$  of treated MWCNT and primary coating MWCNT with PDADMAC 20 ml were mixed with 20 ml of different *pH* buffer (*pH* 2 to 11). The mixture solution was stored at the room temperature for 24 hour. The turbidity of the mixture solutions were measured by UV-Vis spectroscopy at a wavelength of 550 nm.

### **3.5.4 Characterization Technique**

UV-Vis spectrophotometer (SPECORD S 100, Analytikjena, Germany) was used to investigate the turbidity of modified carbon nanotubes in aqueous solution in order to identify the stability of modified CNT. To confirm the successful coating on treated carbon nanotubes, the surface charge of modified carbon nanotubes with polycation and polyanion were measured by Zetasizer (NanoZS4700 nanoseries, Malvern Instruments, UK). Transmission electron microscope (TEM model JEM-2100) was used to investigate the morphology of pristine MWCNT and modified MWCNT with polyelectrolyte.

### 3.6 Hydrophilic model drugs: gentian violet and diclofenac loading and recovery on modified multiwalled carbon nanotubes

#### 3.6.1 Chemicals and materials

Treated multiwall carbon nanotubes were obtained from acid treatment.

Poly(diallyldimethylammonium chloride): PDADMAC (medium molecular weight, 20 wt% in water, typical Mw 200,000 – 350,000) and poly(sodium 4-styrene sulfonate): PSS (typical Mw 70,000) were purchased from Aldrich, Thailand. Gentian violet was purchased from Vittayasom Co., Ltd., Thailand. Diclofenac Sodium was purchased from Aldrich, Thailand. Sodium chloride, Disodium hydrogen phosphate, potassium chloride and Potassium dihydrogen phosphate were purchased from Carlo Erba, Thailand.

##### 3.6.1.1 Gentian violet

Gentian violet (crystal violet, Methyl Violet 10B, hexamethyl pararosaniline chloride) is a bactericide and an antifungal agent, the primary agent used in the Gram stain test, perhaps the single most important bacterial identification test in use today, and it is also used by hospitals for the treatment of serious heat burns and other injuries to the skin and gums. The chemical structure of gentian violet was shown in Figure 3.11.

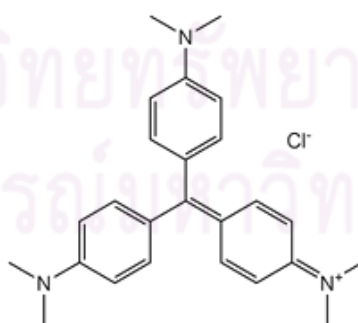


**Figure 3.11** Chemical structure of Gentian violet (crystal violet, Methyl Violet 10B, hexamethyl pararosaniline chloride).

### 3.6.1.2 Diclofenac

Diclofenac (marketed as Voltaren and under a number of other trade names, see Figure 3.12) is a non-steroidal anti-inflammatory drug (NSAID) taken to reduce inflammation and as an analgesic reducing pain in conditions such as arthritis or acute injury. It can also be used to reduce menstrual pain, dysmenorrhea. The name is derived from its chemical name: 2-(2,6-dichloranilino)phenylacetic acid.

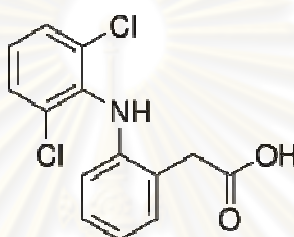


**Figure 3.12** Chemical structure of Diclofenac (2-(2,6-dichloranilino) phenylacetic acid).

### 3.6.2 Preparation of phosphate buffer saline

Phosphate buffer saline *pH* 7.4 was prepared by dissolving 8 g of NaCl, 0.2 g of KCl, 1.44 g of Na<sub>2</sub>HPO<sub>4</sub>, 0.25 g of KH<sub>2</sub>PO<sub>4</sub> in 800 ml of distilled H<sub>2</sub>O. Sodium chloride, Potassium chloride, Potassium dihydrogen phosphate and Disodium hydrogen phosphate were purchased from Carlo Erba, Thailand. The *pH* of aqueous solution was adjusted to 7.4 with HCl or NaOH then added distilled water was added to 1 liter.

### 3.6.3 Layer-by-layer deposition on treated multiwall carbon nanotubes with polyelectrolyte in 0.1xPBS buffer

For the primary coating of the MWCNT, various amounts of MWCNT 20 mg were dispersed in 400 ml of 0.1xPBS by sonicator. In different vials, 20 ml of PDADMAC with concentrations ranging from 0.02 to 0.12 mM were mixed with 20 ml of carbon nanotubes solutions. For the deposition of the secondary layer of polyanionic



PSS on the positively charged primary coated MWCNT, aliquots of 20 ml from a 200 ml of the MWCNT mixed with 0.09 mM PDADMAC, were mixed with 20 ml of PSS having concentration ranging from 0.02 to 0.12 mM. Finally, for the deposition of the tertiary layer of PDADMAC on the negatively charged MWCNT, aliquots of 20 ml were taken from a 200 ml solution containing 0.04 mM of PSS as secondary layers were added to 20 ml of PDADMAC having concentrations ranging from 0.005 to 0.1 mM. All of mixture solutions were investigated on their stability by measuring the turbidity of carbon nanotubes solution using UV-Vis spectroscopy and their surface charge density using zeta potential measurement.

### **3.6.4 Preparation of primary and secondary layers coating on MWCNTs with polyelectrolyte**

#### **3.6.4.1 Deposition of primary layer on carbon nanotubes:**

The amount of treated carbon nanotubes (10 mg) were sonicated in 400 ml of 0.1x PBS buffer *pH* 7.4. While 200 ml of 0.1mM of PDADMAC were stirred, 200 ml of carbon nanotubes solution were added into the PDADMAC solution.

#### **3.6.4.2 Deposition of secondary layer on carbon nanotubes:**

To deposit polyanion as poly(sodium 4-styrene sulfonate): PSS on positive charge of primary coated carbon nanotubes, 20 mg of treated carbon nanotubes were sonicated in 400 ml of 0.1xPBS buffer *pH* 7.4. While 200 ml of 0.15 mM PDADMAC concentration were stirred, 200 ml of treated carbon nanotubes solution were added into the PDADMAC solution. Thereafter, while 200 ml of 0.04 mM of PSS concentration were stirred, 200 ml of primary coating MWCNT with PDADMAC solution were added into the PSS solution.

In this work, we try to load hydrophilic model drug as Gentian violet as a cationic drug and Diclofenac as an anionic drug onto modified MWCNT.

### **3.6.5 Loading and recovery gentian violet from modified multiwall carbon nanotubes; Treated MWCNT, Primary coating MWCNT with PDADMAC and Secondary coating MWCNT with PDADMAC/PSS**

Treated carbon nanotubes, primary coating MWCNT with PDADMAC and secondary coating MWCNT with PDADMAC/PSS were prepared in 0.1xPBS buffer, *pH* 7.4. Gentian violet was prepared at different concentrations (0.0003-0.003  $\mu\text{M}$ ) in 0.1xPBS buffer. 20 ml of modified MWCNT were mixed with 20 ml of gentian violet in different concentrations. The solution were kept for 24 hr, after that the mixture solution were centrifuged at 14,000 rpm for 15 minutes. The supernatant solutions were measured by UV-Vis spectroscopy to determine unbound gentian violet. The decant that consist of gentian violet adsorbed MWCNT were rinsed with 0.1xPBS buffer, thereafter dissolved in ethanol which was the best solvent to dissolve gentian violet. The mixtures were vortexed for 5 minutes then centrifuged again to measure the absorbance of supernatant solution using UV-Vis spectrophotometer.

### **3.6.6 Loading and recovery diclofenac sodium from modified multiwall carbon nanotubes; Treated MWCNT, Primary coating MWCNT with PDADMAC and Secondary coating MWCNT with PDADMAC/PSS**

Treated MWCNT, primary coating MWCNT with PDADMAC and secondary coating MWCNT with PDADMAC/PSS were prepared in 0.1 x PBS buffer, *pH* 7.4. Diclofenac sodium was prepared different concentrations (0.00025-0.01%w/v) in 0.1 x PBS buffer. 20 ml of modified MWCNT were mixed with 20 ml of diclofenac in different concentrations. The solution were kept for 24 hr, after that the mixture solution were centrifuged at 14,000 rpm for 15 minutes. The supernatant solutions were measured by UV-Vis spectroscopy to determine unbound diclofenac concentration. In this case, surprising that modified MWCNT with any coating had no effect on loading efficiency of diclofenac.

### 3.7 Cytotoxicity of modified multiwall carbon nanotubes using MTT assay

#### 3.7.1 Chemicals and Materials

Untreated multiwall carbon nanotubes (baytubes® C 150 P, outer diameter distribution 5-20 nm and length 1 - >10  $\mu\text{m}$  (Figure 3.7)) were kindly donated from Bayer Co., Ltd., Thailand. Treated multiwall carbon nanotubes were received from covalent surface modification process in 3.4. L929 fibroblast mouse cell line were purchased from the American Type Culture Collection (A.T.C.C.) (Rockville, U.S.A). Dulbecco's Modified Eagle Medium (DMEM)-high glucose was purchased from Sigma-Aldrich, U.S.A. MTT (3-(4,5-Dimethylthiazol-2-yl)-2,5-diphenyltetrazolium bromide) was purchased from United States Bio- medical (USB) Corp. (Cleveland, Ohio). Dimethylsulfoxide (DMSO) was purchased from Riedel-de Haën (Seelze, Germany).

MTT (3-(4,5-Dimethylthiazol-2-yl)-2,5-diphenyltetrazolium bromide, a yellow tetrazole) as shown in Figure 3.13, is reduced to purple formazan in living cells. A solubilization solution (usually either dimethyl sulfoxide, an acidified ethanol solution, or a solution of the detergent sodium dodecyl sulfate in diluted hydrochloric acid) is added to dissolve the insoluble purple formazan product into a colored solution. The absorbance of this colored solution can be quantified by measuring at a certain wavelength (usually between 500 and 600 nm) by a spectrophotometer. The absorption maximum is dependent on the solvent employed.

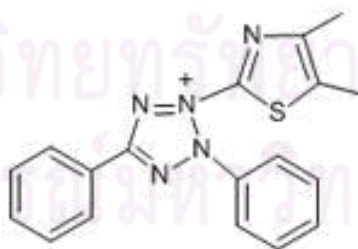


**Figure 3.13** Chemical structure of MTT; (3-(4,5-Dimethylthiazol-2-yl)-2,5-diphenyltetrazolium bromide, a yellow tetrazole)

L929 fibroblast cells, derived from an immortalized mouse fibroblast cell line, are internationally recognized cells that are routinely used in in-vitro cytotoxicity assessments.

### **3.7.2 L929 fibroblast cells preparation**

L929 cells line were frozen with the mixture of serum and DMSO 5-10% in cryo-tube. The cells were defrosted into 37 °C and 5 ml of DMEM were added in the cell. The cell suspensions were centrifuged and the supernatant were removed. DMEM were added in the cells decant and re-suspended by mixing with micropipette. Cells suspended with DMEM were replaced into tissue and tune flash, then incubated in oven 37 °C.

Once, L929 cells were proliferated and adhered at the bottom, the media were removed. Trypsin enzyme was added in order to peel the cells adhesion and re-suspend in the trypsin solution. The trypsinized cells were incubated at 37 °C for 5 minutes. DMEM were added into the cell solution. The cells suspensions were centrifuged and the supernatant was removed. DMEM was added into cell and the cells were counted by hemo-cytometry. The number of L929 cells were prepared at 10,000 cells per well per 100 µl. The cells in 96 wells plate were incubated at 37 °C for 24 hr.

### **3.7.3 Interference of formazan adsorption on untreated and treated multiwall carbon nanotubes**

L929 fibroblast cells were seed at 10,000 cells/well in 96 wells. L929 cells were incubated for 24 hr at 37 °C. Thereafter, the DMEM media were refreshed with the new DMEM media. The L929 cells were incubated for 12 hr. MTT solution was added to cells and incubated for 4 hr. Formazan crystal was dissolved with DMSO then untreated and treated MWCNT concentrations at 6.25, 12.5, 25, 50, 100µg/ml were exposed in formazan solutions for 1 hr. MWCNTs were removed from formazan solution by centrifugation at 4,000 rpm. The remaining formazan solution was measured using UV-Vis spectroscopy at a wavelength of 570 nm. MWCNT samples were sterilized by

exposing with UV lamp for 1-2 hr. 8 replications of samples were tested in each concentration.

### **3.7.4 Cytotoxicity test: MTT Assay**

L929 fibroblast cells were seed at 10,000 cells/well in 96 wells. L929 cells were incubated for 24 hr at 37 °C. Thereafter, the DMEM were refreshed. The L929 cells were incubated for 12 hr. Pristine and treated multiwall carbon nanotubes concentrations 3.125, 6.25, 12.5, 25 and 50 µg/ml were exposed in L929 fibroblast cells and then incubated for 24 hr. Carbon nanotubes were removed after exposing by washing with PBS buffer pH 7.4 twice. MTT solutions was added and incubated for 4 hr at 37 °C. Formazan crystal were dissolved with DMSO and centrifugation at rotation speed 4000 rpm. OD of formazan solutions were measured by UV-Vis spectroscopy at a wavelength of 570 nm. CNT samples were sterilized by exposing on UV lamp for 1-2 hr. 8 replications of samples were tested in each concentration.

### **3.7.5 Effect of functional groups of modified multiwall carbon nanotubes on their cytotoxicity**

#### **3.7.5.1 Preparation of modified carbon nanotubes with poly(diallyldimethyl ammonium chloride) and poly(sodium 4-styrene sulfonate)**

Treated carbon nanotubes 0.05 mg/ml in volume 100 ml were dispersed in 0.1x PBS buffer by sonicator. To prepare the primary coating carbon nanotubes with PDADMAC, treated carbon nanotubes solution (30 ml) were dropped in 0.15 mM poly(diallyldimethyl ammonium chloride)(30 ml) and stirred at the same time. To prepare the secondary coating carbon nanotubes with PSS, the primary coating carbon nanotubes with PDADMAC solution (30 ml) were dropped in 30 ml of 0.1 mM PSS solution. To prepare the tertiary coating carbon nanotubes with PDADMAC, the secondary coating on carbon nanotubes solution 25 ml were dropped in 0.04 mM poly(diallyldimethyl ammonium chloride)(25 ml) and stirred at the same time.

### 3.7.5.2 Preparation of modified multiwall carbon nanotubes for testing MTT assay

**Sample tests;** All of the samples were exposed with UV lamp for 3-4 hr.

**Solution samples:** The modified MWCNT samples were diluted in different concentrations with nutrient broth solution.

- **Primary coating CNT with PDADMAC:** 12.5 µg/ml, 6.25 µg/ml, 3.125 µg/ml, 1.5625 µg/ml and 0.78125 µg/ml.
- **Secondary coating CNT with PDADMAC/PSS:** 6.25 µg/ml, 3.125 µg/ml, 1.5625 µg/ml and 0.78125 µg/ml.
- **Tertiary coating CNT with PDADMAC/PSS/PDADMAC:** 3.125 µg/ml, 1.5625 µg/ml and 0.78125 µg/ml.

**Powder samples:** The modified MWCNT samples were centrifuged to remove the polyelectrolyte excess at 10,000 rpm for 10 minutes. The modified MWCNT powders were collected and re-dispersed in the nutrient broth by sonication.

- **Primary coating CNT with PDADMAC:** 50 µg/ml, 25 µg/ml, 12.5 µg/ml, 6.25 µg/ml, 3.125 µg/ml and 1.5625 µg/ml.
- **Secondary coating CNT with PDADMAC/PSS:** 50 µg/ml, 25 µg/ml, 12.5 µg/ml, 6.25 µg/ml, 3.125 µg/ml and 1.5625 µg/ml.
- **Tertiary coating CNT with PDADMAC/PSS/PDADMAC:** 50 µg/ml, 25 µg/ml, 12.5 µg/ml, 6.25 µg/ml, 3.125 µg/ml and 1.5625 µg/ml.

### 3.7.5.3 Cytotoxicity: MTT Assay

L929 fibroblast cells were seed 10,000 cells/well in 96 wells. L929 cells were incubated for 24 hr. at temperature 37 °C. Thereafter, the old DMEM media were refreshed with the new DMEM media. The L929 cells were incubated with new DMEM media for 12 hr. Untreated and treated MWCNT concentrations 3.125, 6.25, 12.5, 25 and 50 µg/ml and modified MWCNT with polyelectrolyte which were

**Solution samples:**

- **Primary coating CNT with PDADMAC:** 12.5  $\mu\text{g/ml}$ , 6.25  $\mu\text{g/ml}$ , 3.125  $\mu\text{g/ml}$ , 1.5625  $\mu\text{g/ml}$  and 0.78125  $\mu\text{g/ml}$ .
- **Secondary coating CNT with PDADMAC/PSS:** 6.25  $\mu\text{g/ml}$ , 3.125  $\mu\text{g/ml}$ , 1.5625  $\mu\text{g/ml}$  and 0.78125  $\mu\text{g/ml}$ .
- **Tertiary coating CNT with PDADMAC/PSS/PDADMAC:** 3.125  $\mu\text{g/ml}$ , 1.5625  $\mu\text{g/ml}$  and 0.78125  $\mu\text{g/ml}$ .

**Powder samples:**

- **Primary coating CNT with PDADMAC:** 50  $\mu\text{g/ml}$ , 25  $\mu\text{g/ml}$ , 12.5  $\mu\text{g/ml}$ , 6.25  $\mu\text{g/ml}$ , 3.125  $\mu\text{g/ml}$  and 1.5625  $\mu\text{g/ml}$ .
- **Secondary coating CNT with PDADMAC/PSS:** 50  $\mu\text{g/ml}$ , 25  $\mu\text{g/ml}$ , 12.5  $\mu\text{g/ml}$ , 6.25  $\mu\text{g/ml}$ , 3.125  $\mu\text{g/ml}$  and 1.5625  $\mu\text{g/ml}$ .
- **Tertiary coating CNT with PDADMAC/PSS/PDADMAC:** 50  $\mu\text{g/ml}$ , 25  $\mu\text{g/ml}$ , 12.5  $\mu\text{g/ml}$ , 6.25  $\mu\text{g/ml}$ , 3.125  $\mu\text{g/ml}$  and 1.5625  $\mu\text{g/ml}$ .

, were exposed in L929 fibroblast cells and then incubated for 24 hr. MWCNTs were removed after exposing by washing with PBS buffer *pH* 7.4 twice times. MTT solutions was added into cells and incubated for 4 hr at temperature 37 °C. Living cells in each well can convert MTT to be formazan crystal. Formazan crystal were dissolved with DMSO and centrifuged at rotation speed of 4,000 rpm. OD of formazan solutions were measure by UV-Vis spectroscopy at wavelength 570 nm. MWCNT samples were sterilized by exposing on UV lamp for 3-4 hr. 8 replications of samples were tested in each concentration.

**3.8 Characterization Technique****3.8.1 UV-Vis spectroscopy [67]**

Ultraviolet-Visible spectroscopy (UV = 200-400 nm, Visible = 400-800 nm) corresponds to electronic excitations between the energy levels that correspond to the molecular orbitals of the systems. In particular, transitions involving p orbitals and lone pairs (n = non-bonding) are important and so UV-Vis spectroscopy is of most use for

identifying conjugated systems which tend to have stronger absorptions. This technique can be used for analyze the degree of deacetylation of chitosan, stability of carbon nanotubes in chitosan solution, the drug concentration after loading and release from the functionalized carbon nanotubes.

### **3.8.2 Zeta potential measurement [68]**

Zeta potential is a scientific term for electrokinetic potential in colloidal systems. In the colloidal chemistry literature, it is usually denoted using the Greek letter zeta, hence  $\zeta$ -potential. From a theoretical viewpoint, zeta potential is electric potential in the interfacial double layer (DL) at the location of the slipping plane versus a point in the bulk fluid away from the interface. In other words, zeta potential is the potential difference between the dispersion medium and the stationary layer of fluid attached to the dispersed particle. A value of 25 mV (positive or negative) can be taken as the arbitrary value that separates low-charged surfaces from highly-charged surfaces.

### **3.8.3 Transmission electron microscopy (TEM) [69]**

Transmission electron microscopy (TEM) is an imaging technique where a beam of electrons is focused onto a specimen causing an enlarged version to appear on a fluorescent screen or layer of photographic film. Raw carbon nanotubes and functionalized carbon nanotubes can be imaged their morphology clearly in 2 dimensions. This technique will be used for CNTs with diameter less than 100 nm.

### **3.8.4 Scanning electron microscopy (SEM) [69]**

Scanning electron microscopy (SEM) is an imaging technique to produce high resolution images of a sample surface. Due to the manner in SEM, the image is created, its images have a characteristic three-dimensional appearance and are useful to show the surface structure of the sample. This technique will be used for CNTs with diameter more than 100 nm.



### **3.8.5 Gel permeation chromatography (GPC) [70]**

Gel Permeation Chromatography (GPC) is one of the most versatile and powerful analytical techniques available for understanding and predicting polymer performance. GPC is well established for determining the molar mass of polymers. It has the advantage that it determines complete distributions of molar masses as opposed to merely an average molecular weight. This technique indicated the molecular weight of Chitosan with varying degree of deacetylation.

### **3.8.6 Fourier Transform Infrared spectroscopy (FTIR) [71]**

FT-IR is the preferred method of infrared spectroscopy. Infrared spectroscopy, IR radiation is passed through a sample. Some of the infrared radiation absorbed by the sample and some of it is passed through (transmitted). The resulting spectrum represents the molecular absorption and transmission, creating a molecular fingerprint of the sample. Like a fingerprint no two unique molecular structures produce the same infrared spectrum. This technique will be used to analyze functional groups of modified CNTs.

### **3.8.7 Raman spectroscopy [72]**

Raman spectroscopy (named after C. V. Raman) is a spectroscopic technique used to study vibrational, rotational, and other low-frequency modes in a system. It relies on inelastic scattering, or Raman scattering, of monochromatic light, usually from a laser in the visible, near infrared, or near ultraviolet range. The laser light interacts with phonons or other excitations in the system, resulting in the energy of the laser photons being shifted up or down. The shift in energy gives information about the phonon modes in the system.

## **CHAPTER IV**

### **RESULTS AND DISCUSSION**

#### **4.1 Surface modification of carbon nanotubes**

In this set of experiments, the modification of multiwall carbon nanotubes (MWCNTs) by noncovalent surface modification was performed because this approach provided good dispersion and stability in aqueous solution while maintaining the integrity of CNT. However, the modified MWCNTs with various degree of deacetylation of chitosan by noncovalent surface modification were not adequate to provide their stability in aqueous solution. Therefore, covalent surface modification was needed to modify MWCNTs in smaller diameter to provide charged surface and short lengths of MWCNTs. To increase charged density and obtain different functional groups on MWCNTs surface, polyelectrolyte; PDADMAC and PSS, were selected to deposit on treated MWCNT by layer-by-layer self assembly technique with simplified method. The satisfied dispersion and stability properties of modified MWCNT were an important reason that MWCNT can be possibly integrated as a drug carrier for drug delivery application.

##### **4.1.1 Noncovalent surface modification of multiwall carbon nanotubes with various degree of deacetylation of chitosan**

Chitosan biopolymer was selected as a dispersing agent to modify nanotubes surface because of their biocompatibility and nontoxic. Generally, chitosan has been proposed to improve CNT dispersion before being applied in biosensor devices. Recently, chitosan and alginate were coated on singlewall carbon nanotubes surface by noncovalent surface modification and successfully load anticancer drug; doxorubicin onto them [73]. However, most of the publications the chitosan used, had a high degree of deacetylation (>80%) because it can easily be dissolved in aqueous solution. Degree of deacetylation (%DD) of chitosan was an important parameter that controlled the ratio of hydrophobic (N-acetyl-D-glucosamine) and hydrophilic (D-glucosamine) parts of chitosan structure [74, 75] (Figure 4.1). Degree of deacetylation of chitosan was calculated from the ratio of

D-glucosamine to total composition consist of N-acetyl-D- glucosamine and D-glucosamine.

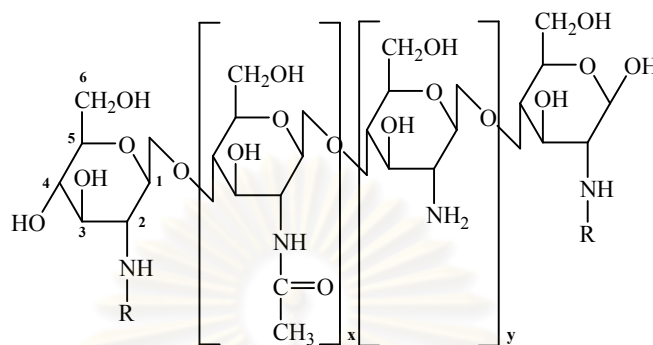


**Figure 4.1** Chemical structure of Chitosan:  $x$  = N-acetyl-D-glucosamine unit,  $y$  = D-glucosamine unit:  $x > 50\%$  = Chitin,  $y > 50\%$  = Chitosan.

#### 4.1.1.1 Chitosan synthesis

To control the hydrophobic/hydrophilic parts of chitosan by varying degree of deacetylation, the hydrophobic parts of chitosan were interesting key point to improve the chitosan adsorption efficiency on nanotubes surface while their stability in aqueous solution is still provided by hydrophilic parts. In the relevant literatures, the improvement of MWCNT's dispersion has been proposed with surfactant or polymer and even dye molecules by attaching hydrophobic part on nanotubes surface while the hydrophilic part stabilize modified MWCNT in aqueous solution. The hypothesis of our research was that the hydrophobic part of chitosan possibly attach on the nanotubes surface while the hydrophilic parts of chitosan stabilize carbon nanotubes in the aqueous solution.

Since chitosan with low %DD were not available as a commercial product, various degree of deacetylation of chitosan were needed to synthesize. Chitin, extracted from shrimp was deacetylated with concentrated sodium hydroxide at ambient temperature. When the reaction time was increased from 2 to 7 days, the degree of deacetylation of chitosan was increased as shown in Figure 4.2.

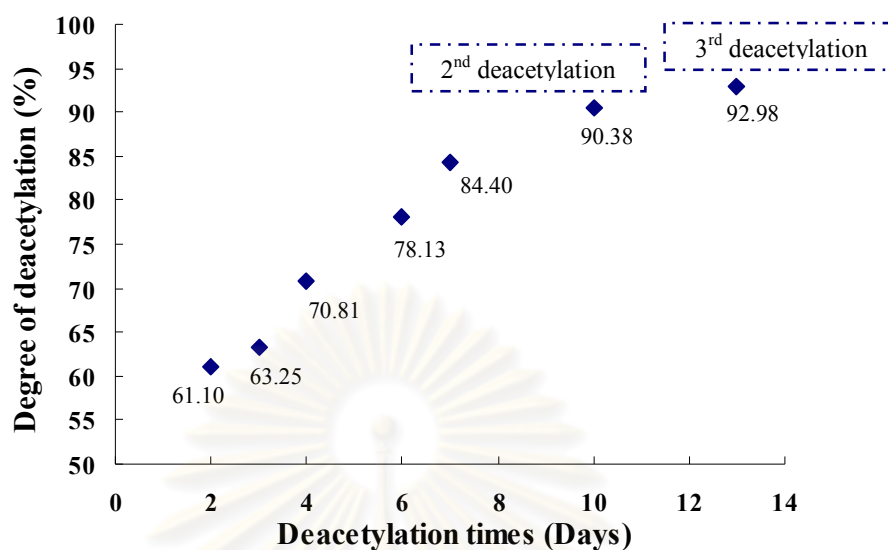


**Figure 4.2** Plot of degree of deacetylation of chitosan which investigated by first derivative UV-Visible spectroscopy technique as a function of deacetylation time.

Under concentrated alkaline, sodium hydroxide reacted with chitin consist of N-acetyl-D-glucosamine as a repeating unit by nucleophilic substitution pathway, the acetyl groups become ammine groups and received sodium acetate as a by product as shown in Figure 4.3.

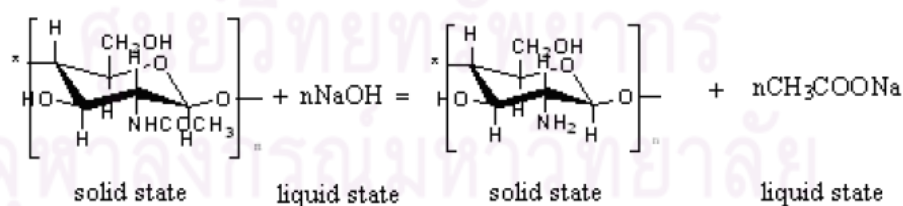


**Figure 4.3** Schematic of deacetylated reaction of chitin under concentrated alkaline [76]

To receive the chitosan, the various reaction time from 2 to 7 days at ambient temperature can produce different %DD of chitosan in a range of 61% to

84 %*DD*. In addition, to increase degree of deacetylation of chitosan, the obtained chitosan from a reaction time of 7 days were reacted with fresh concentrated sodium hydroxide in the second and third rounds in order to deacetylate the remaining acetyl groups in their structure and receive the increasing of degree of deacetylation chitosan (90 and 93%*DD*). The obtained chitosan with different reaction time were investigated on degree of deacetylation of chitosan by first derivative UV-Vis spectroscopy technique.

Infrared spectroscopic method is commonly used to investigate the degree of deacetylation because it is relatively fast technique and does not require the dissolution of chitosan in aqueous solvent. The use of different baseline would inevitably contribute a variation in the degree of deacetylation value. Moreover, sample preparation, type of instrument and condition especially moisture might influence the sample analysis. Therefore, first derivative UV-Vis spectroscopy was selected instead of IR spectroscopy technique in order to solve this problem. The advantage of first derivative UV-Vis spectroscopy to investigate degree of deacetylation of chitosan was that it required only a small amount of sample and relied on simple reagent molecules. In addition, the method allowed a simple, convenient, time saving and was sensitive enough to detect the concentration of N-acetyl-D-glucosamine as low as 0.5 mg/l in 0.01 M acetic acid [77]. The results were reasonable with less interference of protein contaminants, which provided the good precision and accuracy for N-acetyl-D-glucosamine residue in chitosan.

Molecular weight of chitosan was another important parameter that should be considered because it might influence on adsorption efficiency as well. In this case, molecular weight of obtained chitosan was monitored using gel permeation chromatography (GPC). The results in Figure 4.4 showed that molecular weight was decreased in a range of 630 to 530 kDa when the reaction time increased at ambient temperature. Although the relevant literature has been reported that the synthesis temperature affect molecular weight especially at temperature over 40°C [78], in this case, in spite of different reaction time, the % difference of molecular weight of chitosan between 2 days and 13 days was slightly changed in 15.87 % when synthesized under ambient temperature. The nearly molecular weight of chitosan was the good point that we possibly neglected the effect of molecular weight of chitosan on MWCNTs dispersion.

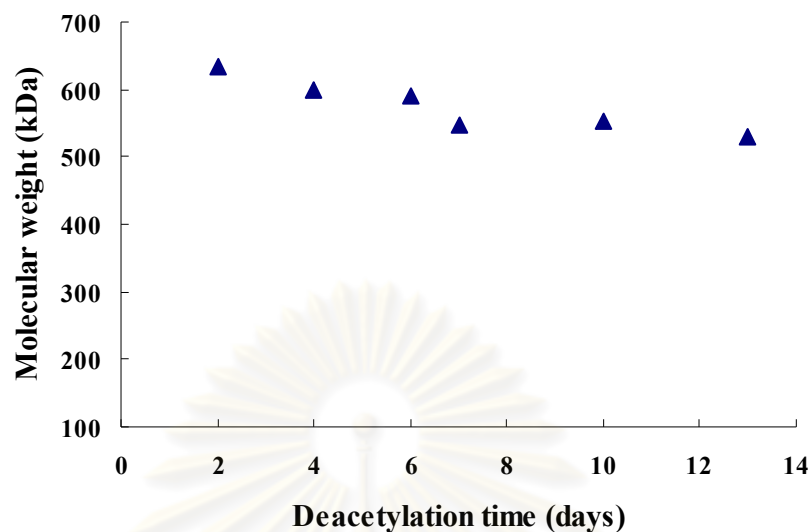


**Figure 4.4** Molecular weight of chitosan as a function of deacetylation time

Therefore, the obtained chitosan with various degree of deacetylation (61, 71, 78, 84, 90 and 93 %DD) and molecular weight in a range of 630-530 kDa were used to noncovalently modify MWCNTs for improving their dispersion and stability in aqueous solution. The hypothesis of this experiment was that the hydrophobic parts (N-acetyl-D-glucosamine) of chitosan possibly attach on MWCNTs to separate to individual MWCNT while the hydrophilic parts (D-glucosamine) of chitosan stabilize MWCNTs by repel each other in aqueous solution as shown in Figure 4.5.

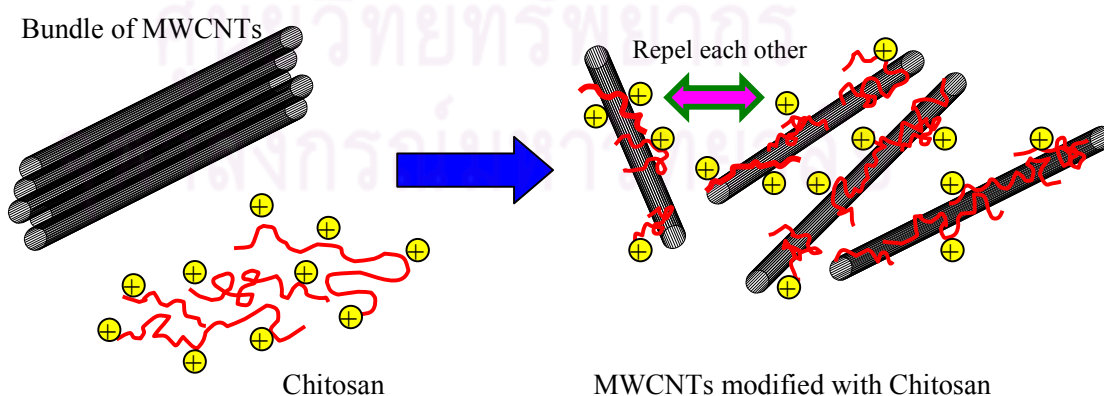


**Figure 4.5** Hypothesis model of surface modification of MWCNTs with chitosan.

To achieve MWCNTs dispersion with chitosan, the sonication process was necessary step to temporarily disperse pristine MWCNTs in aqueous solution. Although pristine MWCNTs was sonicated, it was still hardly dispersed in solution because of their superhydrophobic property. Therefore, the diluted chitosan concentration was used as a starting solution for increasing probability of pristine MWCNTs to attach the solution in order to disperse by sonicator.

#### **4.1.1.2 Effect of sonication times on carbon nanotubes dispersion with chitosan**

The sonication time is also affected to the pristine MWCNTs dispersion efficiency. The temporary dispersion of MWCNTs led the chitosan having time to attach on MWCNT surface. The increasing in sonication time increased the dispersion of MWCNTs by increasing the absorbance at 550 nm as shown in Figure 4.6. Until the sonication time reach to 30 minutes, the dispersion of MWCNTs was not significantly changed in absorbance. In addition, the lower %DD of chitosan provided the better dispersion than higher %DD because of the amount of hydrophobic parts. The carbon nanotubes are totally dispersed at sonication time 45 minutes. However, in the next experiment, we still used the minimum sonication time for 30 minutes in order to avoid the effect of increasing of temperature that heating up during the sonication process. Furthermore, low %DD as 61% chitosan provide high dispersion efficiency compare with chitosan 78 and 93%DD.

ศูนย์วิทยทรัพยากร  
จุฬาลงกรณ์มหาวิทยาลัย

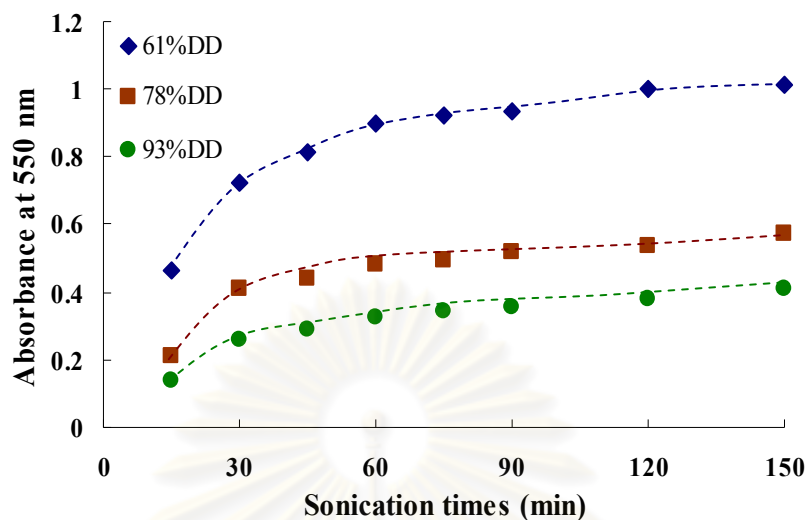


**Figure 4.6** The dispersion of MWCNTs with 5 mM of different degree of deacetylation chitosan (61, 78 and 93%DD) as a function of sonication time.

#### 4.1.1.3 Effect of chitosan concentration on carbon nanotubes dispersion

In these experiments, chitosan was used to disperse the MWCNTs by noncovalent surface modification. If one tries to disperse carbon nanotube in aqueous solution, it is well known that prior to the adjunction of any dispersing agent, the solution will appear clear with the MWCNTs aggregated at the air/water interface. Van der Waals attraction and  $\pi$ - $\pi$  stacking between the abundant double bonds found in MWCNTs are through to be responsible for their aggregation and poor solubility in aqueous solution.

Shown in Figure 4.7 is a plot of the changes in absorbance of the solution as a function of the added chitosan concentration. From the initial solution of aggregated carbon nanotubes, as chitosan concentration is increased up to 1 mM, the adsorption of the polymer onto the carbon nanotubes leads to dispersion, which in turn leads to a sharp increase the absorbance at 550 nm. This increase in absorbance quickly levels off suggesting that all the carbon nanotubes, present in the solution, have been dispersed. Further increase of the chitosan solution to 9 mM does not induce any increase in



absorbance. When chitosan is added to the solution, noncovalent adsorption of chitosan on the nanotube surface is thought to take place, which initiates the dispersion by repulsion of the nanotubes. Since it has been reported that the acetyl groups represent the most hydrophobic part of the chitosan, the authors suggest that these functional groups could adsorb preferentially on the surface of the MWCNTs. In the mean time, the hydrophilic parts of chitosan ( $\text{NH}_3^+$ ) induce a positive charge at the vicinity of the nanotubes surface, which allow their stabilization in aqueous solution by electrostatic repulsion. This dispersion process can be studied using UV–Visible spectroscopy by recording the changes in absorbance of the solution at 550 nm, and is therefore equivalent to a turbidity measurement. As carbon nanotubes absorb all the wavelengths in the visible part of the electromagnetic spectrum, increases in dispersion of the carbon nanotubes render the solution more and more pitch-black.

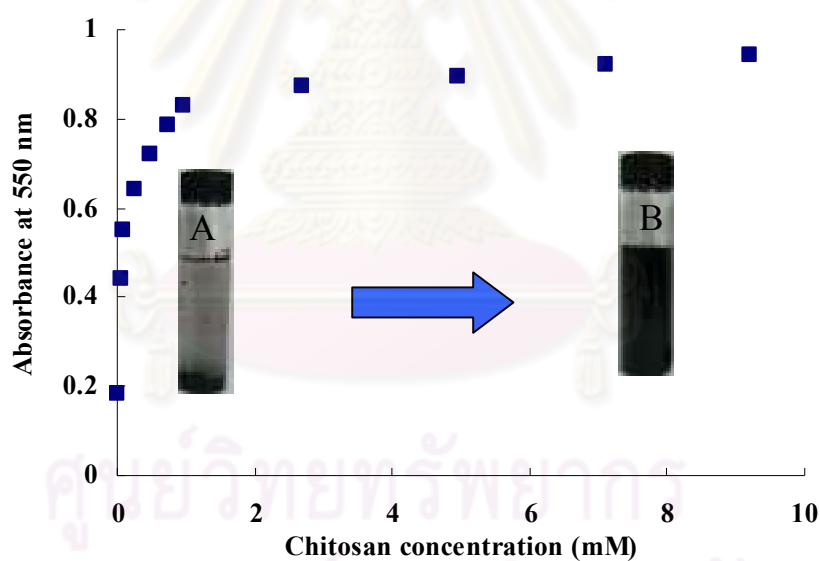


**Figure 4.7** Plot of the changes in absorbance of a MWCNT solution as function of the 61%DD chitosan concentration (0-10mM).

#### 4.1.1.4 Effect of degree of deacetylation of chitosan on carbon nanotubes dispersion

Since our hypothesis was that the more hydrophobic acetyl groups present in chitosan might allow a better interaction with the MWCNTs, our interest turned toward the preparation of chitosan having a higher molar fraction of acetyl groups thus a lower %*DD*.

Our hypothesis was that when the hydrophobic character of chitosan is controlled by the fraction of acetylated functional groups, chitosan with a lower %*DD* should be a better molecule for the dispersion of MWCNTs. Chitosan with a lower %*DD* can simply be prepared by a shorter reaction time of the chitin biopolymer in the 50% w/w sodium hydroxide solution.

In our work, we chose to use 61%*DD* chitosan as the lowest degree of deacetylation because the resulting chitosan molecules were not sufficiently soluble and led to very scattered results. Shown in Figure 4.8 (squares), is the absorbance of different solutions containing MWCNTs dispersed with chitosan having different degree of deacetylation (61, 71, 78, 84, 90 and 93%*DD*). Although it was shown in Figure 4.7 that a 1 mM chitosan concentration is sufficient to dispersed carbon nanotubes, a concentration of 5 mM chitosan was used to insure total dispersion of the MWCNTs in an excess solution of chitosan. From the absorbance measurements of the solutions, it can be seen that the efficiency of the dispersion of the carbon nanotubes, decrease when increasing the chitosan %*DD*. The final absorbance of the solution when using 61%*DD* is double than when using the 93%*DD* chitosan. These results suggest that, as expected, more hydrophobic chitosan segments found in the lower 61%*DD* are more efficient to adsorb onto the MWCNTs leading to a better dispersion of the carbon nanotube in solution. The mechanism through which CNT interact with chitosan is though to be due to hydrophobic interaction from hydrocarbon backbones and acetyl groups, and  $\pi$  system of the MWCNTs. CH- $\pi$  interaction which is a weak hydrogen bonding attraction between soft acid C-H bond and soft base  $\pi$  system are also though to take part in the adsorption of chitosan onto the MWCNTs [79]. At low degree of deacetylation 61%*DD*, the bonding force between chitosan and MWCNTs is based on hydrophobic interaction

due to the acetyl groups that can interact with the surface of the nanotubes. For higher degree of deacetylation from 71%*DD* to 93%*DD*, the dispersion efficiency of the MWCNTs decreases due to the more hydrophilic character of the high %*DD* chitosan which is more soluble.

The efficiency of the surface modification of MWCNTs is often evaluated in term of stability against aggregation and sedimentation. Sedimentation occurs when the repulsion between MWCNTs is not strong enough to prevent the aggregation of the nanotube, leading to their precipitation. After surface modification of the MWCNTs by chitosan, the excess surface charges provided by the amino groups on the chitosan induce nanotube–nanotube repulsion and therefore prevent sedimentation. In our experiment, the sedimentation of the MWCNTs was accelerated with a centrifuge having a rotation rate of 2000 rpm for 10 minutes. In Figure 4.8 (triangles), is shown the absorbance of each MWCNTs solutions after centrifugation for each %*DD*. When compared to the initial absorbance (Figure 4.8, squares), a much lower absorbance as a result of the accelerated sedimentation by centrifugation was measured. Yet, it is interesting to observe that the lower 61%*DD* perform again better than the higher 93%*DD* although the former present a lower charge density when compare with the later. This would suggest that the adsorption of the lower %*DD* chitosan is greater than for higher %*DD*.

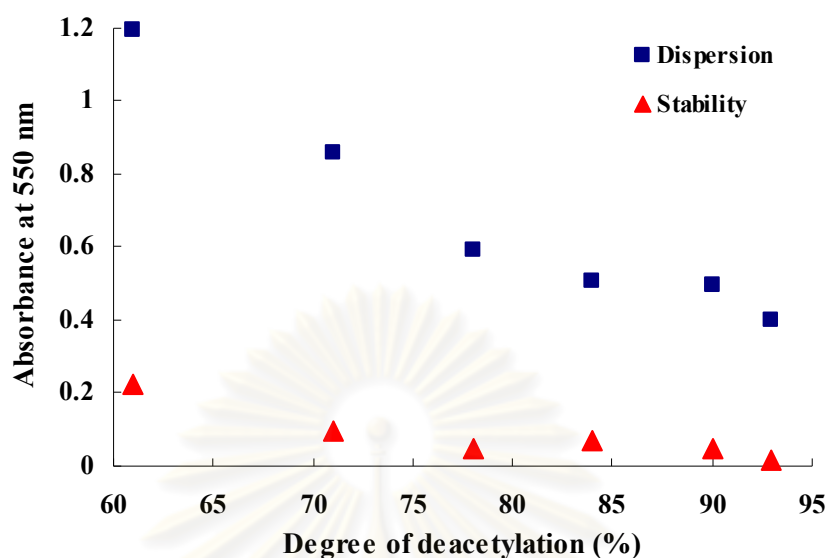


**Figure 4.8** Plots of the changes in absorbance of a dispersion of MWCNTs in a 5 mM chitosan solution of various degree of deacetylation before (squares) and after (triangles) centrifugation at 2000 rpm for 10 minutes.

#### 4.1.1.5 Surface charge of modified carbon nanotubes with different degree of deacetylation of chitosan

In term of resistance to sedimentation, this improved stability suggests that the MWCNTs modified with the lower %*DD* have a higher surface charge density, which provides a better stability against sedimentation. In order to access the value of the surface charge, we further characterized the MWCNTs surface by zeta potential measurements.

The surface charge density of colloidal particles dispersed in solution can be estimated by measuring the zeta potential, which represents the difference in potential between the slip plane of the double layer near the particles surface and the bulk solution. The zeta potential of the pristine carbon nanotube is expected to be initially nearly neutral but should become largely positive after adsorption of chitosan due to the presence of cationic amino groups. In our experiments, zeta potential values of the modified MWCNTs were ranging from 34 to 42 mV, which confirm the successful immobilization

of chitosan on the MWCNTs. Shown in Figure 4.9 (circles), the zeta potential values are plotted as a function of the %*DD*, which range from 42 mV (61%*DD*) to 34 mV (93%*DD*). These values decrease with increasing %*DD* and suggest that all MWCNTs dispersed in solutions have similar surface charged. Yet, because the 61%*DD* chitosan has a lower linear charge density when compared to 93%*DD*, these values need to be corrected if we want to compare the amount of polymer adsorbed at the surface of the MWCNTs. This lower linear charge density is due to the fact that the 61%*DD* contain only 61 groups for 100 monomers while the 93%*DD* contain 93 per 100 monomers.

Since the zeta potential is proportional to the density of charges, equal zeta potential for two nanotubes would require 1.5 times more 61%*DD* than 93%*DD* chitosan. Therefore the 93%*DD* has a linear charge density 1.5 times higher than the 61%*DD*. In Figure 4.9 (triangles) is plotted the corrected normalized chitosan monomer ration adsorbed onto the MWCNTs for each %*DD*. This plot is obtained by dividing the measured zeta potential by the corresponding %*DD* of the chitosan used and normalized. From the plot it can be seen that 1.9 times more 61%*DD* chitosan adsorb onto the MWCNTs when compared with the 93%*DD*. Several factors can justify the much lower adsorption of the 93%*DD* when compared with the 61%*DD*. The 93%*DD* has a better solubility, which means it will tend to remain in solution and will be more thermodynamically stable in solution. The higher charge density on the 93%*DD* chitosan can induce electrostatic repulsion of the groups, which in turn would lead to lower adsorption density of the chitosan while the 61%*DD* could adsorb in a more packed fashion.

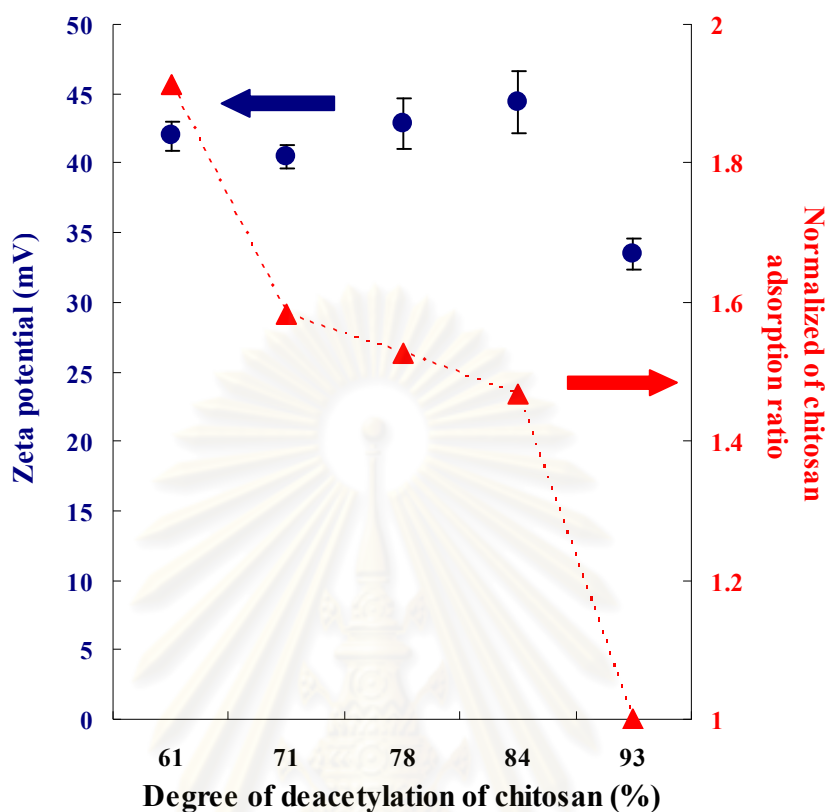


**Figure 4.9** Zeta potential of modified MWCNT (circles) and normalized chitosan adsorption ratio onto the MWCNT (triangles) as a function of the %DD of chitosan.

Multiwall carbon nanotubes have been noncovalently modified with chitosan having different %DD. Using chitosan having different %DD had a strong effect on the quality of the nanotubes dispersion. UV–Visible spectroscopy results suggest that the nanotubes dispersion was improved when using chitosan with a lower degree of deacetylation (61%DD) when compared with higher degree of deacetylation (93%DD). The MWCNT modified with the lower %DD also displayed the best stability against centrifugation. Zeta potential measurements finally confirmed that the amount of chitosan adsorbed onto the nanotubes surface was twice as high with the lower %DD as with the high %DD. These modified MWCNTs with chitosan biopolymer could be used for the immobilization of hydrophobic and hydrophilic drug for drug delivery application.

#### **4.1.2 Molecular Dynamics Simulation: Dispersion and separation of chitosan wrapping on SWCNTs by noncovalently modification.**

In our previous experiment, MWCNTs were modified with chitosan having different degree of deacetylation by noncovalent surface modification. The conclusion of this work was that low %*DD* as 61% of chitosan provided the best dispersion efficiency of MWCNTs. However, during modification process, pitch black mixture solution of MWCNT and chitosan still consist of two species which were the sedimentary CNT and stabilized CNT. As the behavior of modified MWCNTs with chitosan when it dispersed in the aqueous solution is not clearly known yet, molecular dynamics simulation was used to understand the behavior of dispersion and sedimentation of CNTs during modification process.

Molecular dynamics simulation was used to predict the interaction between singlewall carbon nanotubes (SWCNTs) and 60%*DD* of chitosan and interaction of modified CNTs with 60%*DD* of chitosan. Molecular dynamics simulation done on the three models: *i*) two pristine CNTs (*p*CNT-*p*CNT), *ii*) a pristine CNT–a chitosan-wrapped CNT (*p*CNT-*cw*CNT) and *iii*) two chitosan wrapped CNTs (*cw*CNT-*cw*CNT) as shown in Figure 4.10.

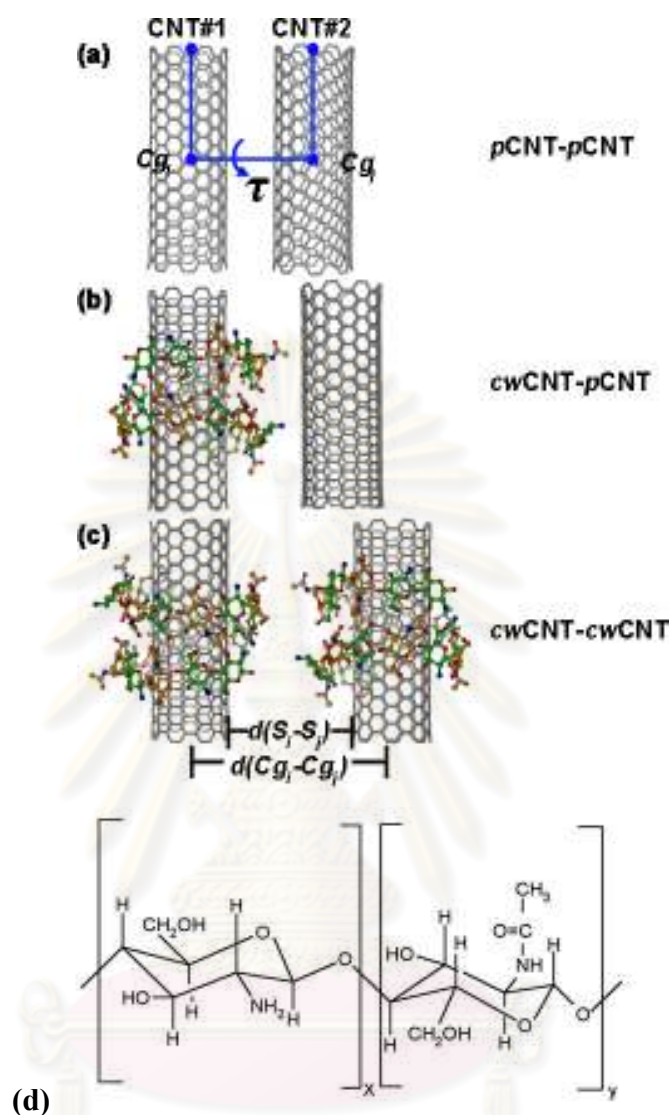


**Figure 4.10** Schematic views of (a) two pristine CNTs (*pCNT-pCNT*), (b) a pristine CNT – a wrapped CNT with chitosan (*pCNT-cwCNT*), and (c) two chitosan-wrapped CNTs (*cwCNT-cwCNT*) where the SWCNT and the polymer used are the (8,8) armchair and 60%*DD* chitosan, respectively. The distances ( $d(Cg_i-Cg_j)$ ) and ( $d(S_i-S_j)$ ) and torsion angle ( $\tau$ ) between the two SWCNTs were defined through the center of gravity ( $Cg$ ) and the surface of each tube in which  $\tau = 0^\circ$  and the two tubes are parallel. The molecular structure of the chitosan's repeating units was shown (d).



#### 4.1.2.1 Dispersion and solubility of CNTs

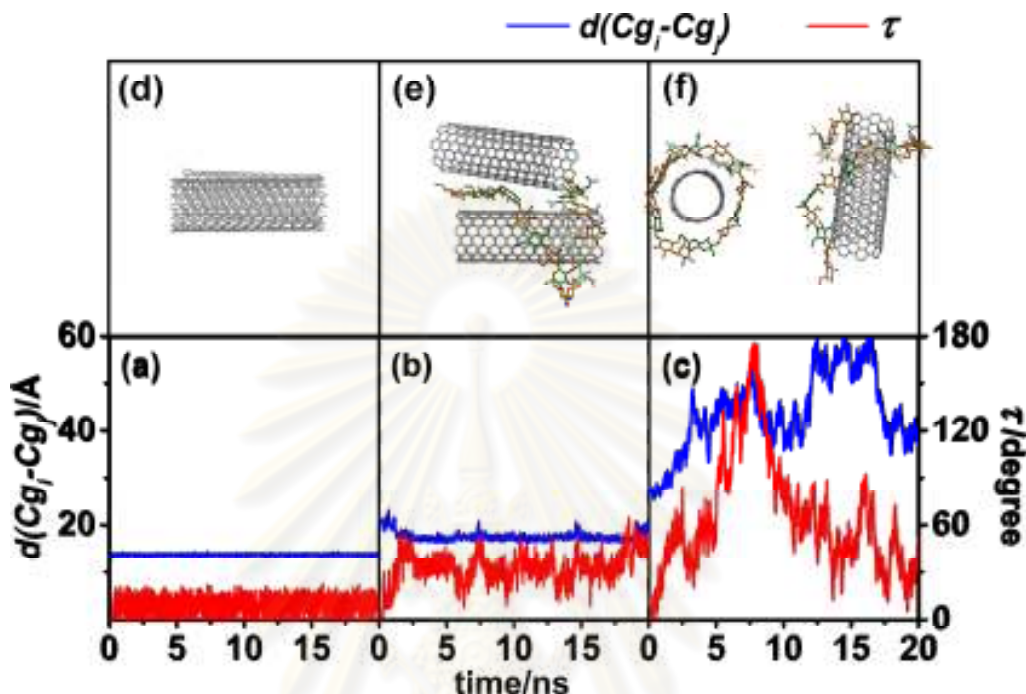


**Figure 4.11** Distance (blue line),  $d(Cg_i-Cg_j)$ , between the two centers of gravity of SWCNT and torsion angle (red line),  $\tau$  (see Figure 4.10 for definition), as a function of the simulation time for the three systems, (a) *pCNT-pCNT*, (b) *pCNT-cwCNT* and (c) *cwCNT-cwCNT*, where their corresponding structures taken from the MD simulation were also shown in (d), (e) and (f).

To understand the chitosan-assisted dispersion and separation of the CNTs in aqueous solution, the tube-tube displacement and orientation were monitored in terms of the distance from the center of gravity of tube  $i^{\text{th}}$  ( $Cg_i$ ) to that of tube  $j^{\text{th}}$  ( $Cg_j$ ),  $d(Cg_i-Cg_j)$ , and the torsion angle between the two SWCNTs' axis,  $\tau$ , respectively (see Figure 4.10 for definitions). The calculated results were shown in Figure 4.11.

In the system of two pristine SWCNTs (*pCNT-pCNT*), the averaged tube-tube displacement represented by the between the centers of tube gravity,  $d(Cg_i-Cg_j)$ , is  $\sim 14$  Å equivalent to that distance between the tube surfaces,  $d(S_i-S_j)$ , of 3 Å (Figure 4.11(a)). In addition, the tilt angle denoted by  $\tau$  angle is  $\sim 11^\circ$ . All values are almost

constant over the period of simulation time. The  $\tau$  data indicated that the two pristine SWCNTs were oriented in almost parallel configuration (Figure 4.11(d)) while the distance between the surfaces,  $d(S_i-S_j)$ , of the two tubes of  $\sim 3 \text{ \AA}$  implied that the hydrophobic and van der Waals interactions between the aromatic rings of both CNTs were observed to play role. This can be a clear answer why the pristine CNTs were found to aggregate experimentally in solution.

With low concentration of chitosan represented by the  $p\text{CNT}-c\text{wCNT}$  system, the  $d(Cg_i-Cg_j)$  was increased by  $\sim 3 \text{ \AA}$  from  $14 \text{ \AA}$  to  $17 \text{ \AA}$  and the tilt angle was increased from  $11^\circ$  to  $33^\circ$ , relative to those of the  $p\text{CNT}-p\text{CNT}$  system. Interestingly, one end of the chitosan fragments was found to unwrap from one tube (CNT#1 in Figure 4.10(b)) and change its configuration to interact with another CNT (pristine, CNT#2 in Figure 4.10(b)), *i.e.*, the chitosan rearranges its conformation to locate in between both CNTs. Although the  $d(Cg_i-Cg_j)$  distance of  $\sim 17 \text{ \AA}$ , with the corresponding  $d(S_i-S_j)$  of  $\sim 6 \text{ \AA}$ , is rather long for molecular interactions but the detected CNT-chitosan-CNT configuration signifies that the chitosan fragments can act as the linker to hold the two tubes together. The simulated phenomenon was firmly supported by the experimental data where the CNT was found to participate in the low concentration of the 60%DD chitosan [80].

Situation is different for the system where both CNTs were wrapped by chitosan fragment,  $c\text{wCNT}-c\text{wCNT}$ . This supposes to represent the CNT in the solution of high concentration of chitosan. As the results, the two wrapped CNTs were found to separate totally and rotate freely, *i.e.*, the noncovalently modified CNTs is highly soluble. This fact was definitely supported by the  $d(Cg_i-Cg_j)$  distance and the  $\tau$  angle ranging from  $\sim 35-60 \text{ \AA}$  and  $\sim 60-180^\circ$ , respectively (Figure 4.11 (c) and Figure 4.11 (f)). The dispersion and solubility of the two modified CNTs is mainly due to the strong repulsion between the positively charged ammonium groups on the glucosamine units of the chitosan.

#### 4.1.2.2 Role of chitosan fragments

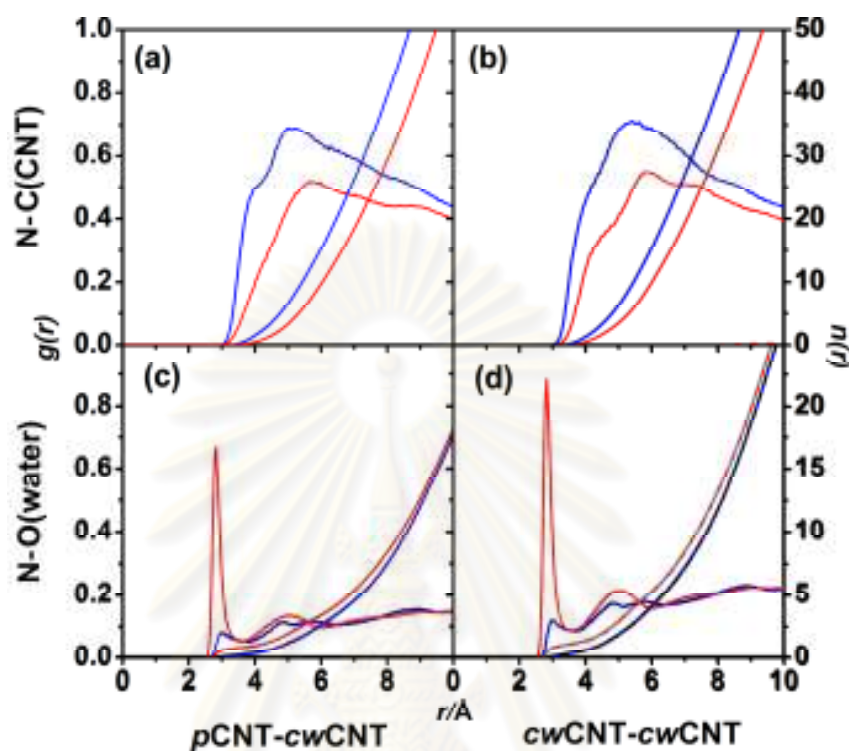


**Figure 4.12** RDFs from the nitrogen atoms on the N-acetyl-D-glucosamine (N(NAG), blue line) and D-glucosamine (N(GLS), red line) of chitosan (see Figure 4.10(d) for definition) to the carbon atoms of the wrapped CNTs (a) CNT#1 for the *p*CNT-*cw*CNT, (b) both CNT#1 and CNT#2 for the *cw*CNT-*cw*CNT and (c) oxygen atoms of water.

According to our previous study on the chitosan-wrapped CNT, the aggregation of the surface modified CNT is possibly due to the hydrophobic interactions between the acetyl groups of chitosan and the aromatic rings of CNT. In order to provide detailed information at molecular level to understand the mechanism of action, the atom-atom radial distribution functions (*RDFs*,  $g_{xy}(r)$ ), that is the probability of finding a particle of type  $y$  within a sphere radius  $r$  around the particle of type  $x$ , were calculated. Here,  $x$  represents the nitrogen atoms of chitosan fragments (the N-acetyl-D-glucosamine (NAG), and D-glucosamine (GLS)), and  $y$  denotes all the carbon atoms of the CNTs

(only the wrapped CNTs shown in Figure 4.10, CNT#1 for the *p*CNT-*cw*CNT and both CNT#1 and CNT#2 for the *cw*CNT-*cw*CNT systems) or the water oxygen atoms. The results were plotted and compared in Figure 4.12.

In the *p*CNT-*cw*CNT system (Figure 4.12(a)), the RDF plots from the N atom on the acetyl group of the NAG unit, N(NAG), and the ammonium group of the GLS unit, N(GLS), to all carbon atoms CNTs show broad maxima at 5.2 Å (blue line) and 5.7 Å (red line) with high and low intensities, respectively. This means that the acetyl group of NAG approaches closer to the outer surface of the tube than the ammonium group of GLS, *i.e.*, the hydrophobic acetyl group (NAG) better interacts with the two tubes through van der Waals interaction than the hydrophilic ammonium group (GLS), causing the CNT aggregation. As expected, the corresponding running integration number, number of water molecule at the distance  $r$ , around the neutral NAG (blue line) is higher than that of the positively charged GLS group (red line) at any distances. This is consistent with the intensity of both plots that of the NAG at any distances is higher than that of the GLS groups.

Similarly for the *cw*CNT-*cw*CNT system (Figure 4.12(b)), the RDF for the NAG (5.6 Å, blue line) takes place at shorter distance than that of the GLS group (6.2 Å, red line) with higher density and higher coordination number. Interestingly, both N(NAG)-C(CNT) and N(GLS)-C(CNT) distances of 5.2 Å and 5.7 Å (Figure 4.12(a)) of the *p*CNT-*cw*CNT system are shorter than those of 5.6 Å and 6.2 Å (Figure 4.12(b)) of the *cw*CNT-*cw*CNT system, respectively. This fact can be described based on the molecular configurations shown in Figure 4.10(b) and 4.10(c), *i.e.*, the chitosan fragment in the high soluble chitosan-wrapped CNT (*cw*CNT-*cw*CNT) can be easily accessed by water molecules than that of the aggregated one (*p*CNT-*cw*CNT). Due to this solvation effect, the chitosan fragment in the *cw*CNT-*cw*CNT system was, then, pulled out to locate at longer distance than that of the *p*CNT-*cw*CNT one.

As expected, the positively charged N(GLS) atom was found to be much better solvated than the N(NAG) atom (Figure 4.12(c) and 4.12(d)). For both systems, *p*CNT-*cw*CNT and *cw*CNT-*cw*CNT, the RDFs for the N(GLS) are much sharper with much higher density than those of the N(NAG). The corresponding coordination numbers,

integrated to their first minima, of the N(GLS) for both systems of 0.9 is higher than that of 0.3 water molecules of the N(NAG) atom.

Molecular dynamics simulation approach was applied to investigate an increase in dispersion and solubility of single-walled carbon nanotube in solution by 60%*DD* chitosan noncovalently wrapped on the outer surface using the three models: *pCNT-pCNT*, *pCNT-cwCNT* and *cwCNT-cwCNT*. In the *pCNT-pCNT* and *pCNT-cwCNT* systems, the distance between the centers of tube gravity and the tube-tube orientation indicated the aggregation of carbon nanotube. This is due to the hydrophobic and van der Waals interactions between the aromatic rings of the two pristine CNTs, and the chitosan wrapped on CNT#1 acting as a linker interacted with both tubes, respectively. In contrast, the two *cwCNTs* were totally separated, freely rotated and well dispersed in aqueous solution owing to the charge-charge repulsive force of the ammonium groups of GLS, a fragment of 60%*DD* chitosan, wrapping on each tube. Interestingly, the hydrophobic acetyl group of NAG fragment is likely to interact with the aromatic rings of carbon nanotube via van der Waals interaction while the positively charged ammonium group of GLS fragment was strongly solvated by waters. These theoretical results can support the previous experimental work in the fact that the hydrophobic acetyl parts of chitosan favored to attach on the nanotubes surface while the hydrophilic ammonium parts provided nanotubes stabilize in the solution by charge-charge repulsive force to each others.

#### **4.1.3 Covalent surface modification of multiwall carbon nanotubes with acid oxidation ( $\text{H}_2\text{SO}_4$ and $\text{HNO}_3$ )**

The multiwall carbon nanotubes (MWCNTs) were oxidized by strong acid,  $\text{H}_2\text{SO}_4$  and  $\text{HNO}_3$ , the oxidation reaction is known to generate various at the open end or the defect sites of carbon nanotubes structure, thereafter functional groups as follow -COOH, -OH, -C=O and another group as sulfur-containing might be introduced in the carbon nanotubes structure.

From the raman spectra of treated and pristine MWCNTs, the characteristic of carbon nanotubes, G band in  $1600\text{ cm}^{-1}$ , and D band in  $1300\text{ cm}^{-1}$  was shown in Figure

4.13. D band presents the amorphous carbon or disordered C in carbon nanotubes while G band was presents the C-C bond in graphene sheet. D band was presented the shoulder of G band that also induced the disordered C. The increasing in intensity of D band suggest disordered structure by carboxylation increased. The  $I_G/I_D$  ratio is used to the assess of the ratio of  $sp^2/sp^3$ . The ratio  $I_G/I_D$  of pristine MWCNTs equal to 0.5056 while the ratio  $I_G/I_D$  of treated MWCNTs equal to 0.2773. This suggests that D band was increased in case of treated MWCNTs because of carboxylic acid groups.

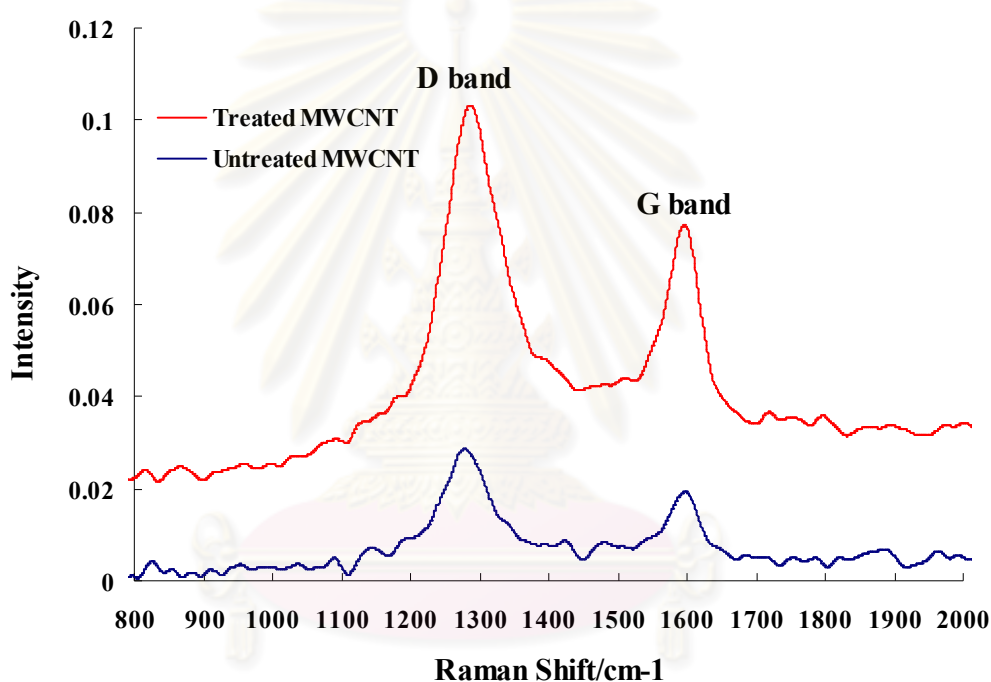


**Figure 4.13** Raman spectra of pristine MWCNT and treated MWCNTs.

The results of FTIR transmission shown that the shoulder peak of carbonyl at  $1710\text{ cm}^{-1}$  shown in Figure 4.14. Although the characteristic peak of carbon nanotubes was not shown clearly in different position, the intensity of the % transmission were increased in case of treated carbon nanotubes. In addition, the height peak of C-H stretching in  $2845$  and  $2912\text{ cm}^{-1}$  decreased after treat MWCNTs with acid.

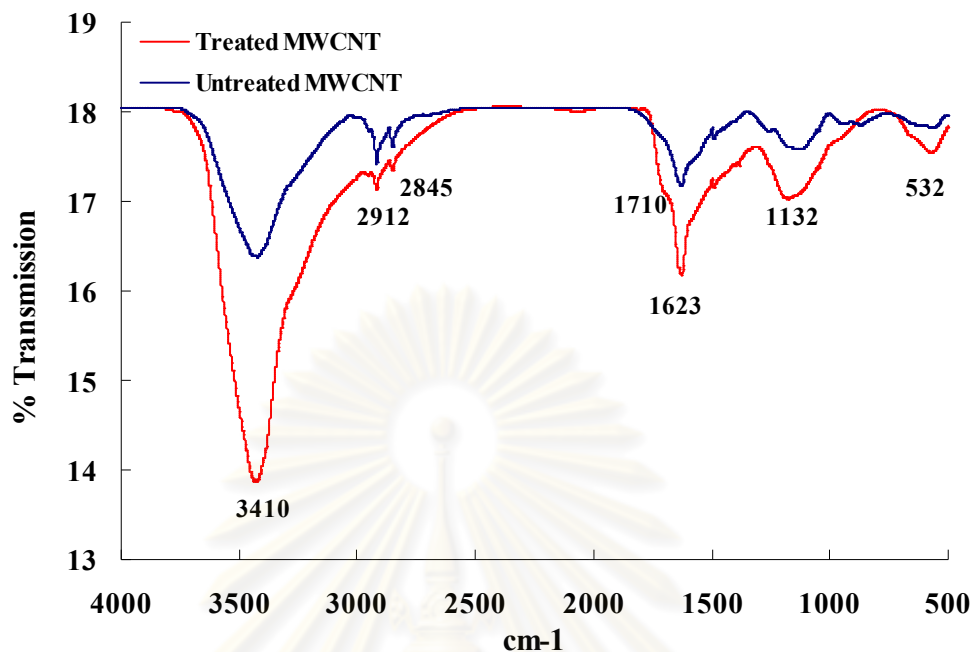


**Figure 4.14** FTIR spectra of pristine MWCNT and treated MWCNTs.

To confirm the functional groups on treated MWCNT, especially carboxylic group, FTIR spectra show the evidence that, 3410 cm<sup>-1</sup> is -OH stretching, 1710 cm<sup>-1</sup> is C=O of carboxylic acid, 1623 cm<sup>-1</sup> is C-C stretching of aromatic and 1132 cm<sup>-1</sup> is C-O of carboxylic acid.

During the oxidation MWCNTs, treated MWCNTs not only have the functional groups on their surface but also obtained in the shorter length. This result was received from the sonication process and as shown in Figure 4.15.

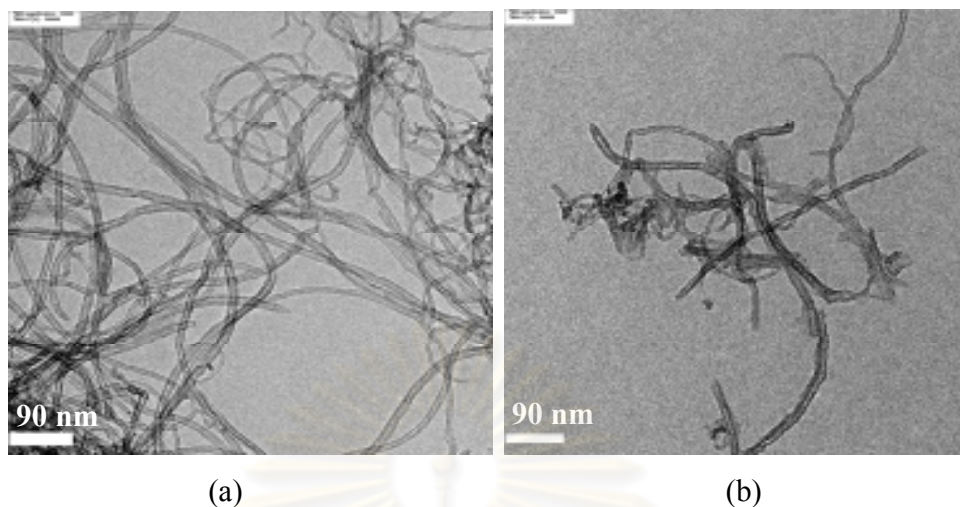


**Figure 4.15** Transmission electron micrograph of (a) pristine MWCNTs and (b) treated MWCNTs.

#### **4.1.4 Layer-by-layer deposition on treated multiwall carbon nanotubes with polyelectrolyte; PDADMAC and PSS without centrifugation process**

The key approach to provide good dispersion and improve the stability of CNT in aqueous solution is to develop a high anionic or cationic charge density at the surface of nanotube. Our previous work has been recently reported the improved adsorption of chitosan around CNT when the degree of deacetylation (%*DD*) of chitosan was lowered from 93%*DD* down to 61%*DD*. However, in term of the stability of modified MWCNTs with chitosan, it was insufficient to prepare as a drug carrier. Therefore, recent literature search is pointing toward a broader usage of the noncovalent surface modification of the nanotubes via layer-by-layer technique.

The functionalized CNT have been proposed by loading polyelectrolytes by layer-by-layer approach [81,82]. Layer-by-layer technique is a major breakthrough of noncovalent surface modification which has been used as a tool to construct polyelectrolyte multilayers with oppositely charged polyelectrolyte onto any type, shape and size of substrates even one dimension of nanomaterials as carbon nanotubes[29, 83].



To modify CNT surface via layer-by-layer technique, polyelectrolytes, enzyme, antibody, nucleic acid, proteins and nanoparticles such as gold and silver nanoparticles [84,85] have been successfully used to deposit on CNT. Moreover, after coating CNT with multilayers, modified CNT was utilized in a wide variety of applications such as a control release anticancer drug [40], cancer biomarker [39] and biosensor [38].

No matter what agent is used in the noncovalent surface modification, the methods usually rely on exposing the nanotubes solution to an excess of polymer followed by tedious centrifugation steps to remove the excess of unbound polymer from the solution. This method provide satisfying results with small volumes but the numerous centrifugation steps as well as the supernatant removal followed by re-dispersion make this method unpractical for scaling up to hundreds of milliliters of CNT solution.

Although this method provides satisfying results with small volumes, the major problem is that it can promote CNTs aggregation during centrifugation step because the carbon nanotubes are forced into dense pack [86]. In addition, the numerous centrifugation steps as well as the supernatant removal followed by re-dispersion make this method unpractical for scaling up to hundreds of milliliters of CNT solution. Moreover, significant amount of carbon nanotubes is lost during the removal of the supernatant. Filtration is another method which can be used to remove unbound polyelectrolyte through the membrane. This way is no forced modified carbon nanotubes into dense pack and it is not necessary to have a density difference between the particle and surrounding media [87]. However, the obstacle of this method is that it's hard to ensure that we can avoid the adsorption of excess polyelectrolyte even modified carbon nanotubes on the filter membrane during the solution pass through the filter membrane. Therefore, the amount of modified carbon nanotubes might possibly be lost during the filtration and re-dispersion process.

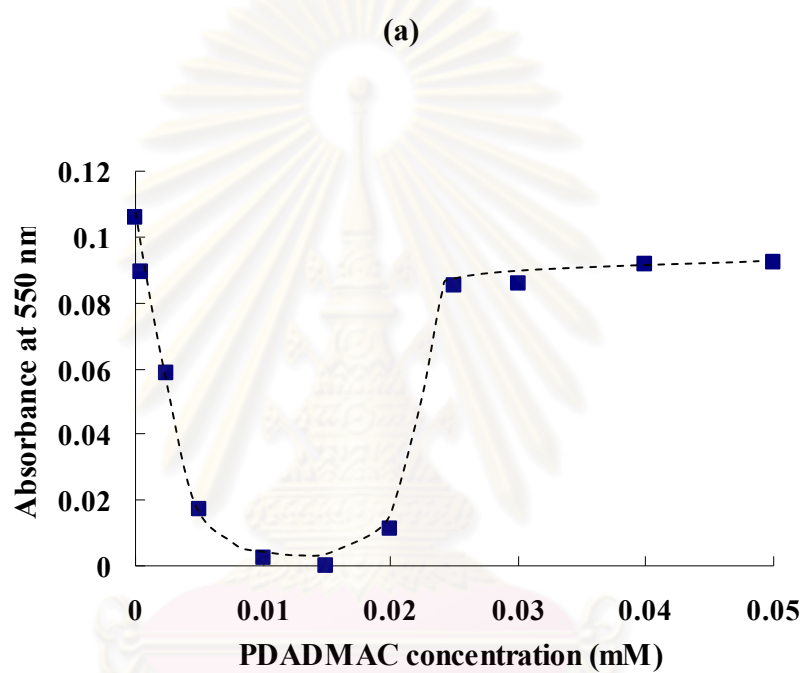
While working on the surface modification of MWCNT with biopolymer, our interest turned toward trying to find a simple method for the “just enough” surface modification of MWCNT by polyelectrolytes solution in order to remove the centrifugation step. Using this method, we have prepared up to 500 ml of MWCNT solutions in a single step but based on the proper adjunction of the polymer amount. Furthermore, the absence of polyelectrolyte excess in solution allowed for the utilizations

of the layer-by-layer deposition techniques with which up to tertiary layer of polyelectrolytes were successively deposited onto the MWCNT surface. The stability of modified MWCNT were identified by measuring turbidity of solution using UV-Visible spectroscopy at wavelength 550 nm combined with zeta potential measurements were used to evaluate and confirm the surface modification of the MWCNT.

#### **4.1.4.1 Primary layer coating on treated MWCNTs with PDADMAC**

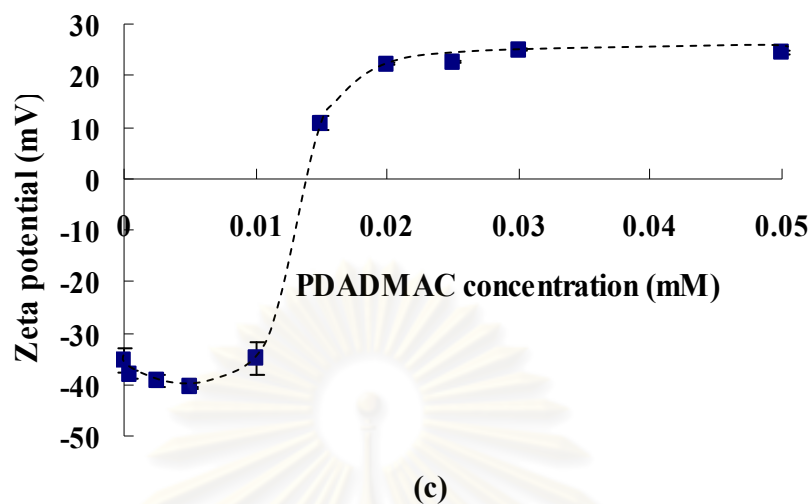
##### **4.1.4.1.1 Effect of PDADMAC concentration on the stability of treated MWCNTs**

As they become more available, MWCNTs will be more present in commercial product and their preparation will need to be scaled up to large batches. The commonly used centrifugation of MWCNT post surface treatment will be unpractical and need to be replaced with simpler method. An alternative method to the previously described centrifugation procedure relies on the adjunction of the “just enough” polyelectrolyte to the MWCNT solution thus limiting the excess polyelectrolyte in solution to the minimum. In order to find the appropriate amount of PDADMAC that need to be added to each MWCNT solution, vials containing fixed amount of MWCNT were mixed with solution of increasing PDADMAC concentrations. The treated MWCNT were sonicated in order to temporarily overcome van der Waals attractive interactions and immediately mixed with the PDADMAC solutions. As the final concentration of PDADMAC was increased, the turbidity of the MWCNT dispersion was recorded by UV-Vis spectroscopy as evidence of the MWCNT stability.



(b)

ศูนย์วิทยทรัพยากร  
จุฬาลงกรณ์มหาวิทยาลัย



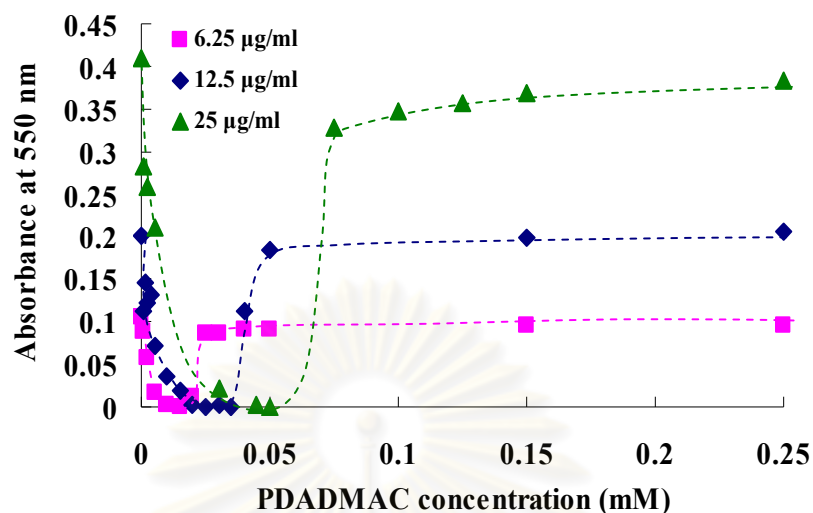
**Figure 4.16** Stability of modified MWCNT 6.25  $\mu\text{g}/\text{ml}$  with different poly(diallyldimethylammonium chloride) concentration (0-0.05 mM) (a) Solutions of treated MWCNT and the modified MWCNT with various PDADMAC concentrations, (b) Plots of the changes in absorbance of modified MWCNT with various PDADMAC concentration after preparing for 1 week, (c) Plots of reversal zeta potential of modified MWCNT with various PDADMAC concentrations.

Figure 4.16(a) showed pictures of the solutions corresponding to various added amount of PDADMAC (vial #2 to #11) compared with the original uncoated MWCNT in vial #1. It can be seen that when increasing the PDADMAC concentration from vial #2 to #6, the solution appeared clearer as the MWCNT precipitated. The appearance of a precipitate at low PDADMAC content is due to incompletely coverage of the surface of the anionic MWCNT. In this case, the two species present in solution are the anionic uncoated MWCNT and the cationic PDADMAC coated MWCNT that aggregate through electrostatic attraction and precipitate. Another reason that induce precipitation is because PDADMAC has large molecular weight ( $\sim 200,000$ - $350,000$  g/mol) that can bind with different MWCNT (negatively charged MWCNT from treated MWCNT and in completely covered MWCNT) in solution and induce their bridged flocculation. Nevertheless, when the concentration of PDADMAC exceeds 0.025 mM as

shown vial #8, the MWCNT in solution remain dispersed with no precipitate appearing. All the MWCNT are then coated with the “primary” cationic PDADMAC layer.

UV-Vis spectroscopy was used to record the turbidity of the MWCNT/PDADMAC mixture at 550 nm as evidence of the CNT dispersion. The turbidity measurements are plotted in Figure 4.16(b) and a decrease in absorbance can be seen in the first section of the plot as the MWCNT precipitate out of the solution. Then, as the PDADMAC concentration was increased sufficiently to coat all the MWCNT, provide good dispersion and result in higher absorbance.

Figure 4.16(c) showed the corresponding zeta potential values for each of the prepared solutions. The zeta potential amplitude is proportional to the charge density at the nanoparticles surface and reflects successful adsorption of the charged polyelectrolytes and its sign corresponds to the anionic or cationic character of the surface. As expected, the zeta potential is reversed from negative for low PDADMAC concentration to positive values when PDADMAC is sufficiently adsorbed at the surface of the MWCNT. It can be seen that the initial negative charge due to the carboxylate is reversed to positive charge due to the presence quaternary ammonium of the PDADMAC. A lower absolute zeta potential value of +24 mV when compared to the -40 mV for the treated MWCNT is probably due to the low charge density of the PDADMAC as well as the fact that some negative carboxylic groups might remain from uncoated segment of the carbon nanotubes.



**Figure 4.17** Plots of the changes in absorbance of modified MWCNT (6.25, 12.5 and 25 µg/ml) with various PDADMAC concentrations (0-0.25mM) after preparing for 1 week.

Using these plots it is possible to identify the concentration of PDADMAC that is needed to modify the surface of the MWCNT and limit its excess in solution. The amount of PDADMAC that need to be added to the MWCNT solution is proportional to the amount of MWCNT present in solution and when different carbon nanotubes concentrations (6.25, 12.5 and 25 µg/ml) were used, it can be seen on Figure 4.17 that PDADMAC concentration of 0.025 mM, 0.05 mM and 0.075 mM are respectively needed. The zeta potential of primary coating MWCNT with PDADMAC in different MWCNTs and PDADMAC concentrations was shown in Figure 4.18.

จุฬาลงกรณ์มหาวิทยาลัย

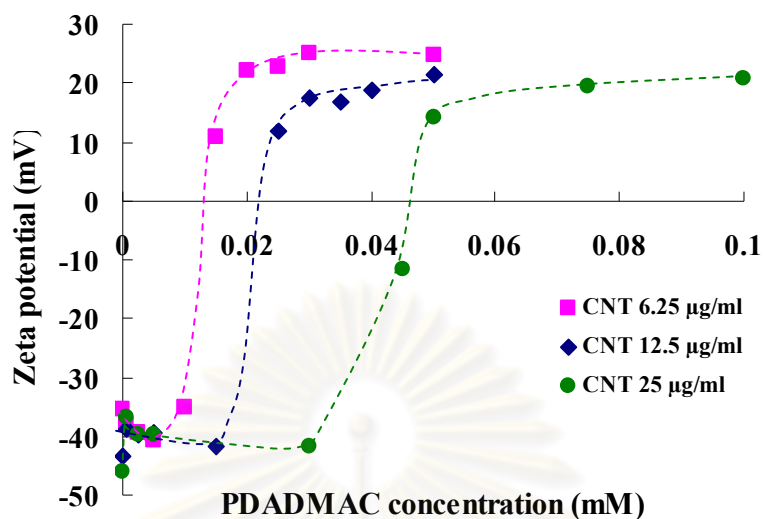


**Figure 4.18** Plots of zeta potential of modified CNT 12.5, 25, 50 µg/ml with various PDADMAC concentrations.

A linear relationship between various MWCNT and PDADMAC content was found in Figure 4.19 to be equal to 0.48 mg of PDADMAC per 1 mg of CNT.

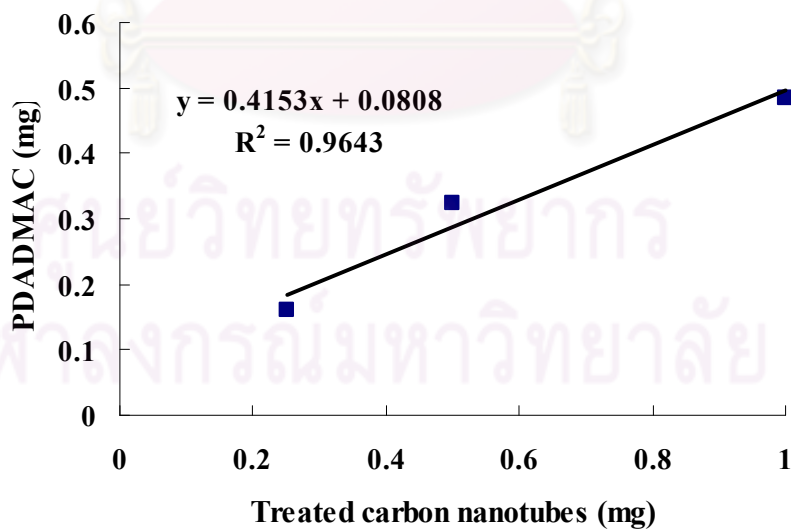


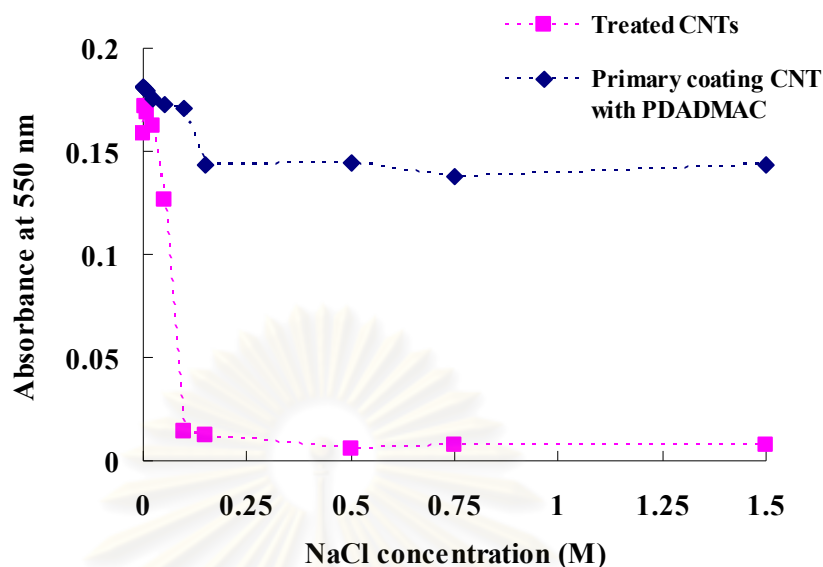
**Figure 4.19** Mass ratio between PDADMAC and treated carbon nanotubes as a primary layer.

Considering the densities of the MWCNT and the PDADMAC layer to have the values of 2.1 and 1.04 g/cm<sup>3</sup> respectively, an average thickness of 3.5 nm per layer can be calculated. Values of 1 nm per PDADMAC monolayer after adsorption on silicon wafer have been previously reported independently of the ionic strength of the solution by Decher but these values are expected to be smaller than that on carbon nanotubes as the electrostatic interaction are much greater on silicon wafer. The layer thickness reported here is also greater probably due to the fact that some PDADMAC segments form loops in the solution leading to a higher amount of PDADMAC adsorbed. These results imply that the polyelectrolytes do not wrap perfectly around the nanotubes and form a loose coating around the nanotubes with some segment adsorbed and some extending largely in solution. This result was confirmed later using TEM imaging.

#### **4.1.4.1.2 Stability of treated and primary coating on MWCNT in different salt concentrations and pH condition.**

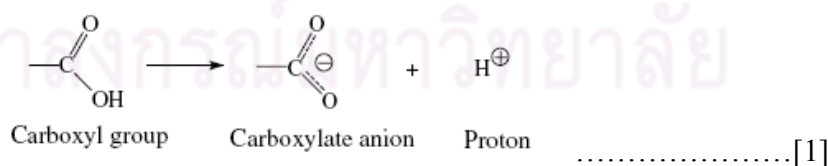
The stability of two modified MWCNT, treated MWCNT and MWCNT coated with PDADMAC in different salt concentration were investigated. Normally, blood in body contain NaCl ~0.15 M, for applying MWCNT as a drug carrier, it was necessary to investigate the CNT stability in various salt concentration to prove that the modified MWCNT can stabilize without any precipitation in NaCl 0.15 M. The absorbance of treated MWCNT starts decreasing at salt concentration 0.1 M and dramatically decreased when the salt concentration reach 0.15 mM (Figure 4.20, squares). While MWCNT coating with PDADMAC were stable in all range of salt concentration (Figure 4.20, diamonds). The carboxylate group of treated CNT were possibly attracted with sodium ion as a counterion to reduce the repulsion between negatively charged nanotubes and finally, aggregation by van der Waals interaction. The MWCNT coated with PDADMAC can be stable in aqueous solution with any salt concentration because the PDADMAC was the pH independent polyelectrolyte.





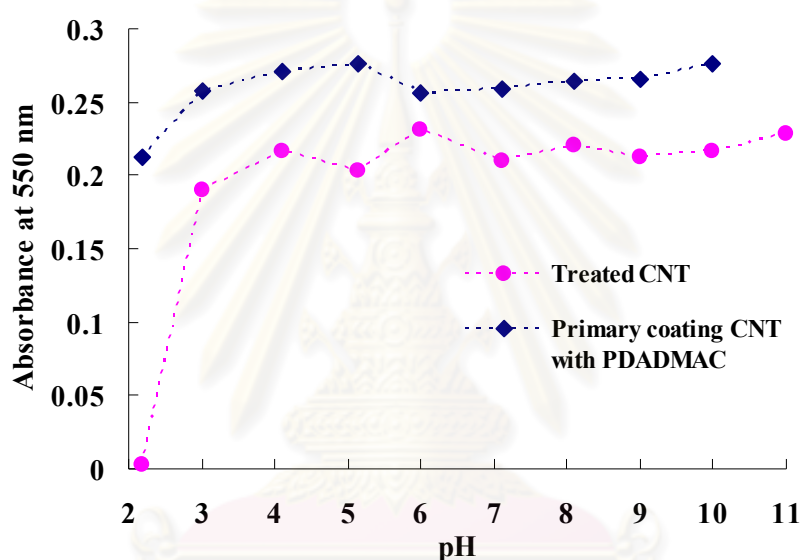
**Figure 4.20** Stability of modified MWCNT, treated MWCNT and PDADMAC coated on MWCNTs, as a function of salt concentration for 1 week.

Figure 4.21 shows the stability of treated MWCNT and primary coating on MWCNT with PDADMAC after dispersed in various  $pH$  solutions. The carboxylic groups were different extent of deprotonation in aqueous solution of various  $pH$  condition. At higher  $pH$ , the extent of deprotonation were increased which lead to higher carboxylate contents. *Yeong-Tarnng Shieh et al.* [88] suggested that the negative charge delocalized over the two oxygen atoms in the carboxylate anion as in reaction [1] below would expel each other and this provides solubility of the treated MWCNTs in aqueous solution.



Although  $pK_a$  of carboxylic acid groups equal 4.5 which means that at  $pH$  4.5, the same proportion of neutral and ionized species present in solution, treated MWCNT can be stable in aqueous solution  $pH \geq 3$  while treated MWCNT were

precipitated at  $pH$  2. The results agree with research work of *Barron et al.* [89]. They found that the carboxylic acid-functionalized CNTs was fully protonated in water of below  $pH$  3 in which the MWCNTs were closed to neutral. The fully protonated carboxylic acid of treated CNTs were aggregated by intermolecular hydrogen bonding of carboxylic acid groups and tend to precipitate. At high  $pH$ , treated CNTs were stable even the  $pH$  of aqueous solution equal 11. However, the ionic strength in the system were possibly increased at  $pH$  higher than 11 and treated CNT can be precipitated.



**Figure 4.21** Stability of modified MWCNT, treated MWCNT and primary coating MWCNTs with PDADMAC, as a function of  $pH$  for 1 day.

#### 4.1.4.2 Secondary layer coating on MWCNTs

Using the MWCNT modified with the primary layer of PDADMAC, a similar procedure was used to deposit another layer of anionic PSS. An increase in PSS concentration leads the primary coating MWCNT with PDADMAC to precipitate because the secondary coating MWCNT with PDADMAC/PSS complex with primary coating MWCNT with PDADMAC inadequate PSS concentrations. The changed of

absorbance at 550 nm in modified MWCNT solution can be observed in term of turbidity was shown in Figure 4.22. Until the PSS concentration reach to 0.04 mM, the primary coating MWCNTs can disperse in the aqueous solution and provide the reversal of the MWCNT surface charge to negative as shown from the zeta potential's evidence in Figure 4.23. The zeta potential result confirmed that the secondary coating on MWCNT were successfully prepared.

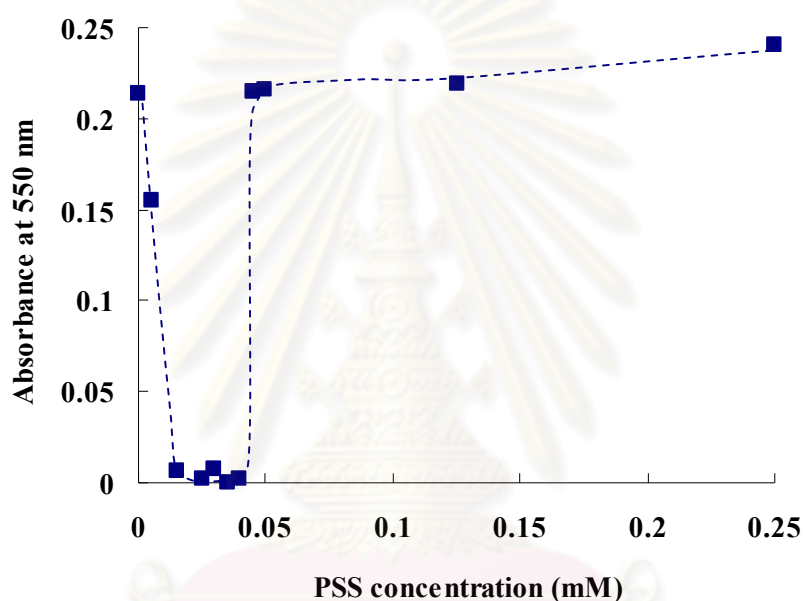


**Figure 4.22** Plots of changes in absorbance of primary coating MWCNT with PDADMAC as a function of PSS concentrations, final amount of MWCNT: 12.5  $\mu\text{g/ml}$ .

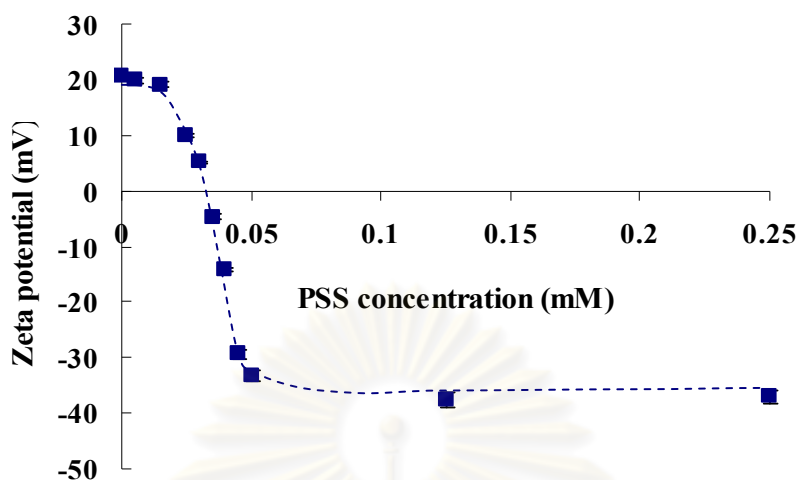


**Figure 4.23** Plots of the reversal zeta potential of primary coating MWCNT with PDADMAC as a function of PSS concentrations, final amount of MWCNT: 12.5  $\mu\text{g/ml}$ .

The amount of PSS added to reverse the surface charge from the PDADMAC top layer was found to be nearly equimolar than that of the previous PDADMAC layers suggesting the nearly 1:1 ratio of the polyelectrolytes for surface charge compensation. Also because the primary solution did not contain excess PDADMAC, it was possible to mix it directly with the PSS solution without the need of a centrifugation step and without the appearance of any precipitate in the solution.

#### 4.1.4.3 Tertiary layer coating on MWCNTs

To demonstrate the usefulness of this technique a third layer of PDADMAC was deposited onto the anionic PSS coated secondary MWCNT. The benefit of this technique rely on the possible successive deposition of polyelectrolytes layers onto the MWCNT without having to centrifuge the MWCNT.

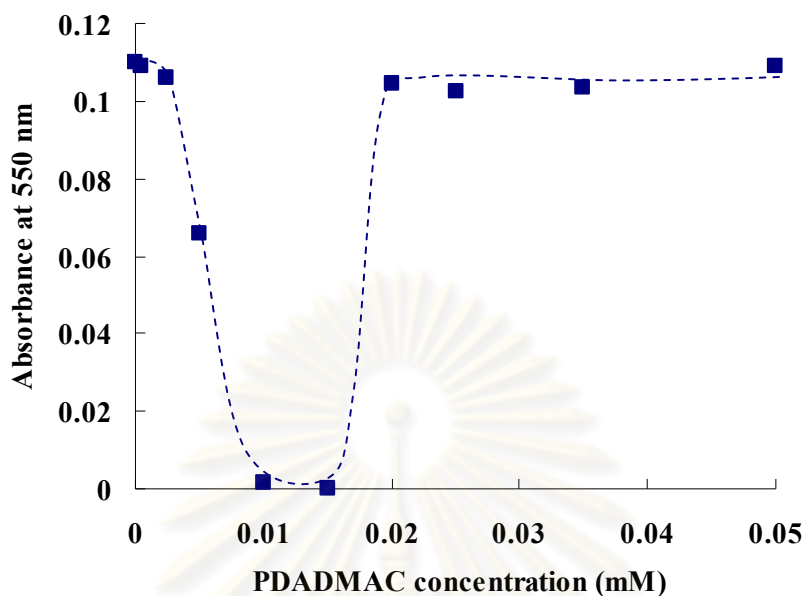


**Figure 4.24** Plots of changes in absorbance of secondary coating MWCNT with PDADMAC/PSS as a function of PDADMAC concentrations, final amount of MWCNT: 6.25  $\mu\text{g/ml}$ .

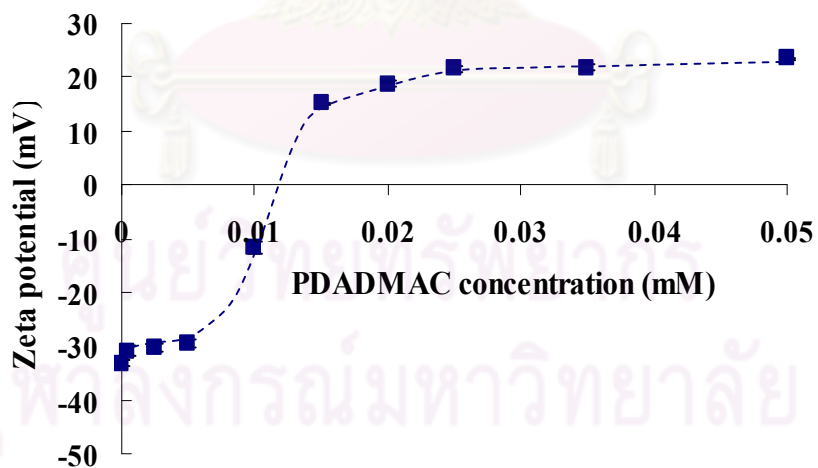


**Figure 4.25** Plots of the changed in zeta potential of secondary coating MWCNT with PDADMAC/PSS as a function of PDADMAC concentrations, final amount of MWCNT: 6.25  $\mu\text{g/ml}$ .

In Figure 4.24, the changes in zeta potential values are plotted for the deposition of the primary, secondary and tertiary layer as a function of the added polyelectrolyte concentrations. The zeta potential values for each layer are presented in Figure 4.25 and can be seen to alternate between positive and negative after the deposition of each layers in Figure 4.26.

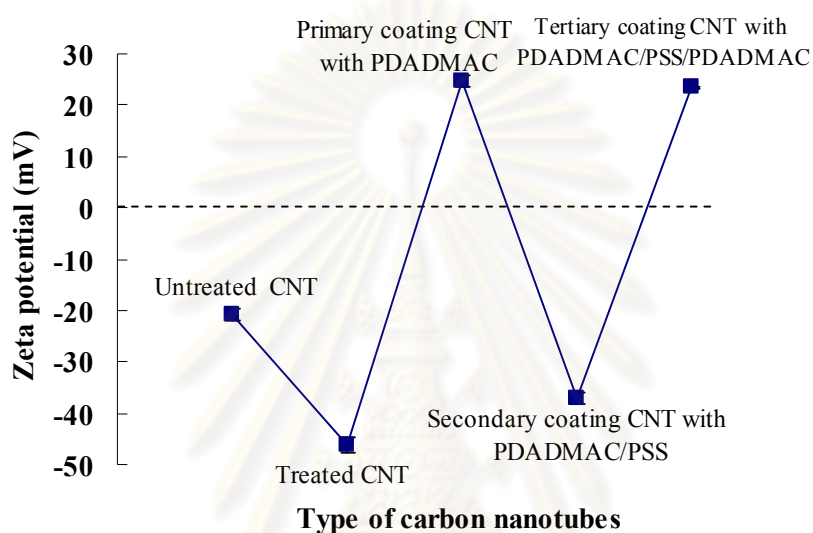


**Figure 4.26** Zeta potential of untreated MWCNT, treated MWCNT, primary coating MWCNT with PDADMAC, secondary coating MWCNT with PDADMAC/PSS, and tertiary coating MWCNT with PDADMAC/PSS/PDADMAC.

Transmission electron microscopy (TEM) was used to measure the thickness of the three layers coating on the MWCNT (Figure 4.27). The calculated thickness for each deposited polyelectrolytes layers was 3.5 nm per layer which would lead to 10.5 nm of three layers coating. Evidence of the fast growth of the PEM onto the MWCNT surface can be seen from TEM images of the bare MWCNT and the 3 layers (PDADMAC/PSS/PDADMAC) coating. The multiwall carbon nanotubes used in this study have a diameter of 14 nm and the thickness of the final coating can be estimated to be 13.4 nm (+/- 2 nm) which value is closed to the calculated value from polyelectrolytes adsorption. The coating of three PDADMAC/PSS layers is thicker than the deposition on

flat silicon wafer. This is probably due to the formation of a large number of loops and tails in solution. Nevertheless this is beneficial to the coating efficiency, suggesting that the coating thickness is sufficient for drug loading and can be achieved much faster than expected from flat substrates. The layer-by-layer technique is a method of choice for the modification of MWCNT as it provides a good control over the surface chemistry and the surface charge can be tuned by the number of deposited layers. The fast growth of the PEM coating by formation of a loose structure can then be used for the selective adsorption of either cationic or anionic drugs depending on the charge of the top layer.

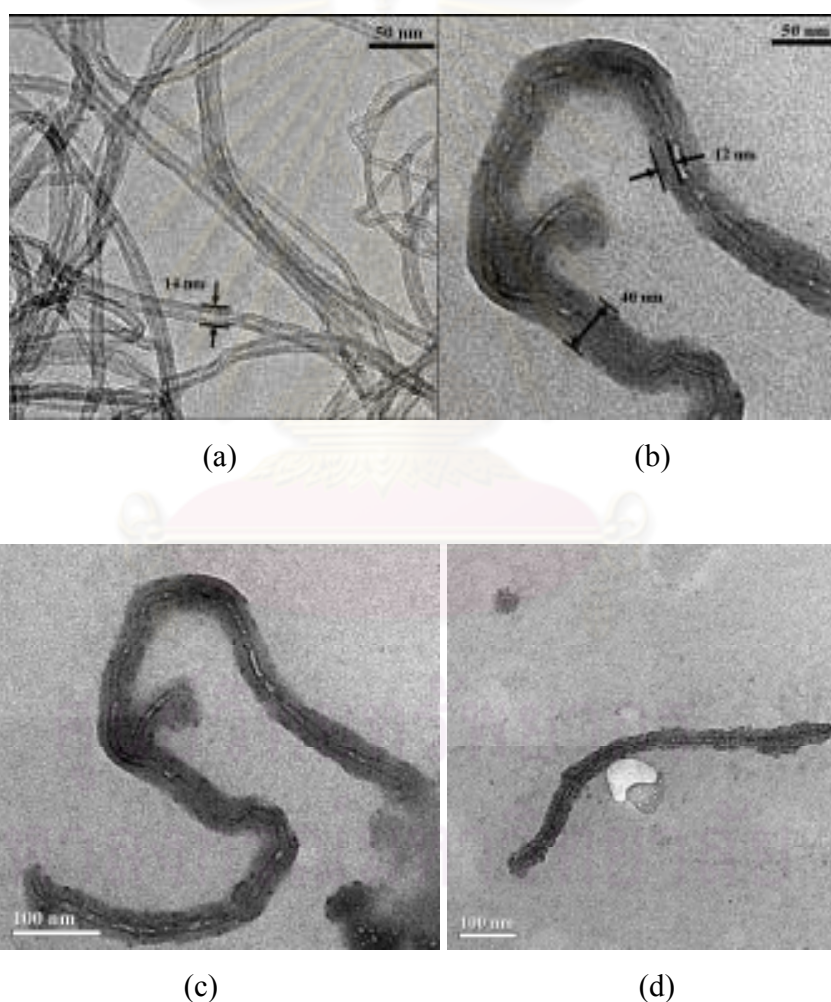


**Figure 4.27** Transmission electron micrograph of (a) pristine MWCNT scale bar 50 nm, (b) tertiary coating MWCNT with PDADMAC/PSS/PDADMAC scale bar 50 nm, (c),(d) tertiary coating MWCNT with PDADMAC/PSS/PDADMAC scale bar 100 nm.

In conclusion, by carefully controlling the concentration of polyelectrolytes in solution, the layer-by-layer deposition of polyelectrolytes multilayers on MWCNT is simplified and do not require tedious centrifugation-sonication steps. Since the sufficient amount of PDADMAC and PSS were deposited on treated carbon nanotubes surface as a primary, secondary and tertiary layer, the modified MWCNT can then be prepared in large scale. The adsorption of the polyelectrolytes for each layers was monitored by turbidity measurement with a UV-Vis spectrophotometer and zeta potential. Using TEM imaging, the thickness of the three layers coating on the MWCNT was measured to be 13.4 nm which suggest the formation of loose polyelectrolyte network onto the MWCNT surface. This simple method can be used to coat large scales of CNT solutions for drug delivery applications.

## **4.2 Loading and recovery of hydrophilic model drugs of modified multiwall carbon nanotubes**

### **4.2.1 Loading and recovery of gentian violet of treated multiwall carbon nanotubes, primary and secondary coating multiwall carbon nanotubes**

Treated MWCNTs which were negative charge in 0.1xPBS buffer were coated with cationic polyelectrolyte: PDADMAC by electrostatic interaction. The insufficient concentration of PDADMAC to coat treated MWCNT lead to the aggregation between two species which were negatively charged species; uncoated MWCNT and positively charged species; PDADMAC coated MWCNT. Therefore, some treated MWCNTs were still suspended but some MWCNTs were precipitated by attracting with a slight concentration of PDADMAC. Until the aggregation between negatively charged of MWCNTs and positively charged of MWCNTs lead all of MWCNT completely precipitate in the solution, the solution become clear and lead the absorbance become nearly zero. When the concentration of PDADMAC was adequate to coat MWCNT, the modified MWCNT in solution can suspend in the solution and providing their stability in the aqueous solution. The lowest concentration of PDADMAC which provide modified MWCNT suspend in the solution was selected to prepare positively charged MWCNT as



a precursor to deposit the secondary layer as PSS in the next step. The amount of PSS added to reverse the charge from the PDADMAC top layer was found. Also because the primary solution did not contain excess PDADMAC, it was possible to mix it directly with the PSS solution without the need of a centrifugation step and without the appearance of any precipitate in the solution. To demonstrate the usefulness of this technique a third layer of PDADMAC was deposited onto the anionic PSS coated secondary MWCNT. The benefit of this technique rely on the possible successive deposition of polyelectrolytes layers onto the MWCNT without having to centrifuge the MWCNT. In Figure 4.28, the zeta potential values for each layer are compiled in and can be seen to alternate between positive and negative after the deposition of each layers in 0.1xPBS.

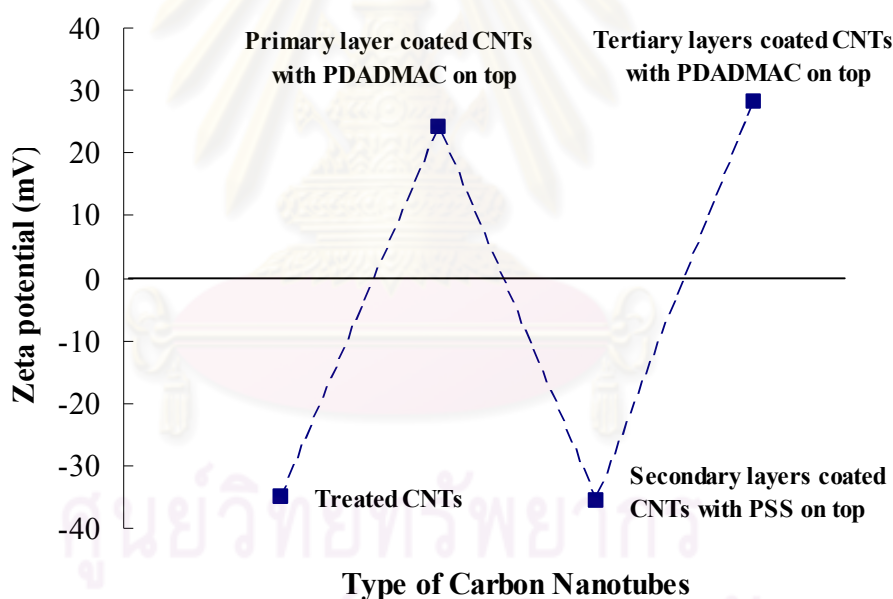


**Figure 4.28** The reversal charge when the CNTs were modified with primary, secondary, and tertiary layer in 0.1xPBS buffer.

As mention above, the multilayers on the carbon nanotubes using layer-by-layer deposition technique was prepared by controlling the added polyelectrolyte

concentrations. Therefore, we can control the negative or positive charge in each layers on carbon nanotubes surface in order to load the hydrophilic drug on their surface.

Gentian violet with different concentrations was used as a cationic model drug for loading on modified MWCNT. After 24 hr of loading time, the remaining gentian violet after loading on modified MWCNT can be investigated using UV-Vis spectroscopy measurement at wavelength 585 nm. The adsorption of gentian violet on MWCNT can be observed by calculate from calibration curve of different gentian violet concentration in Figure 4.29.

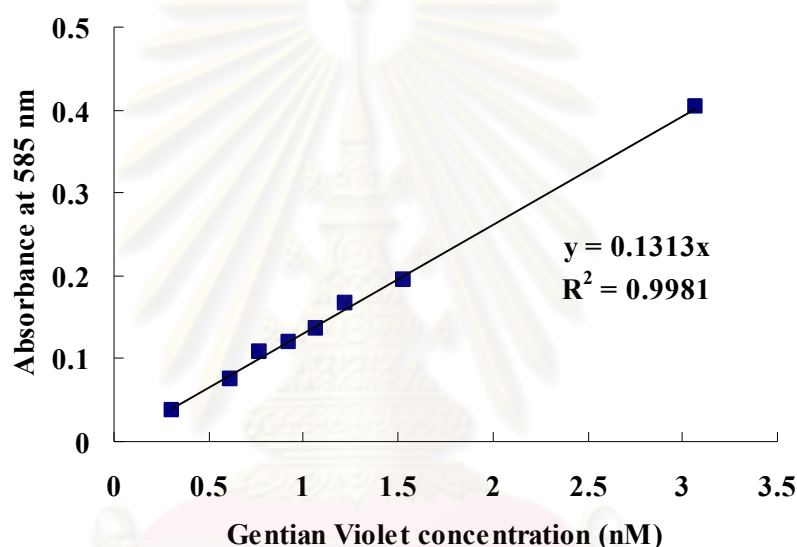


**Figure 4.29** Calibration curve of gentian violet in 0.1 PBS buffer with different concentrations.

Based on our hypothesis, the cationic drug as gentian violet should be favored loading on the negative charged surface by electrostatic attraction. As we expected, negative charged surface which consist of treated MWCNT and the secondary coating MWCNT with PDADMAC/PSS can adsorb gentian violet (shown in Figure 4.30, Figure 4.32) while the primary coating MWCNT with PDADMAC can slightly adsorb in Figure 4.31.

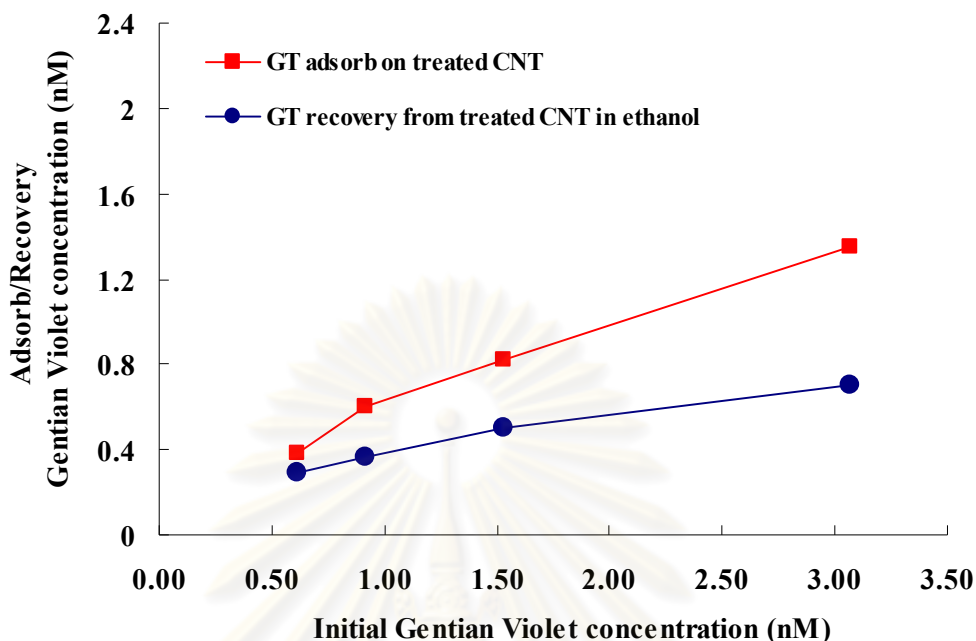


**Figure 4.30** Comparison concentrations of gentian violet adsorption in 0.1 PBS and recover in ethanol from treated MWCNT.

The treated MWCNT were dispersed in the 0.1 PBS pH 7.4, gentian violet was adsorbed on treated MWCNT surface by electrostatic attraction between carboxylate groups and ammonium groups. In addition, gentian violet is possible to attach on treated MWCNT surface by pi-pi stacking between the aromatic ring of both gentian violet and the carbon nanotubes structures. As shown in the Figure 4.30, the increasing of gentian violet concentration increase in gentian violet adsorption on treated carbon nanotubes. The % loading of gentian violet can be calculated when compared with the initial gentian violet concentrations consist of 63.1, 65.9, 53.4 and 44.1%, respectively. After centrifugation process, the gentian violet adsorbed on treated MWCNT were released with ethanol by vortex, we found that the % release for recovering gentian violet from treated MWCNT was follow 76.6, 60.3, 61.3, and 52.2%, respectively. It is possible that the high concentration of gentian violet slightly favored to adsorb on the treated MWCNT surface.

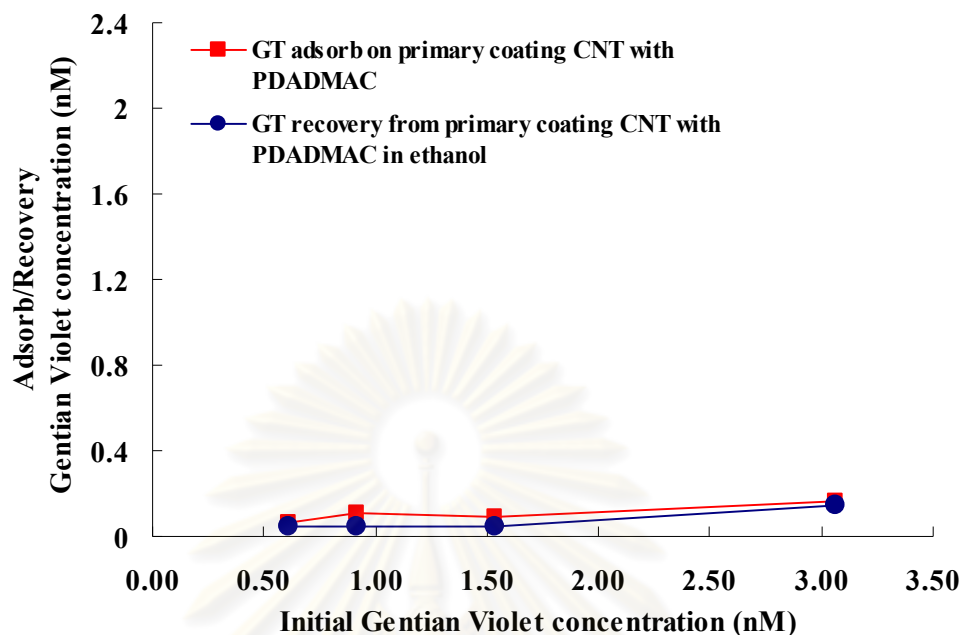


**Figure 4.31** Comparison concentrations of gentian violet adsorption in 0.1 PBS and recover in ethanol from primary coating MWCNT with PDADMAC.

For the primary coating on MWCNT with PDADMAC, the result clearly showed that gentian violet are hardly adsorbed on positive MWCNT because of the repulsion of the ammonium groups between gentian violet and PDADMAC on MWCNT surface (Figure 4.31). The % adsorption were just only 10%. However, just only 10% adsorption are possibly expected that the uncompletely coated MWCNT with PDADMAC remained the small area of uncoated MWCNT which favor to adsorb gentian violet.

ศูนย์วิทยาศาสตร์  
จุฬาลงกรณ์มหาวิทยาลัย

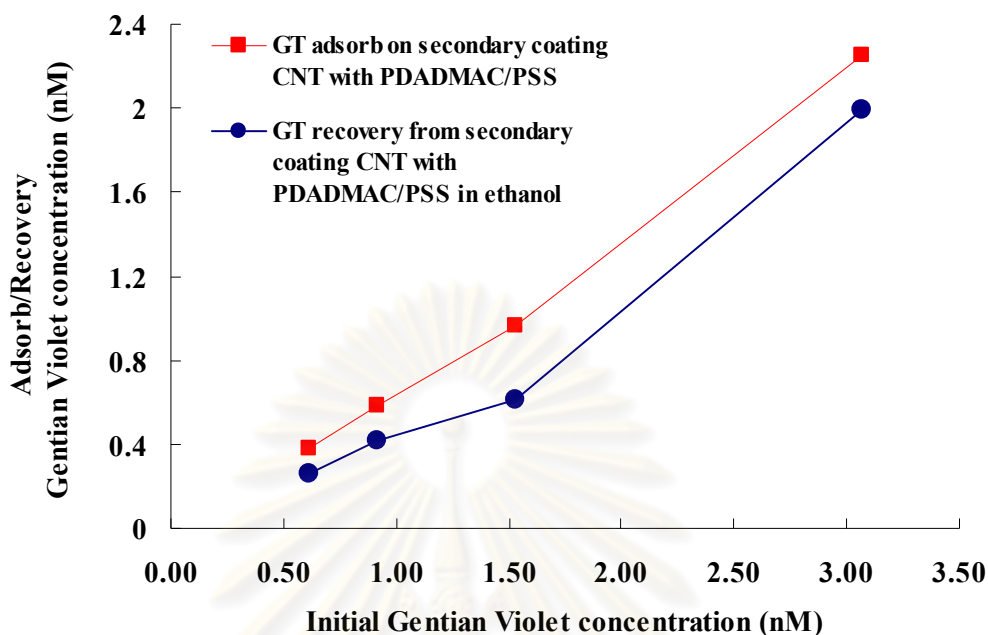


**Figure 4.32** Comparison concentrations of gentian violet adsorption in 0.1xPBS and recover in ethanol from secondary coating MWCNT with PDADMAC/PSS.

According to the quaternary ammonium groups in gentian violet structure, the adsorption of gentian violet onto negative charge on surface of modified MWCNT was based on electrostatic attraction between the oppositely charged molecules. The high gentian adsorption was shown (Figure 4.32) in case of secondary coated layer which was PSS on top because the film coated on MWCNT can provide more adsorption rather than treated CNT which are having the carboxylate groups on their surface.

After loading gentian violet on modified MWCNT, the adsorption of gentian violet on modified MWCNT were quantified by releasing in ethanol which was good solvent for gentian violet. We can see that the gentian violet can be released from the modified carbon nanotubes in different concentrations. For the recovering of gentian violet from different modified MWCNT in ethanol, we found that coating MWCNT with PDADMAC and PSS on top can recover gentian violet more than treated MWCNT. This evidence showed that the affinity attraction between ammonium groups from gentian violet and negatively charged species which were carboxylate and sulfonate group was different. However, gentian violet on modified MWCNT with PDADMAC can be

released less than other condition because of less loading of gentian violet on their surface.

#### **4.2.2 Loading and recovery of diclofenac of treated multiwall carbon nanotubes, primary and secondary coating multiwall carbon nanotubes**

As mentioned treated carbon nanotubes, primary coating MWCNT with PDADMAC and secondary coating MWCNT with PDADMAC / PSS were prepared in 0.1 x PBS buffer, *pH* 7.4. Diclofenac sodium was prepared different concentrations (0.00025-0.01%) in 0.1 x PBS buffer. 20 ml of modified MWCNT were mixed with 20 ml of diclofenac in different concentrations. The solution were kept for 24 hr, after that the mixture solution were centrifuged at 14000 rpm for 15 min. The supernatant solution were measured by UV-Vis spectroscopy to determine unbound diclofenac. In this case, the modified MWCNT with any coating had no effect to load diclofenac as shown in Figure 4.33.

Diclofenac concentrations in the supernatant after centrifugation remain unchanged. This is because at *pH* 7.4, diclofenac were completely ionized and act as a salt which prefer to dissolve rather than adsorb on carbon nanotubes. Especially the negatively charged of treated MWCNT and secondary coating MWCNT possibly repel diclofenac because of their same negative charges. However, even positive charge on top surface as PDADMAC coated on MWCNT can not load diclofenac as well because the remaining diclofenac might possibly come out during the centrifugation process.

ศูนย์วิทยาศาสตร์  
จุฬาลงกรณ์มหาวิทยาลัย

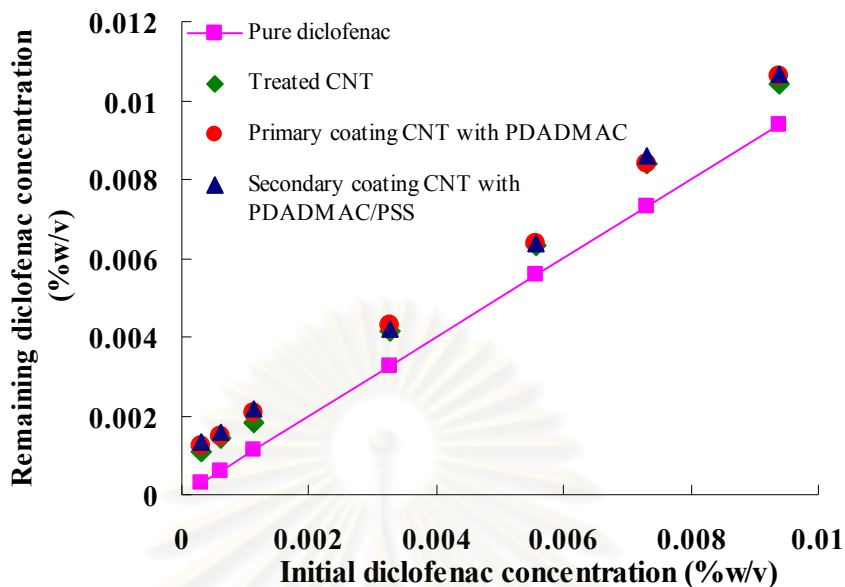


**Figure 4.33** The remaining of diclofenac concentrations in 0.1 PBS after loading to modified carbon nanotubes.

Coating on carbon nanotubes with PDADMAC and PSS in term of primary and secondary layers using Layer-by-Layer technique was successful in this work. The type of charges on nanotubes is affected on drug loading efficiency. Gentian violet can be loaded on secondary coated on nanotubes surface reach to 73% whereas diclofenac sodium can not be loaded in any modified MWCNT because it's ionized and become water soluble at PBS buffer  $pH$  7.4.

#### 4.3 Cytotoxicity of modified carbon nanotubes

According to the hot issue "Toxicity of CNTs", before integrating CNTs into biomedical application, the effect of CNTs on cell have to be considered. Many publications have been proposed that CNTs are toxic while some publications still approved that CNTs are nontoxic. A wide variety of CNT toxicity results was possibly influenced from 5 main factors including size, shape, source, surface chemistry and surface area of CNTs. Therefore, toxicity issue of CNTs are still argued and discussed in wide academic research while the attempt to apply CNTs in biomedical application is

also increased. However, it is hard to find the suitable assay for cytotoxicity test, which is based on colorimetric indicator because pristine CNT surface having high hydrophobic property that possibly adsorb the dye during testing and affecting to the obtainable result. Therefore, the toxic results that we get might be false positive data.

MTT assay has been widely used as a common assay for testing cytotoxicity even there are still ongoing discussion for suitable approach. In this study, the formazan adsorption interference of untreated MWCNT and treated MWCNT was compared.

#### 4.3.1 Interference of adsorption formazan by carbon nanotubes

The untreated MWCNT can adsorb the formazan solution more than treated MWCNT as shown in Figure 4.34. Due to the surface chemistry of pristine MWCNT which are hydrophobic, it is easily adsorbed with hydrophobic formazan more than hydrophilic surface of treated MWCNT. The result clear that pristine MWCNT can interfere with toxicity results while the treated MWCNT is less interfered although the concentrations increased.

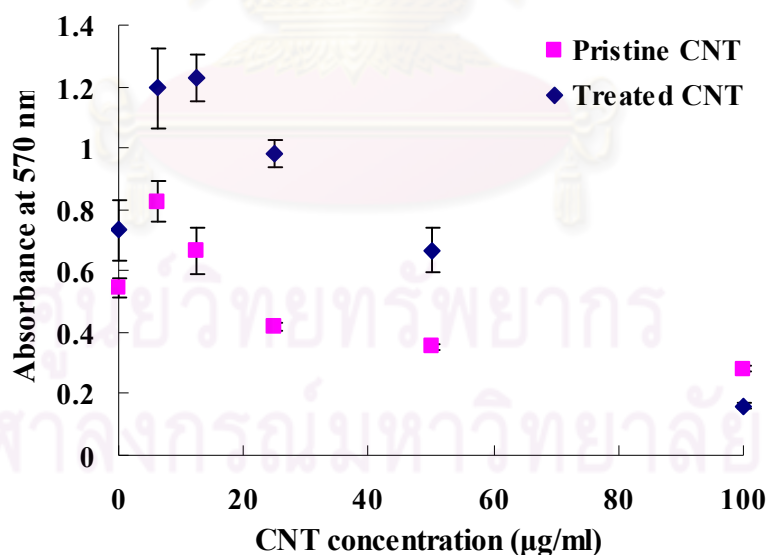


**Figure 4.34** The absorbance of formazan solution at 570 nm after exposed with Untreated and treated MWCNT with various concentrations.



This result, we indicated that the treated MWCNT adsorbed formazan less than untreated MWCNT because of their charged surface. Although MWCNT still effected to the cytotoxicity results, the modified MWCNT which are water soluble, might not affect much for MTT assay and we can get more accurate results.

However, we attempt to avoid the interference of adsorption formazan from MWCNT by removing the MWCNT samples after expose with L929 cells by PBS before adding MTT solution

#### **4.3.2 Cytotoxicity of untreated, treated, primary coating MWCNT with PDADMAC, secondary coating MWCNT with PDADMAC/PSS, tertiary coating MWCNT with PDADMAC/PSS/PDADMAC on L929 fibroblast cells**

##### **4.3.2.1 Cytotoxicity of untreated and treated MWCNT**

The cytotoxicity of MWCNT was evaluated with MTT assay. After exposing pristine and treated MWCNT into L929 cells for 24 hr, the samples were washed out by PBS and MTT was exposed to the cells. The living cells can reduce MTT to Formazan crystal inside the cells while the function of death cell were lost, therefore they cannot convert MTT to formazan.

After dissolving formazan crystal with DMSO, the absorbance of formazan solutions were measured and compared with the cell control. The results (Figure 4.35) showed that the increasing of both untreated and treated MWCNT concentration from 3.125 until 12.5  $\mu\text{g/ml}$  provide the nearly formazan absorbance value. When the concentration of both types of MWCNT reach 25  $\mu\text{g/ml}$ , the treated MWCNT become toxic to the L929 cells while the untreated MWCNT are nontoxic.

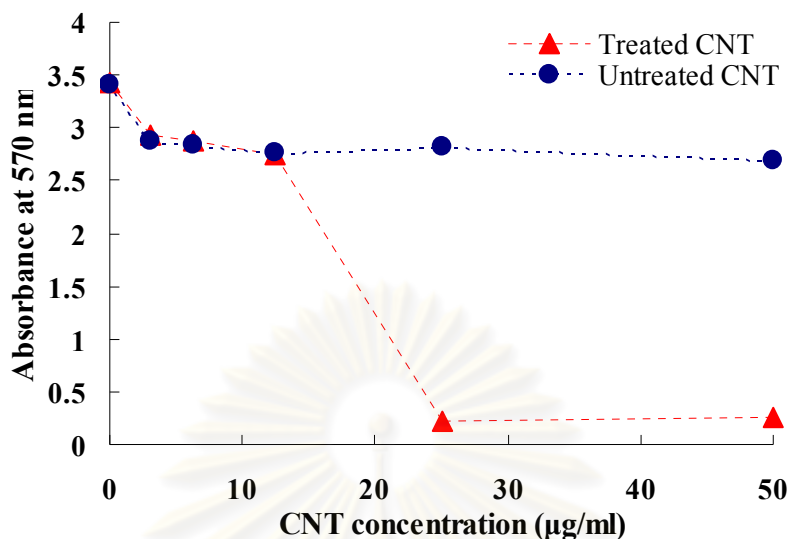


**Figure 4.35** The absorbance of formazan after convert from MTT by exposing L929 cells with different concentrations of untreated and treated CNT for 24 hr.

When we calculated the % cell viability which compare with cell control as shown in Figure 4.35, the result showed that % cell viability after exposed the pristine MWCNT with different concentration provide high cell viability in range 78-83% while %cell viability of treated MWCNT provide 85-80% in treated MWCNT concentration range 3.125-12.5 µg/ml. At high concentration of treated MWCNT, the treated MWCNT reach to 25 µg/ml and 50 µg/ml, the % cell viability were dramatically decreased in to 21.4 % and 7.41%, respectively as shown in Figure 4.36. We expected that the treated MWCNT which were the shorter length provide the high dispersion because of their carboxylic groups. Therefore, treated MWCNT can easily penetrate into the cell membrane compared to the untreated MWCNT which were aggregated and having long length in term of several µm. The untreated MWCNT were hardly penetrated into the cells because of their large size of aggregation.

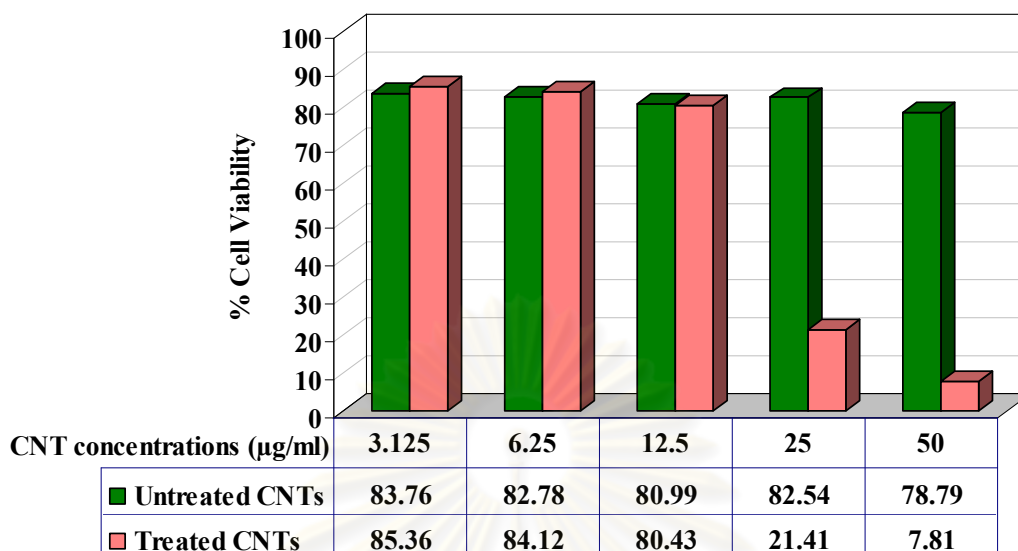


**Figure 4.36** % Cell viability of L929 cell after exposed with untreated and treated MWCNT with different concentrations for 24 hr.

#### 4.3.2.2 Cytotoxicity of primary coating MWCNT with PDADMAC, secondary coating MWCNT with PDADMAC/PSS and tertiary coating MWCNT with PDADMAC/PSS/PDADMAC

However, we attempt to modified MWCNT with different functional groups by deposition of PDADMAC and PSS in order to improve cell viability by selective functional groups. Primary (PDADMAC), secondary (PDADMAC/PSS), and tertiary (PDADMAC/PSS/PDADMAC) coating on MWCNT surface were prepared in 0.1xPBS buffer, thereafter, the modified MWCNT were separated into two type which were tested with the solution. Another were centrifuged in order to remove the excess polymer and kept as a powder. All samples were exposed into L929 cells for 24 hr, the cytotoxicity of polyelectrolyte were tested as a control. PDADMAC and PSS with the different concentrations were exposed into L929 cells for 24 hr. An increase in PDADMAC concentration from 0.001 to 0.01 mM does not affect cell viability. However,

when the concentration of PDADMAC reach 0.05 mM, formazan absorbance dramatically decreased due to lost functions of cells (Figure 4.37).

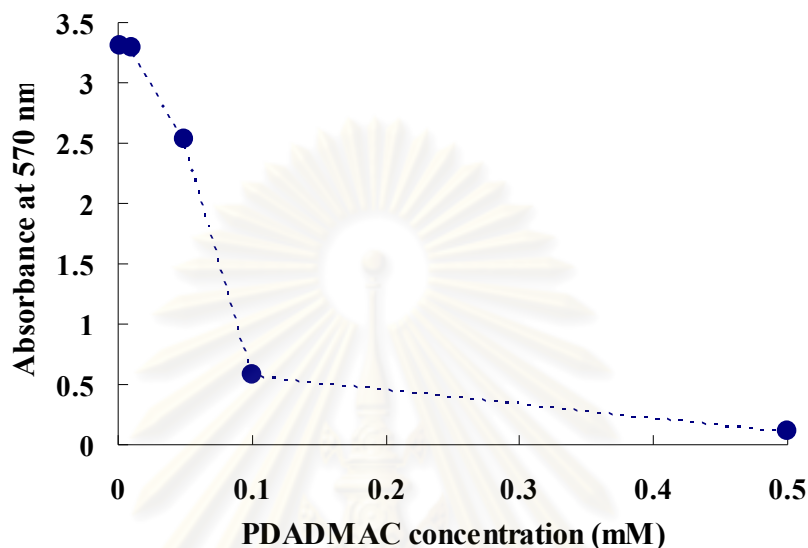


**Figure 4.37** The absorbance of formazan after convert from MTT by exposing L929 cells with different concentrations of PDADMAC solution for 24 hr.

The % cell viability can be calculated from the changed in absorbance of formazan when compare with the cell control. In Figure 4.38, % cell viability dramatically decreased after exposed PDADMAC solution reach to the concentration 0.05 mM. As shown the cell morphology after exposed PDADMAC (Figure 4.39), the L929 cells morphology were changed from the spread to shrink into round shape. Due to the synthetic polymer and their structure consist of positive charge from ammonium groups. The cationic groups can attach on the negatively charged surface of cell membrane by electrostatic attraction. In addition, the molecular weight of PDADMAC might affect the cell. However, the low concentration of PDADMAC still provide cell viability that we can use to modify CNT surface in the next step.

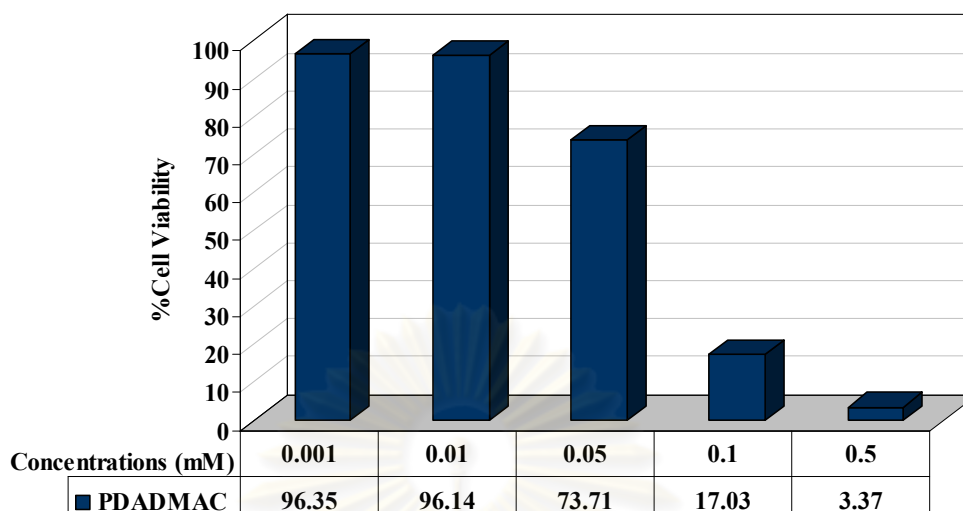


**Figure 4.38** % Cell viability of L929 after exposed with PDADMAC solution with different concentrations for 24 hr.

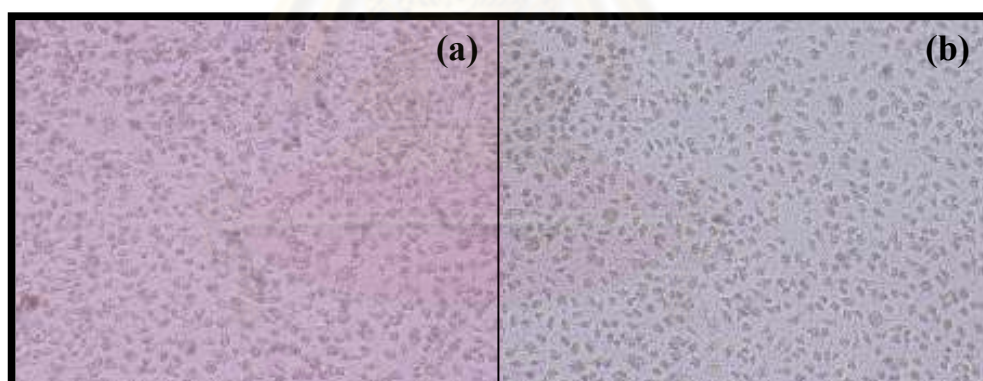


**Figure 4.39** L929 cells morphology after exposed with PDADMAC concentration (a) 0.1 mM and (b) 0.5 mM for 24 hr.

PSS solution were added into L929 cells with different concentration, the cell L929 were shrink . At high concentration of PSS 0.1 and 0.5 mM were toxic to L929 cells. The cell morphology after exposed with the PSS solution were shown in Figure 4.40.

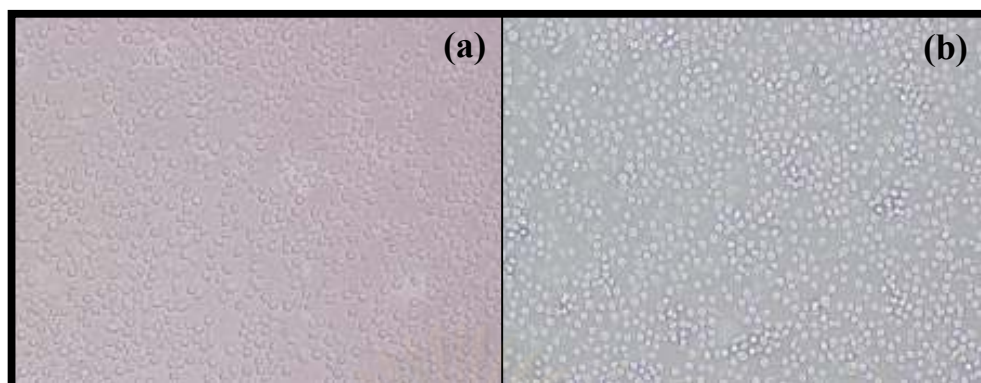


**Figure 4.40** L929 cells morphology after exposed with PSS concentration (a) 0.1 mM and (b) 0.5 mM for 24 hr.

#### **4.3.2.2.1 Cytotoxicity of primary coating MWCNT with PDADMAC, secondary coating MWCNT with PDADMAC/PSS and tertiary coating MWCNT with PDADMAC/PSS/PDADMAC : In case of solution.**

The surface modification of MWCNT with polyelectrolyte as PDADMAC and PSS were used to evaluate their cytotoxicity with L929 cells by MTT assay. Three kind of coating on MWCNT which consist of primary coating MWCNT with PDADMAC, secondary coating MWCNT with PDADMAC/PSS and tertiary coating MWCNT with PDADMAC/PSS/PDADMAC were prepared in the solutions. In Figure 4.41, the MWCNT coated with PDADMAC/PSS and PDADMAC/PSS/PDADMAC with different concentrations were not significantly changed in the concentration of formazan. While the MWCNT coated with PDADMAC were toxic on L929 cells when the concentration reach to 6.25 and 12.5  $\mu\text{g/ml}$ . % Cell viability in Figure 4.42 can be confirmed the toxicity of MWCNT coated with PDADMAC on top were toxic on L929 cells. This evidence might be from the effect of cationic polyelectrolyte which can attract with the negative charged of phospholipid in the cell membrane and provide the complex. In addition, the excess of polyelectrolyte in the MWCNT solution remained which might affect on cytotoxicity because PDADMAC and PSS at higher concentrations than 0.1 mM provide cytotoxicity on the cells.

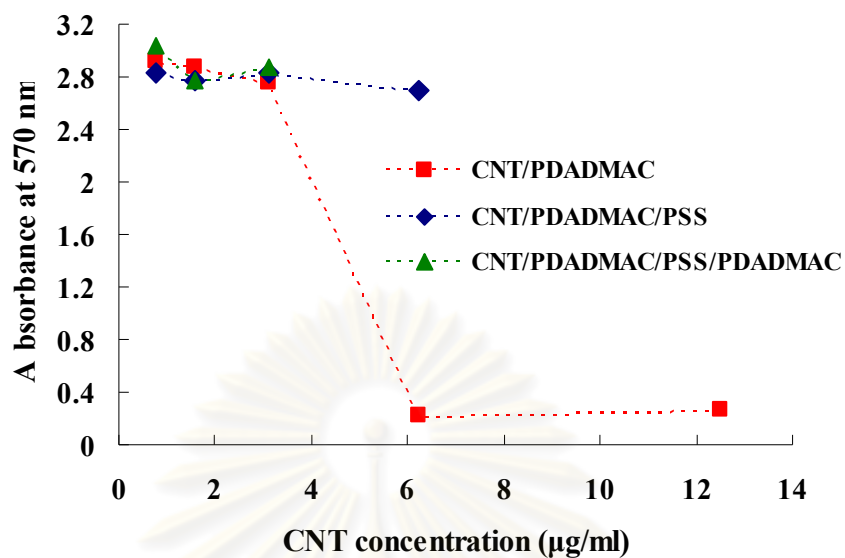


**Figure 4.41** The absorbance of formazan after L929 cells were exposed with different concentrations of primary coating MWCNT with PDADMAC, secondary coating MWCNT with PDADMAC/PSS, tertiary coating MWCNT with PDADMAC/PSS/PDADMAC (In case of solution) for 24 hr.

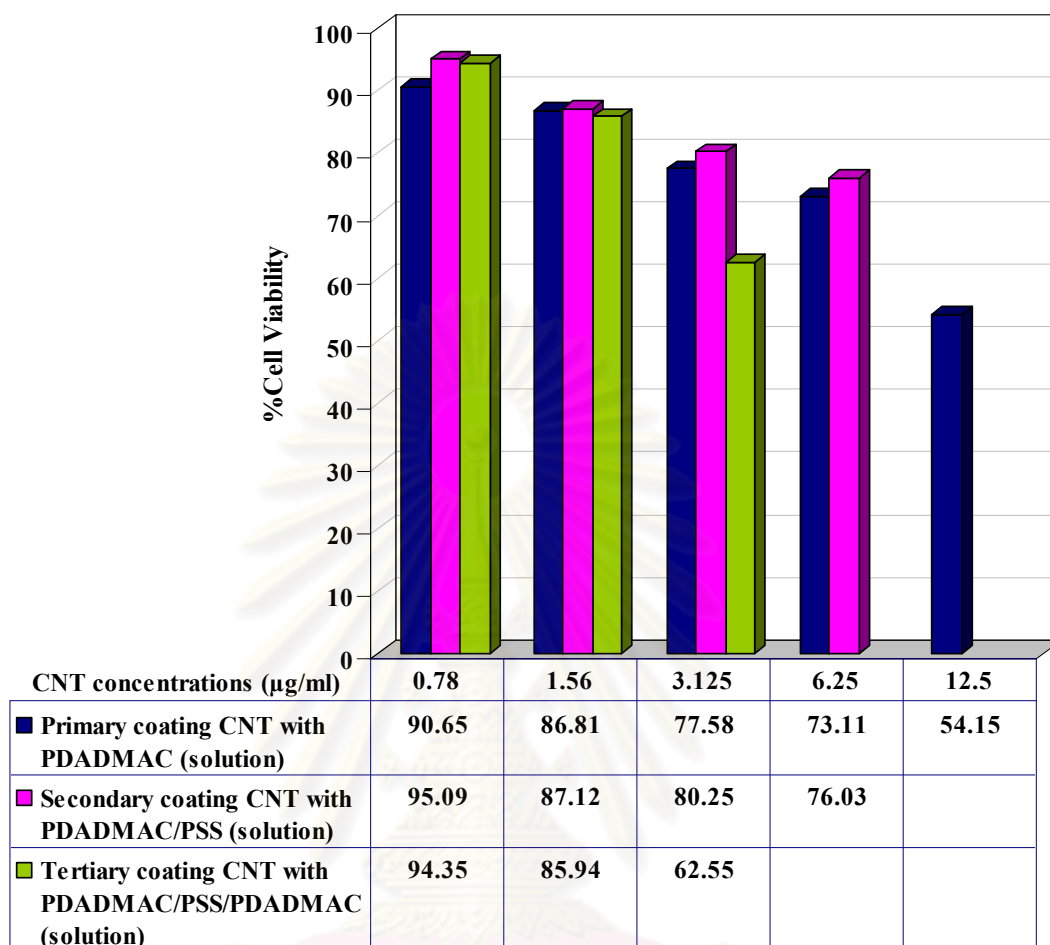


**Figure 4.42** % Cell viability of L929 cells after exposed with primary coating MWCNT with PDADMAC, secondary coating MWCNT with PDADMAC/PSS, tertiary coating MWCNT with PDADMAC/PSS/PDADMAC (In case of solution) with different concentrations for 24 hr.

Cell morphology of L929 after exposed with modified MWCNT with different functional groups and different concentrations was shown in the Figure 4.43



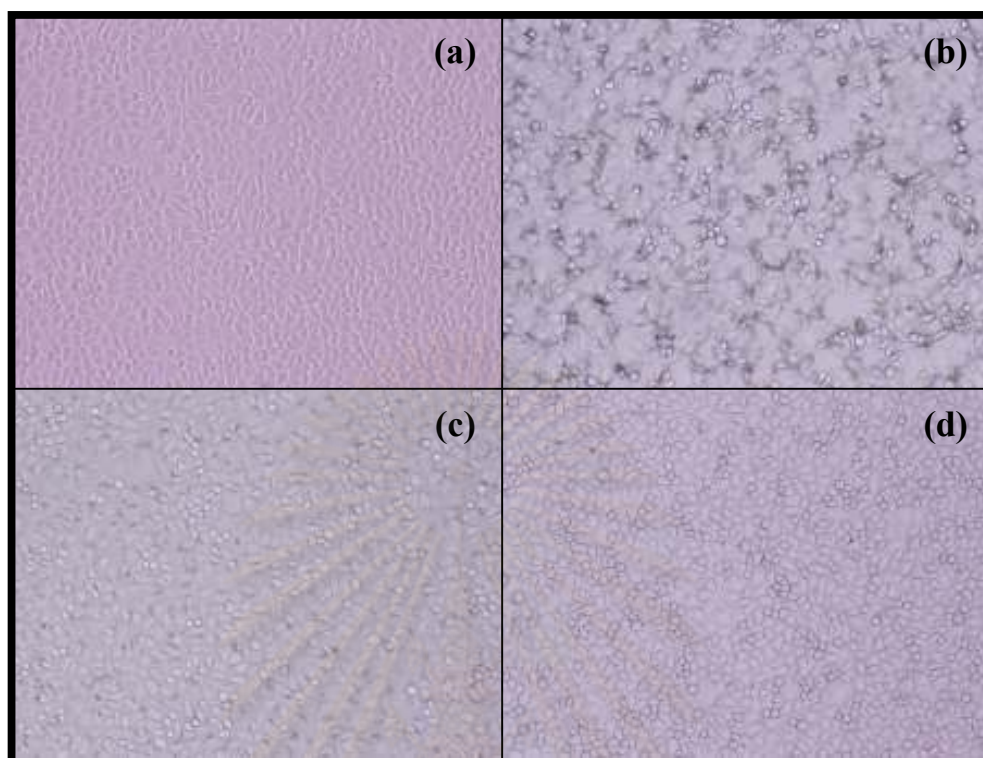


**Figure 4.43** L929 cells morphology, (a) Cell control (b) Cell after exposed with primary coating MWCNT with PDADMAC 12.5 µg/ml, (c) secondary coating MWCNT with PDADMAC/PSS 6.25 µg/ml, and (d) tertiary coating MWCNT with PDADMAC/PSS/PDADMAC 3.125 µg/ml.

#### **4.3.2.2.2 Cytotoxicity of primary coating MWCNT with PDADMAC, secondary coating MWCNT with PDADMAC/PSS and tertiary coating MWCNT with PDADMAC/PSS/PDADMAC : In case of powder.**

However, the modified MWCNT with polyelectrolyte PDADMAC and PSS were centrifuged with 4000 rpm in order to remove the excess polyelectrolyte. The modified MWCNT were redispersed in DMEM which consist of the amino acid and exposed into L929 cells. The results were shown in Figure 4.44, there is no change in the absorbance of formazan with an increase in concentration of MWCNT. Figure 4.45 showed that %cell viability does not change because it is no excess polyelectrolyte which

effect on the cell toxicity. The disadvantage of the centrifugation process was that the MWCNT were densely packed and hardly redisperse in solution. Therefore, the aggregation of modified MWCNT was hardly penetrated into L929 cells. Cell morphology after exposed modified MWCNT were illustrated in Figure 4.46.

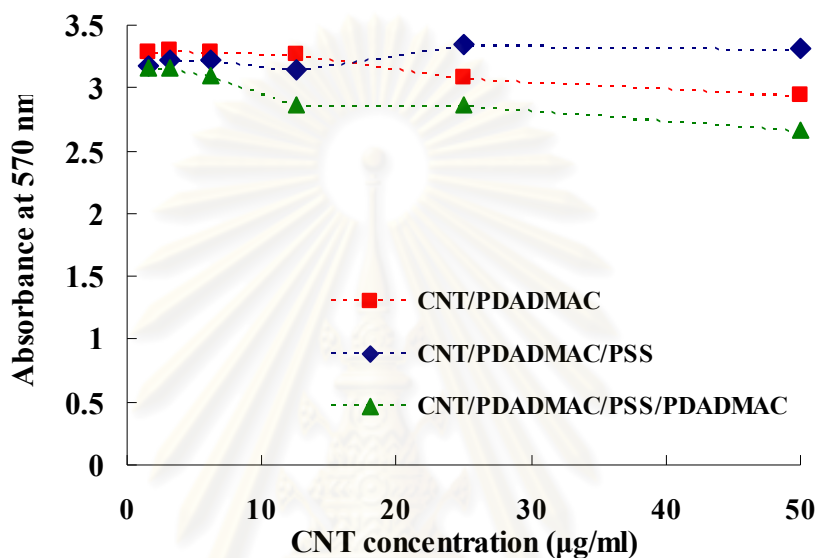


**Figure 4.44** The absorbance of formazan after L929 cells were exposed with different concentrations of primary coating MWCNT with PDADMAC, secondary coating MWCNT with PDADMAC/PSS, tertiary coating MWCNT with PDADMAC/PSS/PDADMAC (In case of powder) for 24 hr.

ศูนย์วิทยทรัพยากร  
จุฬาลงกรณ์มหาวิทยาลัย

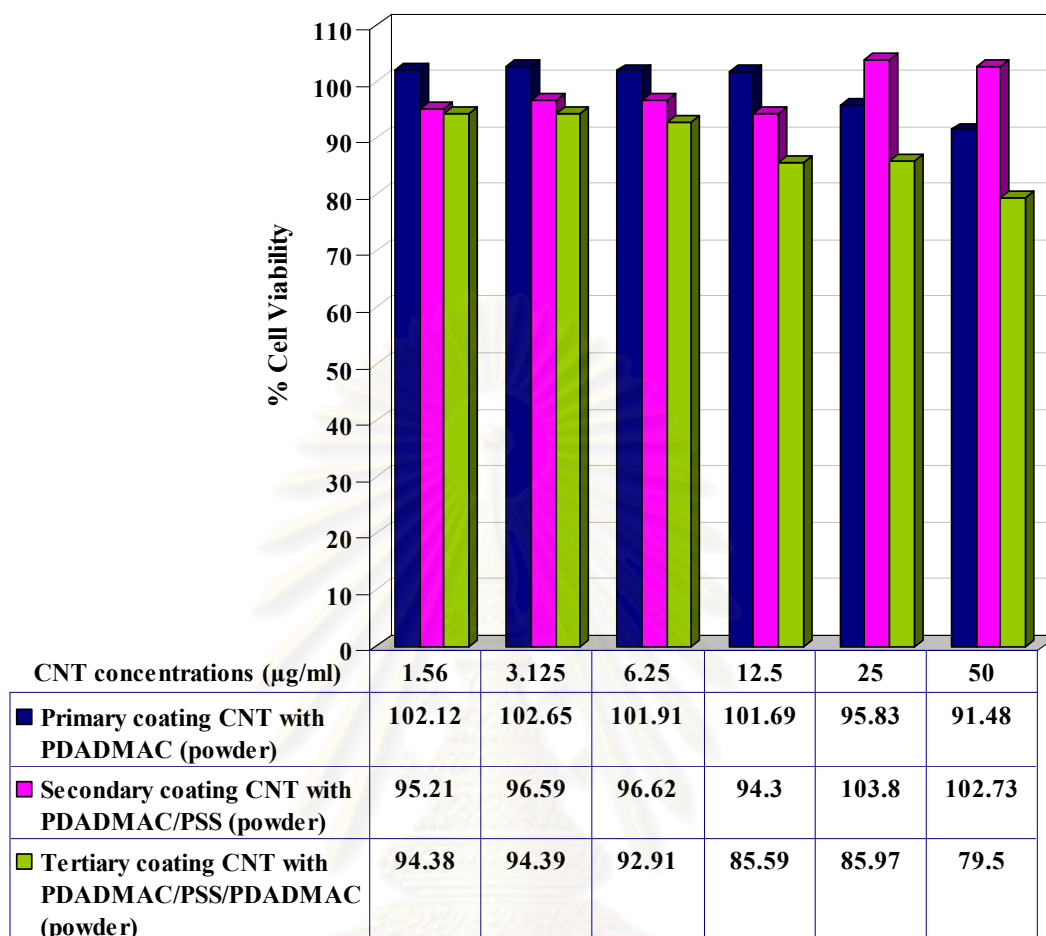


**Figure 4.45** % Cell viability of L929 cells after exposed with primary coating MWCNT with PDADMAC, secondary coating MWCNT with PDADMAC/PSS, tertiary coating MWCNT with PDADMAC/PSS/PDADMAC (In case of powder) with different concentrations for 24 hr.

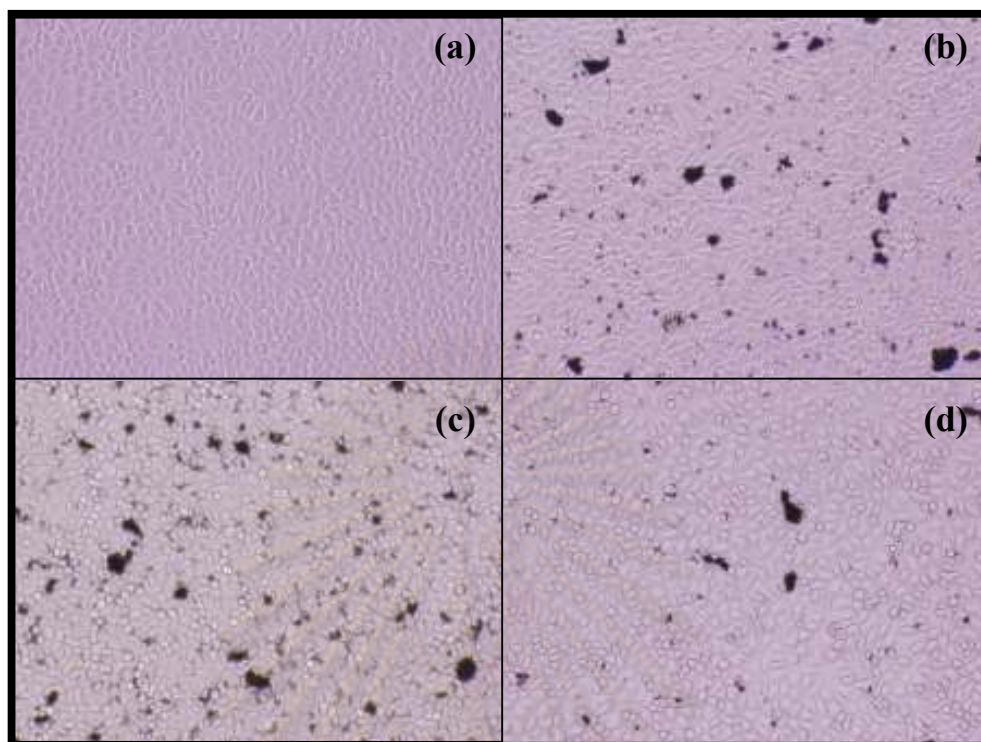


**Figure 4.46** L929 cells morphology, (a) Cell control (b) Cell after exposed with primary coating MWCNT with PDADMAC 50 µg/ml, (c) secondary coating MWCNT with PDADMAC/PSS 50 µg/ml, and (d) tertiary coating MWCNT with PDADMAC/PSS/PDADMAC 50 µg/ml.

ศูนย์วิทยทรัพยากร  
จุฬาลงกรณ์มหาวิทยาลัย

## CHAPTER V

### CONCLUSIONS

Multiwall carbon nanotubes (MWCNTs) have been noncovalently modified with chitosan having different %*DD* (61%, 71%, 78%, 84%, 90% and 93%). Using chitosan having different %*DD* had a strong effect on the dispersion efficiency of the nanotubes. UV-Visible spectroscopy results suggest that the nanotubes dispersion was improved when using chitosan with a lower degree of deacetylation (61%*DD*) when compared with higher degree of deacetylation (93%*DD*). The MWCNT modified with the lower %*DD* also displayed the best stability against centrifugation. Zeta potential measurements finally confirmed that the amount of chitosan adsorbed onto the nanotubes surface was twice as high with the lower %*DD* as with the high %*DD*. These modified MWCNTs with chitosan biopolymer could be used to immobilize hydrophobic and hydrophilic drug for drug delivery application.

Molecular dynamic simulation was used as a complementary tool to predict the sedimentation and stability of modified singlewall carbon nanotube (SWCNT) with 60%*DD* chitosan in three pair species: a pristine-a pristine SWCNT, a pristine SWCNT-wrapped SWCNT with chitosan, and a wrapped SWCNT with chitosan- wrapped SWCNT with chitosan. The behavior of modified SWCNT with 60%*DD* chitosan in aqueous solution; in term of both sedimentation and stability, can be successfully proved. Two pristine carbon nanotubes were aggregated in the solution because of van der Waals force between intertubes which is confirmed by the closer distance in equilibrium. Nitrogen atoms on acetyl groups of N-acetyl-D-glucosamine units were located near the carbon atoms on nanotubes surface while nitrogen atoms on ammonium groups of D-glucosamine units were far away from the nanotube surface. These theoretical results support the previous experimental work which is noncovalently modified MWCNTs with chitosan having different %*DD* in the fact that the hydrophobic acetyl parts of chitosan favored to attach on the nanotube surface while the hydrophilic ammonium parts provided nanotubes stabilize in the solution by repulsive force to each others. Although the monolayer coating MWCNTs with low %*DD* chitosan was successful, their stability was inadequate to prepare as a drug carrier.

By carefully controlling the concentration of polyelectrolytes in solution, the layer-by-layer deposition of polyelectrolytes multilayers on MWCNT is simplified and do not requires the tedious centrifugation-sonication steps. Since the sufficient amount of PDADMAC and PSS were deposited on treated carbon nanotubes surface as a primary, secondary and tertiary layer, the modified MWCNT can then be prepared in large scale. The adsorption of the polyelectrolytes for each layer was monitored by turbidity measurement with a UV-Vis spectrophotometer and zeta potential. Using TEM imaging, the thickness of the three layers coating on the MWCNT was measured to be 13.4 nm which suggest the formation of loose polyelectrolyte network onto the MWCNT surface. This simple method can be used to coat large scales of MWCNT solutions for drug delivery applications.

With different charged type of functional groups on MWCNTs, the hydrophilic model drugs such as gentian violet and diclofenac were used to load on modified MWCNTs. Gentian violet was successfully loaded on negatively charged surface of MWCNTs while the diclofenac can not be achieved to load in any type of modified MWCNTs. The cytotoxicity of modified MWCNT with different functional groups was evaluated with L929 fibroblast cells by MTT assay. Treated MWCNTs were toxic to L929 cells when the concentration reached 25  $\mu\text{g/ml}$  while primary coating MWCNTs with PDADMAC was toxic at concentration 12.5  $\mu\text{g/ml}$ .

## REFERENCES

- [1] There's Plenty of Room at the Bottom. [Online]. 2010. Available from :  
[http://en.wikipedia.org/wiki/There's\\_Plenty\\_of\\_Room\\_at\\_the\\_Bottom](http://en.wikipedia.org/wiki/There's_Plenty_of_Room_at_the_Bottom)  
[2010, August]
- [2] What are nanoscience and nanotechnologies? [Online]. 2010. Available from :  
<http://www.nanotec.org.uk/report/chapter2.pdf> [2010, August]
- [3] Mamalis, A.G., Vogtländer, L.O.G., Markopoulos, A. Nanotechnology and Nanostructured materials :trends in carbon nanotubes. Precision Engineering 28 (2004): 16–30.
- [4] Carbon nanotube. [Online]. 2010. Available from :  
[http://en.wikipedia.org/wiki/Carbon\\_nanotube](http://en.wikipedia.org/wiki/Carbon_nanotube) [2010, August]
- [5] Thess, A., Lee, R., Nikolaev, P., Dai, H.J., Petit, P., Robert, J., et al. Crystalline ropes of metallic carbon nanotubes. Science 273(1996): 483-487.
- [6] Nanoage. [Online]. 2010. Available from :  
[http://www.thenanoage.com/images/Eight\\_Allotropes\\_of\\_Carbon.png](http://www.thenanoage.com/images/Eight_Allotropes_of_Carbon.png)  
[2010, August]
- [7] Iijima, S. Helical microtubules of graphitic carbon. Nature 354(1991): 56-58.
- [8] Iijima, S., and Ichihashi, T. Single-Shell Carbon Nanotubes of 1-Nm Diameter. Nature 363(1993): 603-605.
- [9] Bethune, D.S., Kiang, C.H., Devries, M.S., Gorman, G., Savoy, R., Vazquez, J., et al. Cobalt-catalyzed growth of carbon nanotubes with single-atomic-layerwalls. Nature 363(1993): 605-607.
- [10] Klumpp, C., Kostarelos, K., Prato, M., and Bianco, A. Functionalized carbon nanotubes as emerging nanovectors for the delivery of therapeutics. Biochemica et Biophysica Acta 1758(2006): 404-412.
- [11] Paradise, M., and Goswami, T. Carbon nanotubes-Production and industrial applications. Materials and design 28(2007): 1477-1489.
- [12] Grobert, N. Carbon nanotubes-becoming clean. Materials Today 10(2007): 28-35.
- [13] Journet, C., and Bernier, P. Production of carbon nanotubes. Applied Physics A Materials Science & Processing 67(1998): 1-9.

- [14] Zeng, Q., Li, Z., and Zhou, Y. Synthesis and application of carbon nanotubes. Journal of Natural Gas Chemistry 15(2006): 235-246.
- [15] History of Carbon Nanotubes Discovery. Available from:  
<http://www.rz.meijo-u.ac.jp/labo/ando/1e.html> [2010, August]
- [16] Carbon nanotubes production. Available from:  
<http://ipn2.epfl.ch/CHBU/NTproduction1.htm> [2010, August]
- [17] Yakobson, B. I., and Smalley, R.E. Fullerene nanotubes: C-1000000 and beyond American Scientist 85(1997): 324-337.
- [18] Hu, C., Chen, Z., Shen, A., Shen, X., Li, J. and Hu, S. Water-soluble single-walled carbon nanotubes via noncovalent functionalization by a rigid, planar and conjugated diazo dye. Carbon 44(2006): 428-434.
- [19] Valerie, C.M., Michael, S.S., Erik, H.H., Robert, H.H., and Richard, E.S. Individually Suspended Single -Walled Carbon Nanotubes in Various Surfactants Nano Letters 3(2003): 1379-1383.
- [20] Zhang, J., Wang, Q., Wang, L. and Wang, A. Manipulated dispersion of carbon nanotubes with derivatives of chitosan Carbon 45(2007): 1917-1920.
- [21] Decher, G. Fuzzy Nanoassemblies: Toward Layered Polymeric Multicomposites Science 277(1997): 1232-1237.
- [22] Decher, G., Eckle, M., Schmitt, J., and Struth, B. Layer-by-layer assembled multicomposite films Current Opinion in Colloid & Interface Science 3(1998): 32-39.
- [23] Zykwincka, A., Radji-Taleb, S., and Cuenot, S. Layer-by-layer functionalization of carbon nanotubes with synthetic and natural polyelectrolytes. Langmuir 26(2010): 2779-2784.
- [24] Carrillo, A., Swartz, J.A., Gamba, J.M., Kane, R.S., Chakrapani, N., Wei, B., and Ajayan, P.M. Noncovalent Functionalization of Graphite and Carbon Nanotubes with Polymer Multilayers and Gold Nanoparticles Nano Letters 3(2003): 1437-1440.
- [25] Tchoul, M.N., Ford, W.T., Lolli, G., Resasco, D.E., and Arepalli, S. Effect of Mild Nitric Acid Oxidation on Dispersability, Size, and Structure of Single-Walled Carbon Nanotubes Chemistry of Materials.19(2007): 5765-5772.



- [26] Tagmatarchis, N., and Prato, M. Functionalization of carbon nanotubes via 1,3-dipolar cycloadditions Journal of Materials Chemistry 14(2004): 437-439.
- [27] Dautzenberg, H., Jaeger, W., and Kotz, J. Polyelectrolytes: Formation, Characterization and Application. New York : HANSER, 1994.
- [28] Decher, G., and Schlenoff, J. B. Multilayer Thin Films. New York : Wiley-VCH Verlag Gmbh&Co, 2002.
- [29] Bertrand, P., and Jonas, A. Ultrathin polymer coating by complexation of polyelectrolytes at interfaces: suitable materials, structure and properties. Macromolecules Rapid Communications 21(2000): 319-348.
- [30] Klitzing, R. V., Wong J. E., Jaeger, W., and Steitz, R. Short range interactions in polyelectrolyte multilayers. Current Opinion in Colloid and Interface Science 9(2004): 158-162.
- [31] Hubsch, E., Ball, V., Senger, B., Decher, G., Voegel, J.C., and Schaaf, P. Controlling the growth regime of polyelectrolyte multilayer films: Changing from exponential to linear growth by adjusting the composition of polyelectrolyte mixtures. Langmuir 20(2004): 1980-1985.
- [32] Steitz, R., Jaeger, W., and von Klitzing, R. Influence of charge density and ionic strength on the multilayer formation of strong polyelectrolytes. Langmuir 17(2001): 4471-4474.
- [33] Voigt, U., Khrenov, V., Thuer, K., Hahn, M., Jaeger, W., and von Klitzing, R. The effect of polymer charge density and charge distribution on the formation of multilayers. Journal of Physics-Condensed Matter 15(2003): S213-S218.
- [34] Steitz, R., Leiner, V., Siebrecht, R., and von Klitzing, R. Influence of the ionic strength on the structure of polyelectrolyte films at the solid/liquid interface. Colloids and Surfaces a-Physicochemical and Engineering Aspects 163(2000): 63-70.
- [35] Kim, B., and Sigmund, W.M., Functionalized multiwall carbon nanotube/gold nanoparticle composites. Langmuir 20(2004): 8239-8242.
- [36] Artyukhin, A.B., Bakajin, O., Stroeve, P., and Noy, A. Layer-by-layer electrostatic self-assembly of polyelectrolyte nanoshells on individual carbon nanotube templates. Langmuir 20(2004): 1442-1448.

- [37] Kong, H., Luo, P., Gao, C., and Yan, D. Polyelectrolyte-functionalized multiwalled carbon nanotubes: preparation, characterization and layer-by-layer self-assembly. Polymer 46(2005): 2472-2485.
- [38] Liu, L.J., Zhang, F., Xi, F.N., and Lin, X.F. Highly sensitive biosensor based on bionanomultilayer with water-soluble multiwall carbon nanotubes for determination of phenolics. Biosensors & Bioelectronics 24(2008): 306-312.
- [39] Bi, S., Zhou, H., and Zhang, S.S. Multilayers enzyme-coated carbon nanotubes as biolabel for ultrasensitive chemiluminescence immunoassay of cancer biomarker. Biosensors & Bioelectronics 24(2009): 2961-2966.
- [40] Zhang, X.K., Meng, L.J., Lu, Q.G., Fei, Z.F., and Dyson, P.J. Targeted delivery and controlled release of doxorubicin to cancer cells using modified single wall carbon nanotubes. Biomaterials 30 (2009): 6041-6047.
- [41] Yang, M., Koutsos, V., and Zaiser, M. Interactions between polymers and carbon nanotubes: a molecular dynamics study. Journal of Physical Chemistry B 109(2005): 10009-10014.
- [42] Tallury, S.S., and Pasquinelli, M.A. Molecular Dynamics Simulations of Flexible Polymer Chains Wrapping Single-Walled Carbon Nanotubes. Journal of Physical Chemistry B 114(2010): 4122-4129.
- [43] Xie, Y.H., and Soh, A.K. Investigation of non-covalent association of single-walled carbon nanotube with amylose by molecular dynamics simulation. Materials Letters 59(2005): 971-975.
- [44] Liu, Y., Chipot, C., Shao, X., and Cai, W. Solubilizing carbon nanotubes through noncovalent functionalization. Insight from the reversible wrapping of alginate acid around a single-walled carbon nanotube. Journal of Physical Chemistry B 114(2010): 5783-5789.
- [45] Pantarotto, D., Singh, R., McCarthy, D., Erhardt, M., Briand, J-P., Prato, M., Kostarelos, K., and Bianco, A. Functionalized carbon nanotubes for plasmid DNA gene delivery. Angewandte Chemie International Edition 43(2004): 5242-5246.

- [46] Kam, N. W. S., Jessop, T. C., Wender, P. A., and Dai, H. Nanotube molecular transporter: Internalization of carbon nanotube-protein conjugates into mammalian cells. Journal of American Chemical Society 126(2004): 6850-6851.
- [47] Kam, N. W. S. and Dai, H. Carbon nanotubes as intracellular protein transporters: Generality and biological functionality. Journal of American Chemical Society 127(2005): 6021-6026.
- [48] Wu, W., Wieckowski, S., Pastorin, G., Benincasa, M., Klumpp, C., Briand, J-P., Prato, M. and Bianco, A. Targeted delivery of Amphotericin B to cells by using functionalized carbon nanotubes. Angewandte Chemie International Edition 44(2005): 6358-6362.
- [49] Kam, N. W. S., O'Connell, M., Wisdom, J. A., and Dai, H. Carbon nanotubes as multifunctional biological transporters and near-infrared agents for selective cancer cell destruction. Proceeding of the Nation Academy of Sciences of the United States of America 102(2005): 11600-11605.
- [50] Liu, Z., Sun, X., Nakayama-Ratchford, N., and Dai, H. Supramolecular Chemistry on Water- Soluble Carbon Nanotubes for Drug Loading and Delivery. Acs Nano 1(2007): 50-56.
- [51] Feazell, R. P., Nakayama-Ratchford, N., Dai, H., and Lippard, S. J. Soluble Single-Walled Carbon Nanotubes as Longboat Delivery Systems for Platinum(IV) Anticancer Drug Design. Journal of American Chemical Society 129(2007): 8438-8439.
- [52] Shao, N., Lu, S., Wickstrom, E., and Panchapakesan, B. Integrated molecular targeting of IGF1R and HER2 surface receptors and destruction of breast cancer cells using single wall carbon nanotubes. Nanotechnology 18(2007): 1-9.
- [53] Kostarelos, K., Lacerda, L., Pastorin, G., Wu, W., Wieckowski, S., Luangsivilay, J., et al. Cellular uptake of functionalized carbon nanotubes is independent of functional group and cell type. Nature Nanotechnology 2(2007): 108-113.
- [54] Jia, G., Wang, H.F., Yan, L., Wang, X., Pei, R.J., Yan, T., et al. Cytotoxicity of carbon nanomaterials: Single-wall nanotube, multi-wall nanotube, and fullerene. Environmental Science & Technology 39(2005): 1378-1383.

- [55] Sayes, C.M., Liang, F., Hudson, J.L., Mendez, J., Guo, W.H., Beach, J.M., et al. Functionalization density dependence of single-walled carbon nanotubes cytotoxicity in vitro. Toxicology Letters 161(2006): 135-142.
- [56] Porter, A.E., Gass, M., Bendall, J.S., Muller, K., Goode, A., Skepper, J.N., et al. Uptake of Noncytotoxic Acid-Treated Single-Walled Carbon Nanotubes into the Cytoplasm of Human Macrophage Cells. Acs Nano 3(2009): 1485-1492.
- [57] Wick, P., Manser, P., Limbach, L.K., Dettlaff-Weglikowska, U., Krumeich, F., Roth, S., et al. The degree and kind of agglomeration affect carbon nanotube cytotoxicity. Toxicology Letters 168(2007): 121-131.
- [58] Casey, A., Herzog, E., Davoren, M., Lyng, F.M., Byrne, H.J., and Chambers, G. Spectroscopic analysis confirms the interactions between single walled carbon nanotubes and various dyes commonly used to assess cytotoxicity. Carbon 45(2007): 1425-1432.
- [59] Belyanskaya, L., Manser, P., Spohn, P., Bruinink, A., and Wick, P. The reliability and limits of the MTT reduction assay for carbon nanotubes-cell interaction. Carbon 45(2007): 2643-2648.
- [60] Herzog, E., Casey, A., Lyng, F.M., Chambers, G., Byrne, H.J., and Davoren, M. A new approach to the toxicity testing of carbon-based nanomaterials - The clonogenic assay. Toxicology Letters 174(2007): 49-60.
- [61] Muzzarelli, A.A.R., and Roccheti, R. Determination of the degree of acetylation of chitosans by first derivative ultraviolet spectrophotometry. Carbohydrate Polymers 5(1985): 461-472.
- [62] Sornmee, P., Rungrotmongkol, T., Saengsawang, O., Arsawang, U., Remsungnen, T., and Hannongbua, S. Understanding of molecular properties of the doxorubicin anticancer drug filling inside and wrapping outside the single-walled carbon nanotube. Journal of Computational and Theoretical Nanoscience (In press).
- [63] Arsawang, U., Saengsawang, O., Rungrotmongkol, T., Sornmee, P., Remsungnen, T., and Hannongbua, S. How does carbon nanotube serve as a carrier for gemcitabine transport in drug delivery system? Journal of Molecular Graphics and Modelling (Revised).

- [64] Duan, Y., Wu, C., Chowdhury, S., Lee, M.C., Xiong, G., Zhang, W., et al. in Wiley Subscription Services, Inc., Wiley Company, 2003: 1999-2012.
- [65] Tessier, M.B., DeMarco, M.L., Yongye, A.B., and Woods, R.J. Extension of the GLYCAM06 biomolecular force field to lipids, lipid bilayers and glycolipids. Molecular Simulation 34(2008): 349-364.
- [66] Case, T.A.D. D.A., Cheatham, T.E., Simmerling, C.L., Wang, J., Duke, R.E., Luo, R., et al. in U.o. California (Ed.), San Francisco, 2008.
- [67] Spectroscopy. [Online]. 2007. Available from :  
<http://www.chem.ucalgary.ca/courses/351/Carey/Ch13/ch13-uvvis.htmf>  
[2010, August].
- [68] Zeta potential. [Online]. 2010. Available from :  
[http://en.wikipedia.org/wiki/Zeta\\_potential](http://en.wikipedia.org/wiki/Zeta_potential)[2010, August].
- [69] Ma, H., Shieh, K.J., Qiao, T. X. Study of Transmission Electron Microscopy (TEM) and Scanning Electron Microscopy (SEM). Nature and Science[Online]. 2006. Available from : <http://sciencepub.org/nature/0403/03-0171-mahongbao-ns.doc>  
[2010, August].
- [70] Gel Permeation Chromatography. [Online]. 2007. Available from :  
<http://www.pssgpcshop.com/faq-1.htm>[2010, August].
- [71] Introduction to Fourier Transform Infrared Spectrometry [Online]. 2007. Available from : <http://mmrc.caltech.edu/FTIR/FTIRintro.pdf> [2010, August].
- [72] Raman spectroscopy. [Online]. 2010. Available from :  
[http://en.wikipedia.org/wiki/Raman\\_spectroscopy](http://en.wikipedia.org/wiki/Raman_spectroscopy) [2010, August].
- [73] Zhang, X.K., Meng, L.J., Lu, Q.G., Fei, Z.F., and Dyson, P.J. Targeted delivery and controlled release of doxorubicin to cancer cells using modified single wall carbon nanotubes. Biomaterials 30(2009): 6041-6047.
- [74] Kumar, M.N.V.R. A review of chitin and chitosan applications. Reactive & Functional Polymers 46(2000): 1-27.
- [75] Bangyekan, C., Aht-Ong, D., and Srikulkit, K. Preparation and properties evaluation of chitosan-coated cassava starch films. Carbohydrate Polymers 63(2006): 61-71.

- [76] Zhang, C., Cui, Y., and Jia, Z. Study on the Reaction Kinetics of Ultrasonic Radiation Non-homogeneous Phase Chitin Deacetylation. International Journal of Chemistry 11(2009): 50-56.
- [77] Khan, T.A., Peh, K.K., and Ch'ng, H.S. Reporting degree of deacetylation values of chitosan: the influence of analytical methods. Journal of Pharmacy and Pharmaceutical Sciences 5(2002): 205-212.
- [78] Jia, Z.S., and Shen, D.F. Effect of reaction temperature and reaction time on the preparation of low-molecular-weight chitosan using phosphoric acid. Carbohydrate Polymers 49(2002): 393-396.
- [79] Nishio, M. CH/pi hydrogen bonds in crystals. Crystengcomm 2004;6:130-58.
- [80] Iamsamai, C., Hannongbua, S., Ruktanonchai, U., Soottitantawat, A., and Dubas, S.T. The effect of the degree of deacetylation of chitosan on its dispersion of carbon nanotubes. Carbon 48(2010): 25-30.
- [81] Kong, H., Luo, P., Gao, C., and Yan, D. Polyelectrolyte-functionalized multiwalled carbon nanotubes: preparation, characterization and layer-by-layer self-assembly. Polymer 46(2005): 2472-2485.
- [82] Huang, S.C.J., Artyukhin, A.B., Wang, Y.M., Ju, J.W., Stroeve, P., and Noy, A. Persistence length control of the polyelectrolyte layer-by-layer self-assembly on carbon nanotubes. Journal of the American Chemical Society 127(2005): 14176-14177.
- [83] Hammond, P.T. Recent explorations in electrostatic multilayer thin film assembly. Current Opinion in Colloid & Interface Science 4(1999): 430-442.
- [84] Kim, B., and Sigmund, W.M. Functionalized multiwall carbon nanotube/gold nanoparticle composites. Langmuir 20(2004): 239-42.
- [85] Lin, J.H., He, C.Y., Zhao, Y., and Zhang, S.S. One-step synthesis of silver nanoparticles/carbon nanotubes/chitosan film and its application in glucose biosensor. Sensors and Actuators B-Chemical 137(2009): 768-773.
- [86] Guzey, D., and McClements, D.J. Formation, stability and properties of multilayer emulsions for application in the food industry. Advances in Colloid and Interface Science 128(2006): 227-248.

- [87] Voigt, A., Lichtenfeld, H., Sukhorukov, G.B., Zastrow, H., Donath, E., Baumler, H., et al. Membrane filtration for microencapsulation and microcapsules fabrication by layer-by-layer polyelectrolyte adsorption. Industrial & Engineering Chemistry Research 38(1999): 4037-4043.
- [88] Shieh, Y.T., Liu, G.L., Wu, H.H., and Lee, C.C. Effects of polarity and pH on the solubility of acid-treated carbon nanotubes in different media. Carbon 45(2007): 1880-1890.
- [89] Zeng, L.L., Zhang, L., and Barron, A.R. Tailoring aqueous solubility of functionalized single-wall carbon nanotubes over a wide pH range through substituent chain length. Nano Letters 5(2005): 2001-2004.



ศูนย์วิทยทรัพยากร  
จุฬาลงกรณ์มหาวิทยาลัย



**APPENDIX**

ศูนย์วิทยทรัพยากร  
จุฬาลงกรณ์มหาวิทยาลัย



## **A. SCHOLARSHIPS**

- 2007-2009 Thailand Graduate Institute of Science and Technology (TGIST)**  
(TG-55-09-50-059D)  
National Science and Technology Development Agency
- 2008-2010 The 90<sup>th</sup> Anniversary of Chulalongkorn University Fund**  
**(Ratchadaphiseksomphot Endowment Fund)**  
Graduate School, Chulalongkorn University
- 2010 Conference Grant for Ph.D. Student**  
Graduate School, Chulalongkorn University

## **B. LIST OF CONFERENCES (Oral Presentation)**

- 1. 33<sup>rd</sup> Congress on Science and Technology of Thailand (STT33)**  
at Walailuk University, Nakhorn Sri Thammarat, Thailand on 18-24 October 2007.  
**Title** “Noncovalent surface modification of multiwalled carbon nanotubes with chitosan: Effect of degree of deacetylation”
- 2. The first Annual Meeting of Thailand Research Fund Senior Research**  
at Faculty of Science, Mahasarakham University, Mahasarakham, Thailand on 22 October 2009.  
**Title** “The effect of degree of deacetylation of chitosan on its dispersion of carbon nanotubes”
- 3. Pure and Applied Chemistry International Conference (PACCON2010)**  
at Sunee Grand Hotel, Ubonratchathani, Thailand on 21-23 January 2010.  
**Title** “Layer-by-layer surface modification of multiwall carbon nanotubes”
- 4. Joint Symposium on Advanced Polymers and Nanomaterials by Inha University and Chulalongkorn University**  
at Pathumwan Princess Hotel, Bangkok, Thailand on 10 July 2010.  
**Title** “Noncovalent Surface Modification of Carbon Nanotubes”
- 5. X International Conference on Nanostructured Materials - NANO 2010**  
at La Sapienza University, Rome, Italy, 13 – 17 September, 2010.  
**Title** “Loading of model drug on layer-by-layer polyelectrolyte coating of carbon nanotubes”

### **C. LIST OF CONFERENCES (Poster Presentation)**

#### **1. The first HOPE Meeting (Advanced courses on Nanoscience and Nanotechnology)**

Tsukuba, Ibaraki, Japan organized by Japan Society for the Promotion of Science (JSPS) held on 24-29 February 2008.

**Title** “Noncovalent Surface Modification of Multiwall Carbon Nanotubes with Chitosan: Effect of Chitosan Concentrations and Degree of Deacetylation”

#### **2. International conference 1<sup>st</sup> Biannual NanoThailand Symposium (NTS)**

Queen Sirikit National Convention Center, Bangkok, Thailand on 6-8 December 2008.

**Title** “Immobilization of curcumin of modified multiwalled carbon nanotubes with chitosan as novel drug carrier”

### **D. LIST OF PUBLICATIONS**

1. **Iamsamai C.**, Hannongbua S., Ruktanonchai U., Soottitantawat A., Dubas S.T. The effect of the degree of deacetylation of chitosan on its dispersion of carbon nanotubes. **Carbon**. 2010; 48(1): 25-30.

2. **Iamsamai C.**, Hannongbua S., Ruktanonchai U., Soottitantawat A., Dubas S.T. Simple method for the layer-by-layer surface modification of multiwall carbon nanotubes. **Submitted**.

#### **Related Publication**

1. Rungrotmongkol T., Arsawang U., **Iamsamai C.**, Vongachariya A., Dubas S.T. and Hannongbua S. How dispersion and separation are the noncovalently modified carbon nanotubes? A case study with a chitosan-polysaccharide biopolymer wrapping on SWCNTs. **In Preparation**.

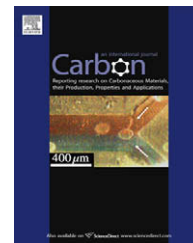
## **E. OTHER EXPERIENCES**

*“The title "HOPE" signifies the promise held for young scientists and the optimism for a bright science and technology future in the Asia-Pacific region.....”*

Chularat Iamsamai was selected from Office of the National Research Council of Thailand (NCRT) to get the great opportunity from Japan Society for the Promotion of Science (JSPS) to engage in interdisciplinary discussions with five Nobel laureates and other distinguished scientists pioneering the frontiers of knowledge in **The first HOPE Meeting (Advanced courses on Nanoscience and Nanotechnology)** at Tsukuba International Congress Center, Tsukuba, Ibaraki, Japan organized by Japan Society for the Promotion of Science held on 24-29 February 2008.

In addition, she was interviewed about her research work in Bangkokbiznews which onlined in column of “IT-Innovations: Innovations” on 5 December 2008. Available from: [http://www.bangkokbiznews.com/2008/12/05news\\_317969.php](http://www.bangkokbiznews.com/2008/12/05news_317969.php).

ศูนย์วิทยทรัพยากร  
จุฬาลงกรณ์มหาวิทยาลัย

available at [www.sciencedirect.com](http://www.sciencedirect.com)journal homepage: [www.elsevier.com/locate/carbon](http://www.elsevier.com/locate/carbon)

# The effect of the degree of deacetylation of chitosan on its dispersion of carbon nanotubes

Chularat Iamsamai <sup>a</sup>, Supot Hannongbua <sup>b</sup>, Uracha Ruktanonchai <sup>c</sup>, Apinan Soottitantawat <sup>d</sup>, Stephan T. Dubas <sup>e,\*</sup>

<sup>a</sup> Nanoscience and Technology Program, Graduate School, Chulalongkorn University, Bangkok 10330, Thailand

<sup>b</sup> Department of Chemistry, Faculty of Science, Chulalongkorn University, Bangkok 10330, Thailand

<sup>c</sup> National Nanotechnology Center, National Science and Technology Development Agency, Pathumthani 12120, Thailand

<sup>d</sup> Department of Chemical Engineering, Faculty of Engineering, Chulalongkorn University, Bangkok 10330, Thailand

<sup>e</sup> Metallurgy and Materials Science Research Institute, Chulalongkorn University, Bangkok 10330, Thailand

## ARTICLE INFO

### Article history:

Received 16 March 2009

Accepted 30 June 2009

Available online 5 July 2009

## ABSTRACT

The effect of the degree of deacetylation (DD) of chitosan biopolymer on the noncovalent surface modification of multiwall carbon nanotubes (MWCNTs) is presented. MWCNTs were modified by chitosan having different degree of deacetylation (61%, 71%, 78%, 84%, 90% and 93%) and UV-Visible spectroscopy was used to evaluate their dispersion efficiency as a function of chitosan concentration and degree of deacetylation. Results showed that the dispersion of MWCNTs could be dramatically improved when using chitosan with the lowest degree of deacetylation (61%DD) possibly due to a higher surface coverage of the MWCNTs. Zeta potential measurements were used to confirm that the chitosan surface coverage on the MWCNTs was twice as high when modifying the nanotubes surface with the 61%DD than when using the 93%DD chitosan. These results suggest that the dispersion of MWCNTs with chitosan can be improved when using chitosan having a degree of deacetylation of 61%. These results are of interest in particular for the improved dispersion of MWCNTs in aqueous solutions such as in drug delivery applications.

© 2009 Elsevier Ltd. All rights reserved.

## 1. Introduction

Among all the carbon nanostructures (fullerene, nanotubes, and nanofibers), the carbon nanotubes (CNTs) are probably being the most studied and used in applications ranging from the electronic to the biomedical [1–6]. Recently, carbon nanotubes have been proposed, as carrier for drug delivery applications [7,8]. Also, due to their high specific surface area combined with the proper surface modification, they have been used as carrier for drug delivery in cancer therapy [9–11]. Although CNTs show great potential in the biomedical

area, they can hardly be dispersed in any solvents due to nanotube–nanotube or van der Waals interactions [12] and tend to aggregate. Their poor solubility is a major problem and can lead to thrombosis of blood vessels when injected in living systems [13]. In order to achieve water dispersion, noncovalent and covalent surface modification of the CNTs surface has been developed. Covalent modification of the CNTs can, for example, be achieved with grafting of functional groups directly on the nanotube by reflux in strong acid for several hours [14]. While water dispersible nanotubes can be obtained using this method, the acidic

\* Corresponding author: Fax: +66 02611 7586.

E-mail address: [stephan.d@chula.ac.th](mailto:stephan.d@chula.ac.th) (S.T. Dubas).

0008-6223/\$ - see front matter © 2009 Elsevier Ltd. All rights reserved.

doi:10.1016/j.carbon.2009.06.060

treatment often leads to fragmentation of the nanotubes in smaller sections, which might impair their properties. In contrast, the noncovalent modification of CNTs surface is an attractive approach since it only involves the adsorption of a surfactant or biopolymer and preserves the CNTs integrity [15–18]. Surfactants such as sodium dodecyl sulfate and sodium dodecyl benzene sulfonate have been proposed as coating agent to promote the dispersion of the CNTs and provide good stability for several months in aqueous solution [19,20]. However, the used of such surfactants in drug delivery applications is not possible as they are thought to be toxic by inducing denaturation of proteins present in the blood [21]. This fact was demonstrated by Dong et al. who recently reported that individual single wall carbon nanotubes modified with surfactants, were toxic to 1321N1 human astrocytoma cells when compare with unmodified single wall carbon nanotubes [22]. As an alternative to potentially toxic surfactant, biopolymers have been proposed to noncovalently modify the CNTs surface [23,24]. Biopolymers such as gum arabic or gelatin have been used in the surface modification of CNTs for the preparation of conducting microelectrode used in bio-electrochemistry [25,26]. Chitosan, a polysaccharide biopolymer obtained from the deacetylation of chitin, has been widely used in medical applications because it can, not only be economically processed from chitin, but is also nontoxic, biocompatible, and biodegradable [27,28]. Chitosan biopolymer is to be treated as a random copolymer of D-glucosamine (deacetylated unit) and N-acetyl-D-glucosamine (acetylated unit) with a degree of deacetylation (%DD) representing the molar fraction of D-glucosamine along the backbone of the polymer [29]. Naturally, chitosan and its derivatives have been reported as polymer of choice for CNTs modification to improve their dispersion [30]. Chitosan structure contains both acetyl hydrophobic groups, which could bind onto the CNTs surface, and the amino groups to provide water dispersion. Furthermore, Peng et al. also demonstrated using computational simulation that chitosan could wrap along the CNTs axis [31]. This was also supported by surface decoration of carbon nanotubes with chitosan, followed by a cross-linking step [32]. In all cited work, chitosan with a high degree of deacetylation was used mainly for the modification of single wall carbon nanotubes probably because high %DD chitosan display a better solubility in aqueous media. Yet the highly hydrophilic character of the high %DD chitosan might be a disadvantage for the surface modification of carbon nanotubes and lead to poor adsorption. In the presented work, our starting hypothesis was that a lower %DD chitosan would be preferable and might allow a better dispersion of the nanotubes. Literature search confirmed that no previous report has been made on the effect of degree of deacetylation of chitosan to the dispersion and stability efficiency of CNTs.

In this article, the effect of the degree of deacetylation (%DD) of chitosan on the dispersion of MWCNTs is reported. The dispersion efficiency and stability against sedimentation of the modified MWCNTs was also investigated a function of the chitosan %DD. The degree of deacetylation of chitosan was found to play a critical role in the dispersion efficiency of MWCNTs and their stability based on noncovalent modification. Our results suggest that lower %DD chitosan is more efficient to disperse MWCNTs.

## 2. Experimental

### 2.1. Chemicals

MWCNTs with a diameter of 110–170 nm and length of 5–9  $\mu\text{m}$  were purchased from Aldrich, Thailand. These nanotubes were synthesized by chemical vapor deposition (information provided by the distributor). Chitin extracted from shrimp and used in the synthesis of chitosan was obtained from A.N. (aquatic nutrition lab) Ltd., Thailand. Concentrated sodium hydroxide 50% w/w was purchased from Vittayasom Co., Ltd., Thailand. Analytical grade glacial acetic acid was purchased from Labscan Asia Co., Ltd., Thailand. All chemicals and solvents were used as received without any further purification. Double distilled water was used in all experiments.

### 2.2. Experimental methods

#### 2.2.1. Synthesis of chitosan with various %DD

Chitosan with various degree of deacetylation (%DD) was prepared by reacting 50 g of chitin in 750 ml of concentrated sodium hydroxide (50% w/w) under constant shaking. Different chitosan batches of increasing %DD were obtained by increasing the reaction time from 2 to 13 days at ambient temperature. The resulting chitosan powder was then filtered and rinsed with water until obtaining neutral pH and finally dried in air. The %DD of each chitosan batches was measured by first derivative spectroscopy using a UV-Visible spectrophotometer (SPECORD S 100, Analytikjena) [33]. In each experiment, the chitosan samples were prepared by appropriate dilution of the stock solutions in order to obtain the needed concentration of chitosan in 20 mM acetic acid.

#### 2.2.2. Effect of chitosan concentration on the dispersion of MWCNTs

UV-Visible spectroscopy was used to determine the efficiency of the dispersion of the carbon nanotubes in solution. As MWCNTs absorb all wavelengths in the visible range, their dispersion can be evaluated by recording the changes in absorbance at fixed wavelength (550 nm) [34,30]. The wavelength of 550 nm was chosen as it represents the midway of the visible range and is often used in turbidity measurements. In each experiments, a fixed amount of MWCNTs (5 mg) was first dispersed in a 100 ml solution of a 0.01 mM chitosan (%DD = 61). The absorbance of the solution was measured after each adjunction of chitosan until the final concentration of 10 mM chitosan was reached. At each step, the mixture was stirred and sonicated for 10 min using an ultrasonic bath (CREST Model 275D, USA).

#### 2.2.3. Effect of chitosan %DD on the dispersion of MWCNTs

To evaluate the effect of the %DD on the dispersion efficiency of MWCNTs by chitosan, 12.5 mg of MWCNTs were added to different solutions of chitosan having a fixed volume of 50 ml and a fixed concentration of 5 mM but having increasing %DD (61, 71, 78, 84, 90 or 93%DD). After mixing, the MWCNTs and the chitosan solutions were stirred and sonicated for 30 min. The absorbance at 550 nm of the pitch-black solutions was then measured by UV-Visible spectroscopy.

#### 2.2.4. Stability of modified MWCNTs

To assess the stability against sedimentation of the CNT modified with various types of chitosan (61, 71, 78, 84, 90 or 93%DD), each prepared solution was centrifuged 10 min at a rotation rate of 2000 rpm. The final absorbance at 550 nm of the supernatant was recorded and plotted as a function of the %DD.

#### 2.2.5. Surface charge of the modified MWCNTs

The zetasizer (NanoZS4700 nanoseries, Malvern Instruments, UK) was used to measure the surface zeta potential of the MWCNTs modified with solutions of chitosan having 61, 71, 78, 84 and 93%DD. Each solution contained 20 mM of acetic acid, which remained from the preparation of the chitosan solutions and provided a final pH value of 3.4. The acidic medium is needed to insuring total ionization of the amino groups present in the chitosan to their  $\text{NH}_3^+$  form. Measurements in neutral or basic conditions would lead to low zeta potential values as well as poor chitosan solubility due to the de-protonation of the  $\text{NH}_3^+$  to  $\text{NH}_2$ . The modified MWCNTs were then centrifuged at 4000 rpm for 15 min in order to remove the excess of chitosan. The precipitant was re-dispersed by vortex in 25 ml of 20 mM acetic acid and sonicated. The precipitation and re-dispersion steps were repeated three times prior to zeta potential measurements.

### 3. Results and discussion

In these experiments, chitosan was used to disperse the MWCNTs by noncovalent surface modification. If one tries to disperse carbon nanotube in aqueous solution, it is well known that prior to the adjunction of any dispersing agent, the solution will appear clear with the MWCNTs aggregated at the air/water interface. Weak van der Waals attraction and  $\pi$ - $\pi$  stacking between the abundant double bonds found in MWCNTs are through to be responsible for their aggregation and poor solubility in aqueous solution. Shown in Fig. 1 is a plot of the changes in absorbance of the solution as a function of the added chitosan concentration. From the initial solution of aggregated carbon nanotubes, as chitosan concentration is increased up to 1 mM, the adsorption of the polymer onto the carbon nanotubes leads to dispersion, which in turn

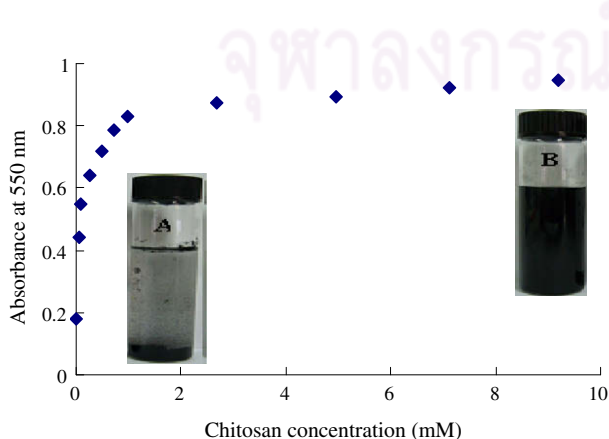


Fig. 1 – Plot of the changes in absorbance of a MWCNTs solution as function of the 61%DD chitosan concentration.

leads to a sharp increase the absorbance at 550 nm. This increase in absorbance quickly levels off suggesting that all the carbon nanotubes, present in the solution, have been dispersed. Further increase of the chitosan solution to 9 mM does not induce any increase in absorbance. When chitosan is added to the solution, noncovalent adsorption of chitosan on the nanotube surface is thought to take place, which initiate the dispersion by repulsion of the nanotubes. Since it has been reported that the acetyl groups represent the most hydrophobic part of the chitosan, the authors suggest that these functional groups could adsorb preferentially on the surface of the MWCNTs. In the mean time, the hydrophilic parts of chitosan ( $\text{NH}_3^+$ ) induce a positive charge at the vicinity of the nanotubes surface, which allow for their stabilization in aqueous solution by electrostatic repulsion. This dispersion process can be studied using UV–Visible spectroscopy by recording the changes in absorbance of the solution at 550 nm, and is therefore equivalent to a turbidity measurement. As carbon nanotubes absorb all the wavelengths in the visible part of the electromagnetic spectrum, increases in dispersion of the carbon nanotubes render the solution more and more pitch-black.

Since our hypothesis was that the more hydrophobic acetyl groups present in chitosan might allow a better interaction with the MWCNTs, our interest turned toward the preparation of chitosan having a higher molar fraction of acetyl groups thus a lower %DD. Our hypothesis was that since the hydrophobic character of chitosan is controlled by the fraction of acetylated functional groups [35], chitosan with a lower %DD should be a better molecule for the dispersion of CNTs. Chitosan with a lower %DD can simply be prepared by a shorter reaction time of the chitin biopolymer in the 50% w/w sodium hydroxide solution. In our work we chose to use 61%DD as the lowest degree of deacetylation because the resulting chitosan molecules were not sufficiently soluble and led to very scattered results. Shown in Fig. 2 (squares), is the absorbance of different solutions containing MWCNTs dispersed with chitosan having different degree of deacetylation (61, 71, 78, 84, 90 or 93%DD). Although it was shown in Fig. 1 that a 1 mM chitosan concentration is sufficient to dispersed carbon nanotubes, a concentration of 5 mM chitosan was used to

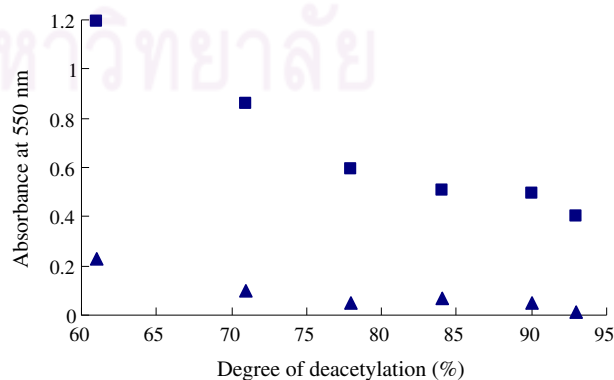
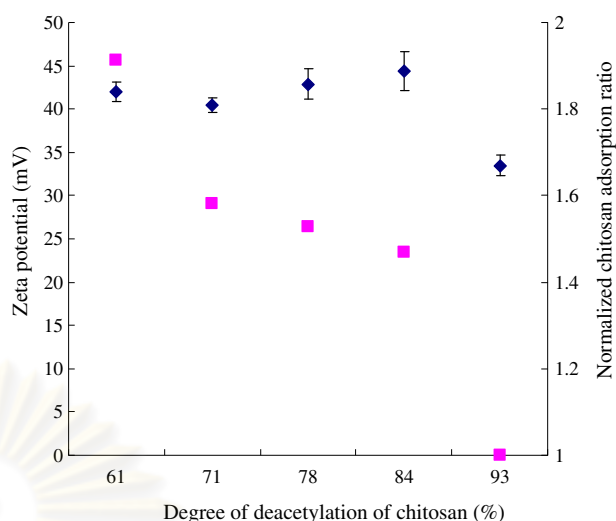


Fig. 2 – Plots of the changes in absorbance of a dispersion of MWCNTs in a 5 mM chitosan solution of various degree of deacetylation before (squares) and after (triangles) centrifugation at 2000 rpm for 10 min.

insure total dispersion of the MWCNTs in an excess solution of chitosan. From the absorbance measurements of the solutions, it can be seen that the efficiency of the dispersion of the carbon nanotubes, decrease when increasing the chitosan %DD. The final absorbance of the solution when using 61%DD is double than when using the 93%DD chitosan. These results suggest that, as expected, more hydrophobic chitosan segment found in the lower 61%DD are more efficient to adsorb onto the MWCNTs leading to a better dispersion of the carbon nanotube in solution. The mechanism through which CNT interact with chitosan is though to be due to hydrophobic interaction from hydrocarbon backbones and acetyl groups, and  $\pi$  system of the MWCNTs. CH- $\pi$  interaction which is a weak hydrogen bonding attraction between soft acid C-H bond and soft base  $\pi$  system are also though to take part in the adsorption of chitosan onto the MWCNTs [36]. At low degree of deacetylation 61%DD, the bonding force between chitosan and MWCNTs is based on hydrophobic interaction due to the acetyl groups that can interact with the surface of the nanotubes. For higher degree of deacetylation from 71%DD to 93%DD, the dispersion efficiency of the MWCNTs decreases due to the more hydrophilic character of the high %DD chitosan which is more soluble.

The efficiency of the surface modification of MWCNTs is often evaluated in term of stability against aggregation and sedimentation. Sedimentation occurs when the repulsion between MWCNTs is not strong enough to prevent the aggregation of the nanotube, leading to their precipitation. After surface modification of the MWCNTs by chitosan, the excess surface charges provided by the amino groups on the chitosan induce nanotube-nanotube repulsion and therefore prevent sedimentation. In our experiment, the sedimentation of the MWCNTs was accelerated with a centrifuge having a rotation rate of 2000 rpm for 10 min. In Fig. 2, is shown the absorbance of each MWCNTs solutions after centrifugation for each %DD (triangles). When compared to the initial absorbance (Fig. 2, square), a much lower absorbance as a result of the accelerated sedimentation by centrifugation was measured. Yet, it is interesting to observe that the lower 61%DD perform again better than the higher 93%DD although the former present a lower charge density when compare with the later. This would suggest that the adsorption of the lower %DD chitosan is greater than for higher %DD. In term of resistance to sedimentation, this improved stability suggests that the MWCNTs modified with the lower %DD have a higher surface charge density, which provides a better stability against sedimentation. In order to access the value of the surface charge, we further characterized the MWCNTs surface by zeta potential measurements.

The surface charge density of colloidal particles dispersed in solution can be estimated by measuring the zeta potential, which represents the difference in potential between the slip plane of the double layer near the particles surface and the bulk solution. The zeta potential of the pristine carbon nanotube is expected to be initially nearly neutral but should become largely positive after adsorption of chitosan due to the presence of cationic amino groups. In our experiments, the modified MWCNTs were found to have zeta potential values ranging from 34 to 42 mV, which confirm the successful immobilization of chitosan on the MWCNTs. Shown in Fig. 3



**Fig. 3 – Zeta potential of modified MWCNTs (diamonds) and normalized chitosan ration adsorbed onto the MWCNTs (squares) as a function of the %DD of chitosan.**

(diamonds) are plotted the zeta potential values as a function of the %DD, which range from 42 mV (61%DD) to 34 mV (93%DD). These values decrease with increasing %DD and suggest that all MWCNTs dispersed in solutions have similar surface charged. Yet, because the 61%DD chitosan has a lower linear charge density when compared to 93%DD, these values need to be corrected if we want to compare the amount of polymer adsorbed at the surface of the MWCNTs. This lower linear charge density is due to the fact that the 61%DD contain only 61  $\text{NH}_3^+$  groups for 100 monomers while the 93%DD contain 93  $\text{NH}_3^+$  per 100 monomer. Since the zeta potential is proportional to the density of charges, equal zeta potential for two nanotubes would require 1.5 times more 61%DD than 93%DD chitosan. Therefore the 93%DD has a linear charge density 1.5 times higher than the 61%DD. In Fig. 3 (squares) is plotted the corrected normalized chitosan monomer ration adsorbed onto the MWCNTs for each %DD. This plot is obtained by dividing the measured zeta potential by the corresponding %DD of the chitosan used and normalized. From the plot it can be seen that 1.9 times more 61%DD chitosan adsorb onto the MWCNTs when compared with the 93%DD. Several factors can justify the much lower adsorption of the 93%DD when compared with the 61%DD. The 93%DD has a better solubility, which means it will tend to remain in solution and will be more thermodynamically stable in solution. The higher charge density on the 93%DD chitosan can induce electrostatic repulsion of the  $\text{NH}_3^+$  groups, which in turn would lead to lower adsorption density of the chitosan while the 61%DD could adsorb in a more packed fashion.

#### 4. Conclusion

Multiwall carbon nanotubes have been noncovalently modified with chitosan having different %DD. Using chitosan having different %DD had a strong effect on the quality of the nanotubes dispersion. UV-Visible spectroscopy results suggest that the nanotubes dispersion was improved when using

chitosan with a lower degree of deacetylation (61%DD) when compared with higher degree of deacetylation (93%DD). The MWCNT modified with the lower %DD also displayed the best stability against centrifugation. Zeta potential measurements finally confirmed that the amount of chitosan adsorbed onto the nanotubes surface was twice as high with the lower %DD as with the high %DD. These modified MWCNTs with chitosan biopolymer could have the potential immobilization of hydrophobic and hydrophilic drug in drug delivery application.

## Acknowledgements

The authors are grateful to Thailand Graduate Institute of Science and Technology (TG-55-09-50-059D) and The 90th Anniversary of Chulalongkorn University Fund (Ratchadaphiseksomphot Endowment Fund) for their financial supports.

## Appendix A. Supplementary data

Supplementary data associated with this article can be found, in the online version, at doi:10.1016/j.carbon.2009.06.060.

## REFERENCES

- [1] Iijima S. Helical microtubules of graphitic carbon. *Nature* 1991;354:56–8.
- [2] Appenzeller J. Carbon nanotubes for high-performance electronics – progress and prospect. *Proc IEEE* 2008;96(2):201–11.
- [3] Martel R. Sorting carbon nanotubes for electronics. *ACS Nano* 2008;2(11):2195–9.
- [4] Avouris P, Chen J. Nanotube electronics and optoelectronics. *Mater Today* 2006;9(10):46–54.
- [5] Bianco A, Kostarelos K, Partidos CD, Prato M. Biomedical applications of functionalised carbon nanotubes. *Chem Commun* 2005(5):571–7.
- [6] Yang WR, Thordarson P, Gooding JJ, Ringer SP, Braet F. Carbon nanotubes for biological and biomedical applications. *Nanotechnology* 2007;18(41):412001 (12 pages).
- [7] Liu Z, Sun XM, Nakayama-Ratchford N, Dai HJ. Supramolecular chemistry on water-soluble carbon nanotubes for drug loading and delivery. *ACS Nano* 2007;1(1):50–6.
- [8] Foldvari M, Bagonluri M. Carbon nanotubes as functional excipients for nanomedicines: II. Drug delivery and biocompatibility issues. *Nanomed-Nanotechnol Biol Med* 2008;4(3):183–200.
- [9] Hilder TA, Hill JM. Probability of encapsulation of paclitaxel and doxorubicin into carbon nanotubes. *Micro Nano Lett* 2008;3(2):41–9.
- [10] Liu Z, Chen K, Davis C, Sherlock S, Cao QZ, Chen XY, et al. Drug delivery with carbon nanotubes for in vivo cancer treatment. *Cancer Res* 2008;68(16):6652–60.
- [11] Hampel S, Kunze D, Haase D, Kramer K, Rauschenbach M, Ritschel M, et al. Carbon nanotubes filled with a chemotherapeutic agent: a nanocarrier mediates inhibition of tumor cell growth. *Nanomedicine* 2008;3(2):175–82.
- [12] Thess A, Lee R, Nikolaev P, Dai HJ, Petit P, Robert J, et al. Crystalline ropes of metallic carbon nanotubes. *Science* 1996;273(5274):483–7.
- [13] Radomski A, Jurasz P, Alonso-Escolano D, Drews M, Morandi M, Malinski T, et al. Nanoparticle-induced platelet aggregation and vascular thrombosis. *Br J Pharmacol* 2005;146(6):882–93.
- [14] Saini RK, Chiang IW, Peng HQ, Smalley RE, Billups WE, Hauge RH, et al. Covalent sidewall functionalization of single wall carbon nanotubes. *J Am Chem Soc* 2003;125(12):3617–21.
- [15] Lisunova MO, Lebovka NI, Melezhyk EV, Boiko YP. Stability of the aqueous suspensions of nanotubes in the presence of nonionic surfactant. *J Colloid Interface Sci* 2006;299(2):740–6.
- [16] Haggemueller R, Rahatekar SS, Fagan JA, Chun JH, Becker ML, Naik RR, et al. Comparison of the quality of aqueous dispersions of single wall carbon nanotubes using surfactants and biomolecules. *Langmuir* 2008;24(9):5070–8.
- [17] Liu YQ, Gao L, Zheng S, Wang Y, Sun J, Kajiura H, et al. Debundling of single-walled carbon nanotubes by using natural polyelectrolytes. *Nanotechnology* 2007;18(36):365702 (6 pages).
- [18] Yang Q, Li SA, Pan XJ. Synthesis of fluorescent chitosan and its application in noncovalent functionalization of carbon nanotubes. *Biomacromolecules* 2008;9(12):3422–6.
- [19] Moore VC, Strano MS, Haroz EH, Hauge RH, Smalley RE, Schmidt J, et al. Individually suspended single-walled carbon nanotubes in various surfactants. *Nano Lett* 2003;3(10):1379–82.
- [20] Priya BR, Byrne HJ. Investigation of sodium dodecyl benzene sulfonate assisted dispersion and debundling of single-wall carbon nanotubes. *J Phys Chem C* 2008;112(2):332–7.
- [21] Gudixen KL, Gitlin I, Whitesides GM. Differentiation of proteins based on characteristic patterns of association and denaturation in solutions of SDS. *Proc Natl Acad Sci USA* 2006;103(21):7968–72.
- [22] Dong L, Joseph KL, Witkowski CM, Craig MM. Cytotoxicity of single-walled carbon nanotubes suspended in various surfactants. *Nanotechnology* 2008;19(25):255702 (5 pages).
- [23] Takahashi T, Luculescu CR, Uchida K, Ishii T, Yajima H. Dispersion behavior and spectroscopic properties of single-walled carbon nanotubes in chitosan acidic aqueous solutions. *Chem Lett* 2005;34(11):1516–7.
- [24] Kang B, Yu DC, Chang SQ, Chen D, Dai YD, Ding YT. Intracellular uptake, trafficking and subcellular distribution of folate conjugated single walled carbon nanotubes within living cells. *Nanotechnology* 2008;19(37):375103 (8 pages).
- [25] Zheng W, Zheng YF. Gelatin-functionalized carbon nanotubes for the bioelectrochemistry of hemoglobin. *Electrochem Commun* 2007;9(7):1619–23.
- [26] Bandyopadhyaya R, Nativ-Roth E, Regev O, Yerushalmi-Rozen R. Stabilization of individual carbon nanotubes in aqueous solutions. *Nano Lett* 2002;2(1):25–8.
- [27] Rinaudo M. Chitin and chitosan: properties and applications. *Prog Polym Sci* 2006;31(7):603–32.
- [28] Mourya VK, Inamdar NN. Chitosan-modifications and applications: opportunities galore. *React Funct Polym* 2008;68(6):1013–51.
- [29] Wu T, Zivanovic S. Determination of the degree of acetylation (DA) of chitin and chitosan by an improved first derivative UV method. *Carbohydr Polym* 2008;73(2):248–53.
- [30] Yan LY, Poon YF, Chan-Park MB, Chen Y, Zhang Q. Individually dispersing single-walled carbon nanotubes with novel neutral pH water-soluble chitosan derivatives. *J Phys Chem C* 2008;112(20):7579–87.
- [31] Peng FB, Pan FS, Sun HL, Lu LY, Jiang ZY. Novel nanocomposite pervaporation membranes composed of poly(vinyl alcohol) and chitosan-wrapped carbon nanotube. *J Memb Sci* 2007;300(1–2):13–9.
- [32] Liu YY, Tang J, Chen XQ, Xin JH. Decoration of carbon nanotubes with chitosan. *Carbon* 2005;43(15):3178–80.



- [33] Muzzarelli AAR, Roccheti R. Determination of the degree of acetylation of chitosans by first derivative ultraviolet spectrophotometry. *Carbohydr Polym* 1985;5:461-72.
- [34] Jeong SH, Kim KK, Jeong SJ, An KH, Lee SH, Lee YH. Optical absorption spectroscopy for determining carbon nanotube concentration in solution. *Synth Met* 2007;157(13-15): 570-4.
- [35] Bangyekan C, Aht-Ong D, Srikulkit K. Preparation and properties evaluation of chitosan-coated cassava starch films. *Carbohydr Polym* 2006;63(1):61-71.
- [36] Nishio M. CH/ $\pi$  hydrogen bonds in crystals. *Crystengcomm* 2004;6:130-58.



ศูนย์วิทยทรัพยากร  
จุฬาลงกรณ์มหาวิทยาลัย

## VITAE

### PERSONAL DATA

**Name** : Chularat Iamsamai  
**Nationality** : Thai  
**Date of Birth** : July 12, 1980  
**E-mail** : iamsamai@yahoo.com

### EDUCATION

- 1999-2003 Bachelor of Engineering**  
 Department of Materials Science and Engineering, Faculty of Engineering and Industrial Technology, Silpakorn University, Nakhon Pathom, Thailand  
**Major:** Petrochemicals and Polymeric Materials
- 2003-2005 Master of Science**  
 Department of Materials Science, Faculty of Science, Chulalongkorn University, Bangkok, Thailand  
**Major:** Applied Polymer Science and Textile Technology  
**Thesis title:** Coating of Polyamide Fibers with Polyelectrolyte Multilayer Thin Films to Improve Wash Fastness
- 2006 - 2010 Doctor of Philosophy**  
 Doctor of Philosophy Program in Nanoscience and Technology, Graduate School, Chulalongkorn University, Bangkok, Thailand  
**Major:** Nanoscience and Technology  
**Thesis title:** Modified Carbon Nanotubes for Drug Delivery Applications

### PUBLICATIONS IN THIS DISSERTATION

- Iamsamai C.**, Hannongbua S., Ruktanonchai U., Soottitantawat A., Dubas S.T. The effect of the degree of deacetylation of chitosan on its dispersion of carbon nanotubes. Carbon. 2010; 48(1): 25-30.
- Iamsamai C.**, Hannongbua S., Ruktanonchai U., Soottitantawat A., Dubas S.T. Simple method for the layer-by-layer surface modification of multiwall carbon nanotubes. **Submitted**.

### **Related Publication**

- Rungrotmongkol T., Arsawang U., **Iamsamai C.**, Vongachariya A., Dubas S.T. and Hannongbua S. How dispersion and separation are the noncovalently modified carbon nanotubes? A case study with a chitosan-polysaccharide biopolymer wrapping on SWCNTs. **In preparation**.